8-2013

PROBLEMS IN THE STUDY AND USE OF AC DIELECTROPHORESIS AND THEIR CONSEQUENCES: A STUDY BASED ON COMSOL MULTIPHYSICS MODELING

Vandana devi Pandian babu
Clemson University, vdevi@clemson.edu

PROBLEMS IN THE STUDY AND USE OF AC DIELECTROPHORESIS AND THEIR CONSEQUENCES: A STUDY BASED ON COMSOL MULTIPHYSICS MODELING

A Thesis
Presented to
the Graduate School of
Clemson University

In Partial Fulfillment
of the Requirements for the Degree
Master of Science
Bioengineering

---

by
Vandana Devi Pandian Babu
August 2013

Accepted by:
Dr. Guigen Zhang, Committee Chair
Dr. Delphine Dean
Dr. Pingshan Wang

ABSTRACT

Dielectrophoresis (or DEP) is an important phenomenon which is induced when a dielectric particle is placed in a non-uniform electric field. The force generated by DEP has been exploited for various micro and nano fluidics applications like positioning, sorting and separation of particles involved in medical diagnostics, drug discovery, cell therapeutics, biosensors, microfluidics, nanoassembly, particle filtration etc. The integration of DEP systems into the microfluidics enables inexpensive, fast, highly sensitive, highly selective, label-free detection and also the analysis of target bioparticles.

This work aims to provide a complete compilation of the factors affecting the DEP force. It elucidates the underlying mechanisms using COMSOL Multiphysics and sheds new insight into the mechanisms for the separation and sorting of different types of particles. This research identifies the problems in the literature and uses COMSOL to analyze the impact of these problems on the end results. It examines four factors that affect the DEP force: physical conditions, electrode setup, properties of the particles and suspension medium. Moreover, it analyzes the influence of the Clausius-Mossotti factor (CM factor) and its cross-over upon the magnitude and direction of the DEP force.

From the analysis, it becomes clear that particle size not only affects the magnitude of the DEP force but also the conductivity of the particle. This factor, which is largely ignored, could lead to a shift in the crossover frequency. Shell model plays an important role in determining the dielectric properties of particles that are not homogenous. In such a situation assuming uniform dielectric properties may lead to

inconclusive results. The presence of an electric double layer surrounding a particle affects the conductivity of the particle. Also, assuming DEP force to be the only force acting on a particle suspended in a non-uniform electric field leads to errors in the end results.

This research provides knowledge on the basic characteristics of the DEP force and its mechanism. It provides a better understanding by examining numerous works carried out in the past and brings out the problems and their consequences.

DEDICATION

I would like to dedicate this work to my parents, brother and my friends for their support, motivation and guidance.

ACKNOWLEDGEMENTS

I would like to sincerely thank my advisor, Dr. Guigen Zhang, for his guidance and motivation. His mentorship and genuine interest in my personal growth as a graduate student is greatly appreciated. I am grateful to my committee members, Dr. Delphine Dean and Dr. Pingshan Wang for being supportive in the completion of this thesis. I would also like to thank all the members of my research groups for their inputs and interest in my work. I am indebted to all my friends at Clemson for their immense support. Last but not the least I would like to thank all the professors and support staff at Clemson University who helped me complete this work and provided their unwavering support through the last two years. This work is partially supported by Tokyo Electron US Holding.

TABLE OF CONTENTS

Page

Table of Contents (Continued)

Table of Contents (Continued)

LIST OF TABLES

LIST OF FIGURES

List of Figures (Continued)

List of Figures (Continued)

Figure Page

List of Figures (Continued)

Figure Page

CHAPTER 1

INTRODUCTION

DEP is demonstrated when dielectric particles are placed in a non-uniform electric field (both in AC and DC electric fields). This is because DEP shows higher dependence on the field gradient than the field direction. In the case of AC-DEP, which is mainly reviewed and studied in this research, fields of a particular frequency are used to manipulate particles with greater selectivity. If particles move in the direction of increasing electric field, the behavior is referred to as positive DEP (pDEP). If particles move away from high field regions, it is known as negative DEP (nDEP).

The strength of the DEP force varies with the properties of these particles and the suspension media used as well as physical parameters and electrode setup. In contrast to electrophoresis, the particles do not have to be charged when manipulating them with DEP forces. When these particles are placed in a non-uniform electric field, they will be polarized to form a dipole. This leads to attraction and repulsion of particles according to the orientation of the dipole, which is dependent on the relative polarizability of the particle and medium. According to Maxwell-Wagner-Sillars theory such polarization occurs at the particle-medium interface on a macroscopic scale, leading to the separation of the charges.

DEP was first observed in early 20^{th} century. However it was explained and named by Herbert A. Pohl in 1950 when he was attempting to separate particles from a polymer solution. The applications of DEP remained unknown and hence not much work was done on it. In the last ten years it has been revived due to development made towards

translating theoretical treatment of microparticles, nanoparticles and cells to practical applications like biosensors, bioassays. In the last three years DEP has been combined with microfluidics to help better manipulation of particles. Currently most of the work is into addressing unmet needs in tissue engineering and stem cell research.

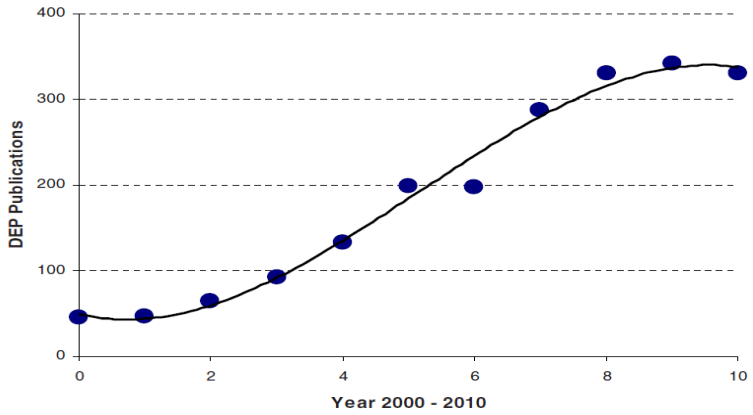

Figure 1.1: Number of publications on DEP for the period 2000–2010

As seen from Figure 1.1, the number of publications has increased in the last ten years. But the number of patents does not correspond to the publications. This shows that there are issues in translating the experimental observations to practical applications. To overcome this, the underlying concepts of DEP have to be studied. This research aims at providing a better understanding of the fundamentals of DEP.

DEP requires the optimization of physical conditions and electrode parameters for each type of particle used. The polarizability of the particles in a suspension medium contributes significantly to the DEP force. It requires particles to be suspended in a low conductivity medium for particle manipulation, which affects the viability of the cells. The electric field applied to in case of highly conductive biological sample leads to Joule heating and bubbling that affects the particle movement. Also, there are several

ambiguities in the mechanism behind particle movement by DEP. This research aims to identify and rectify the associated problems.

1.1 Research Objectives:

The research objectives of this work are summarized below:

- To review the field of DEP and present the theories
- To provide a better understanding of a particle moving in a non-uniform electric field
- To identify and demonstrate the consequences of the common misconceptions, discrepancies and contradicting results from the literature in the application of DEP
- To demonstrate the importance of correcting the issues in the literature
- To explore various factors that might affect the movement of particles placed under the influence of a DEP
- To perform a complete analysis of the properties of the particle, suspension medium, electrodes and physical quantities that affect DEP
- To validate experimental results from the literature using COMSOL multiphysics
- To identify the future work that needs to be done in the field of DEP

1.2 Organization of the thesis

Chapter 1 gives a brief introduction about the objectives of the research and organization of the thesis. Chapter 2 presents a literature review for the work. It gives

detailed background information about the data collected, methods used, conclusions drawn, discussions and suggestions put forward. This chapter covers the applications of DEP force in biomedical engineering. Chapter 3 lists the common problems and challenges that were identified in the literature. Chapter 4 explains the different models used, physics included and input parameters given to the model. It gives an overview of the COMSOL Multiphysics 4.2 which is used in Chapter 5 to illustrate the problems and the consequences of these problems.

Chapter 5 gives the analytical formulae derived for the purpose of this research and the calculation and demonstration of the problems. Sufficient evidence is provided to demonstrate the suggested hypothesis and consequences of these problems on the results are demonstrated. Chapter 6 summarizes the different factors that affect DEP like the effect of different physical conditions, electrode geometry and dimensions of electrode, particle and suspension medium parameters. Chapter 7 contains the conclusions of the work and suggested future on this research.

CHAPTER II

LITERATURE REVIEW

2.1. Fundamentals of DEP

DEP is based on the theory that particles such as synthetic beads, biological cells, proteins and DNA can be manipulated by the forces exerted by non-uniform electric fields. This concept was first studied by Herbert A. Pohl in the 1950s. Pohl described the application of DEP in removing suspended solid particles from polymer solutions during analysis. He thus defined DEP as the phenomenon seen in '*the relative motion of suspension and medium resulting from polarization forces produced by an inhomogeneous electric field*' [1]. Since then, DEP has been studied extensively for numerous applications.

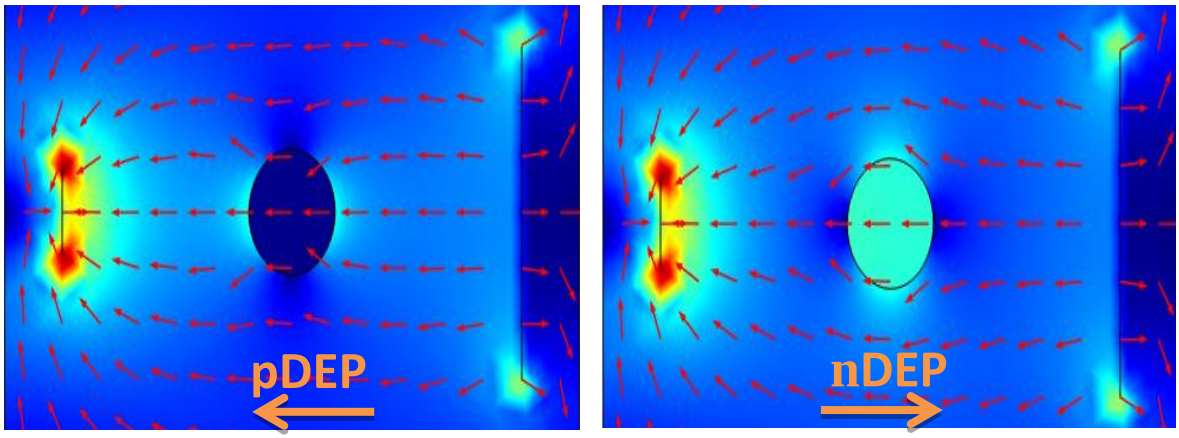

Figure 2.1: Illustration of DEP forces on polarized particle in the case of positive and negative DEP

In Figure 2.1 we can see that when a particle is placed in a non-uniform electric field polarization occurs, leading to an induced dipole moment. When the induced dipole moment is placed in uniform electric field, one end of the dipole is in a weaker field than

the other and electrostatic pull will cause particle movement [2]. Thus, non-uniform electric fields play an important role in generating DEP for particle manipulation.

There are several ways to create non-uniform electric fields. One is the use of different electrode designs. A wide variety of electrode designs, ranging from simple planar geometries to complex three-dimensional (3-D) designs have been explored. Another way is to use insulators to alter the electric field. In recent works, arrays of insulating posts in a channel of a microchip are used to produce the spatially non-uniform fields needed for DEP [3-5]. They provide an attractive alternative to conventional electrode-based systems.

2.1.1. Theoretical Explanation of DEP

The simplest theoretical model for DEP is that of a homogeneous spherical particle immersed in a dielectric medium (see Figure 2.2) [6]. According to Pohl, for a homogeneous sphere of radius R in a medium with permittivity $\boldsymbol{\varepsilon_m}$, the DEP force can be calculated as follows

$$F_{DEP} = 2\pi r^3 \varepsilon_m Re(f_{CM}) \nabla |E|^2 \tag{2.1}$$

where, f_{CM} is the Clausius-Mossotti (CM) factor, r is the radius of the particle and ε_m is the permittivity of the medium.

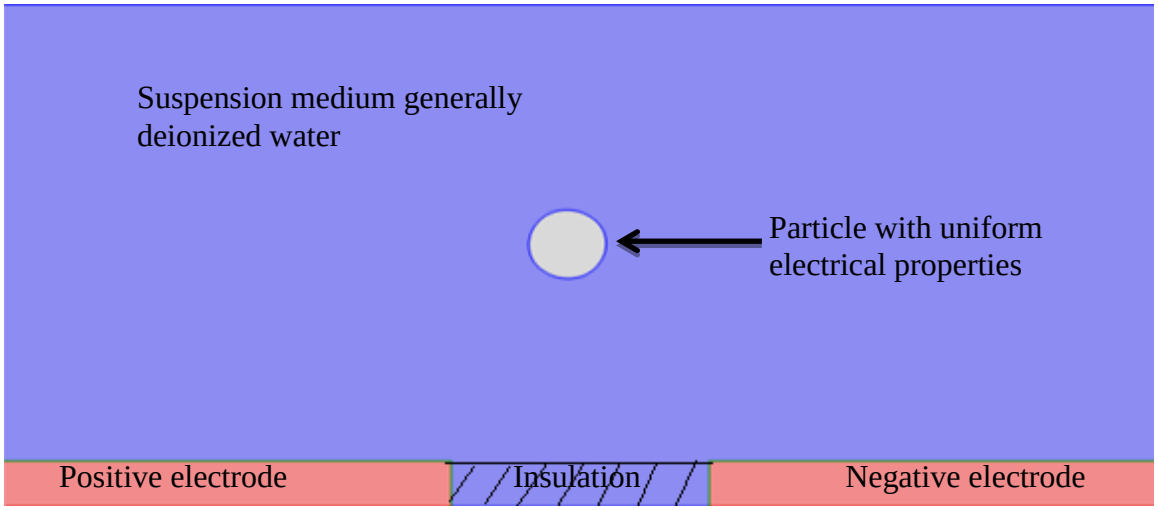

Figure 2.2: Homogeneous particle suspended in a liquid medium. An insulation region is necessary to separate the positive and negative electrodes.

When a particle has a non-spherical shape (e.g., ellipsoidal shape) equation 2.1 cannot be used. The following equation gives the DEP force for a more general field-aligned ellipsoid of radius *r* and length *l* [7]

$$F_{DEP} = \frac{\pi r^2 l}{3} \varepsilon_m Re(f_{cm}) \nabla |E|^2$$

This equation can be used to study the dielectrophoretic response of red blood cells and carbon nanotubes.

2.1.2 Frequency dependence of CM factor

The CM factor introduced in equation 2.1 is defined in terms of complex permittivity as follows [8]

$$f_{CM} = (\varepsilon_p{}^* - \varepsilon_m{}^*)/(\varepsilon_p{}^* + 2\varepsilon_m{}^*) \quad (2.2)$$

where, $\varepsilon_p{}^*$ and $\varepsilon_m{}^*$ are complex permittivity of the particle and the suspension medium respectively. The calculation of the complex permittivity (ε^*) is given below [9]

$$\varepsilon_p{}^* = \varepsilon_p - i\,(\sigma_p/\omega) \tag{2.3}$$

where, σ_p is the conductivity of the particle, ε_p is the permittivity of the particle, i is the imaginary unit and ω is the angular frequency.

The direction of particle movement depends on the sign of the CM factor, which in turn depends on the frequency. From equation 2.1 it can be seen that the real part of the CM factor ($Re(f_{cm})$) plays an important role in determining the DEP force.

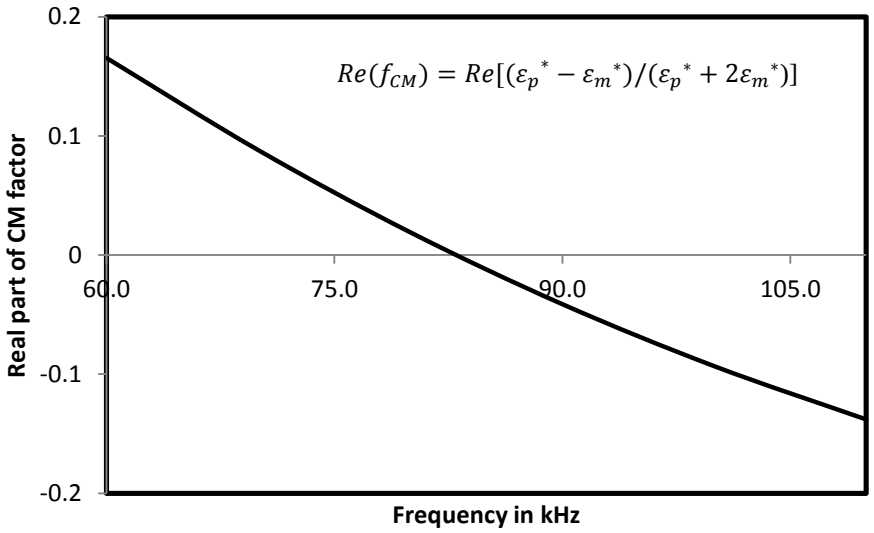

Figure 2.3: CM factor changing from positive to negative with increase in frequency (Theoretical data for CM factor calculation)

In Figure 2.3 $Re(f_{cm})$ is plotted against the frequency for polystyrene beads (particle polarizability is greater than the medium, see section 2.1.4). At lower frequencies $Re(f_{cm})$ is positive and as frequency increases it decreases to negative values after passing through zero. Thus, with change in frequency the $Re(f_{cm})$ changes from

positive to negative. When the polarizability of the particle is less than the medium at low frequencies, Re(f_{cm}) is negative and as frequency increases it becomes positive. Thus, with change in frequency the Re(f_{cm}) changes from negative to positive for polystyrene beads.

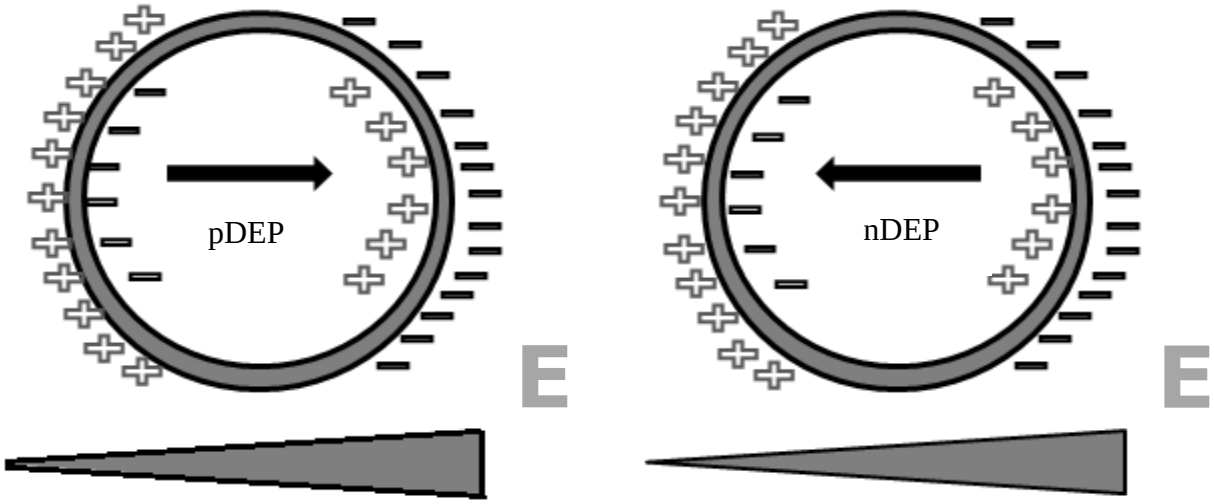

Figure 2.4: Particle polarization and DEP forces under positive and negative DEP

The frequency at which Re(f_{cm}) is zero is called the crossover frequency. The particle moves in the direction of increasing electric field when Re(f_{cm}) is positive, leading to pDEP. The particle moves away from the high electric field regions when Re(f_{cm}) is negative, leading to nDEP. The crossover between positive and negative DEP response is dependent on the properties of the particle and the suspension medium [10]. The crossover frequency is unique for each type of particle and thus can be used to sort particles.

2.1.3. Shell Model of particles

Synthetic beads such as polystyrene and latex beads are isotropic (uniform dielectric properties in all directions) [11] and have a zero-shell model (see Figure 2.5) [12].

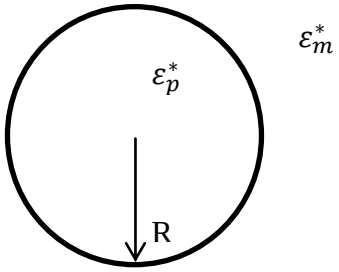

Figure 2.5: Homogenous or zero-shell model for synthetic particles with uniform dielectric properties

In a zero shell model the complex permittivity of particle and medium are given by [13, 14] the following equations

$$\varepsilon_p^* = \varepsilon_p - i\,\sigma_p/\omega \text{ , for particle}$$

$$\varepsilon_m^* = \varepsilon_m - i\,\sigma_m/\omega \text{ , for medium}$$

Unlike synthetic particles, biological particles (e.g., cells) generally have a complex heterogeneous structure containing more than one layer [15]. Cells have a complex internal structure with membranes having different permittivity and conductivity from the cytoplasm [16]. Their structures are better described by a composite dielectric body made of dielectric shells (one or more) representing the cell membrane, cell wall, a homogeneous dielectric core etc.

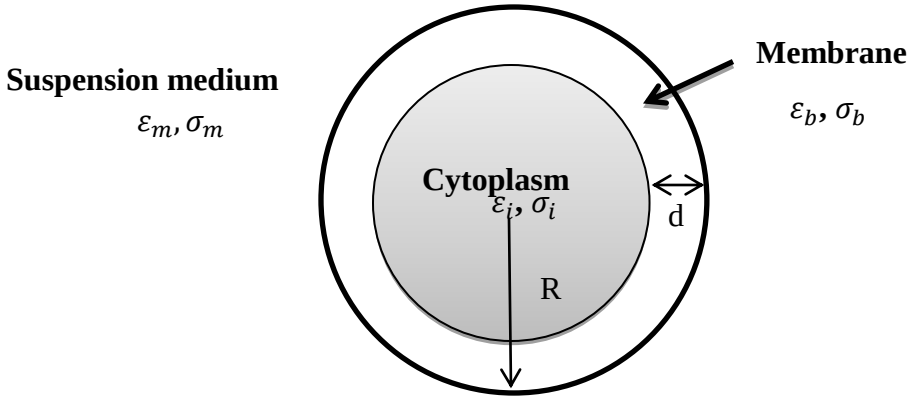

Figure 2.6: Single shell model considering different dielectric properties for the cytoplasm and membrane

Figure 2.6 shows a single shell model having a uniform core surrounded by a membrane of different dielectric properties. Although the inside of a cell is nonhomogeneous there is less effect since the electrical field penetrates very little into the cell at low frequencies [17]. Single shell model is used in these cases. For a cell described in Figure 2.6, the overall dielectric property is obtained from a combination of the properties of the shell and the core [18, 19]

$$\varepsilon_p^*(\omega) = \varepsilon_m^* \frac{(\frac{R}{r})^3 + 2\frac{\varepsilon_o^* - \varepsilon_i^*}{\varepsilon_o^* + 2\varepsilon_i^*}}{(\frac{R}{r})^3 - \frac{\varepsilon_o^* - \varepsilon_i^*}{\varepsilon_o^* + 2\varepsilon_i^*}} \tag{2.4}$$

where, ε_p^* is the complex permittivity of the particle, ε_o^* is the complex permittivity of the outer shell or membrane, ε_i^* is the complex permmitivity of the inner core, r is the inner radius and R is the outer radius. Equation 2.4 can be rearranged as follows:

$$\varepsilon_p^*(\omega) = \varepsilon_m^* \frac{2\varepsilon_m^* + \varepsilon_i^* - 2v(\varepsilon_m^* - \varepsilon_i^*)}{2\varepsilon_m^* + \varepsilon_i^* - v(\varepsilon_m^* - \varepsilon_i^*)}$$

In which, $v = \left(1 - \frac{d}{R}\right)^3$

and *d* is the thickness of outer shell and *R* is the outer radius of the shell.

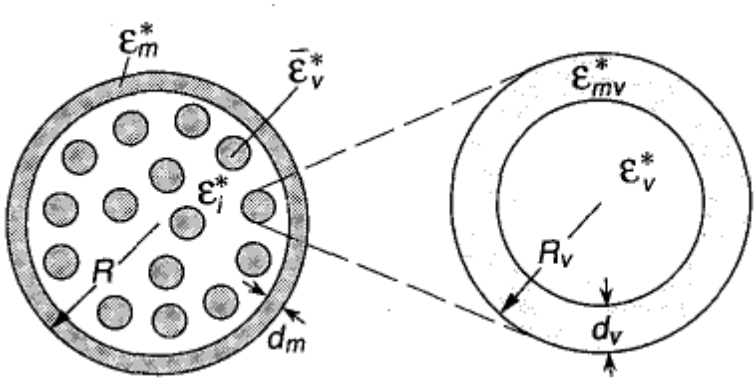

Figure 2.7: Vesicle inclusion model containing structures with different dielectric properties inside the single shell model

Figure 2.7 describes the vesicle inclusion models where the membrane, cytoplasm and the vesicles have different dielectric properties. This can be used for yeast cells that have distinct nucleus, vacuole, fat globules and cell wall.

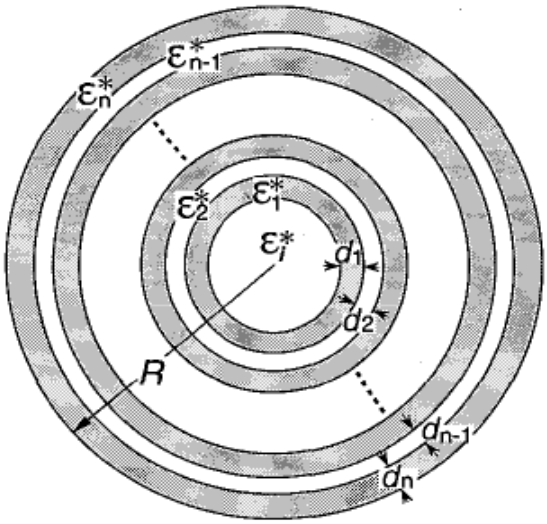

Figure 2.8: Multi-shell model of biological cells and other complex particles

In the case where there exists more than one concentric layer (see Figure 2.8) with different permittivity and conductivity [20], the complex permittivity is given by the following equation

$$\varepsilon_{s_j}{}^{*} = \varepsilon_{s_j} + \frac{\sigma_{s_j}}{i\omega\varepsilon_o} \text{ (j = 1, 2, 3…)}$$

where, *i* is the imaginary unit and *j* is the index number for the layers. This formula can accommodate the permittivity and conductivities of the different layers of the particle.

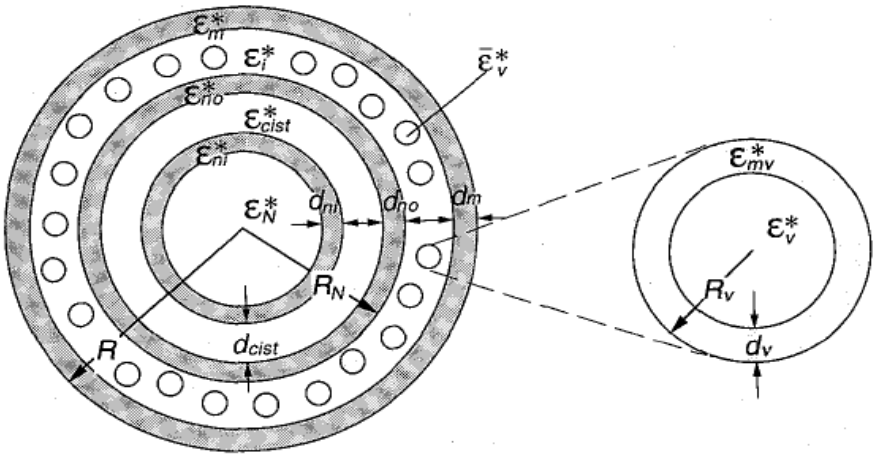

Figure 2.9: Triple shell model with vesicle inclusion, depicting the model of the cell with different organelles

Figure 2.9 shows the triple shell model with vesicle inclusions (e.g., Plant cell with cell wall, cell membrane and vacuoles). The different models mentioned above have unique CM factors. Based on the different dielectric properties in the different regions of the structure a CM factor equation has to be derived to calculate the DEP force. The CM factor derivation for single shell model is done in this research.

2.1.4 Polarizability

The polarizability of a particle is defined in terms of the local electric field at the particle by the following equation

$$\rho \propto \alpha E_{local}$$

where, ρ is the dipole moment and E_{local} is the local electric field at the orbital. It is very important to choose the right medium to suspend the particles because the DEP force changes with the relative polarizability (depending on whether the particle is more polarizable or less polarizable than the medium) according to Maxwell-Wagner-Sillars polarization [21]. This can be illustrated by plotting the Re(f_{cm}) against the frequency.

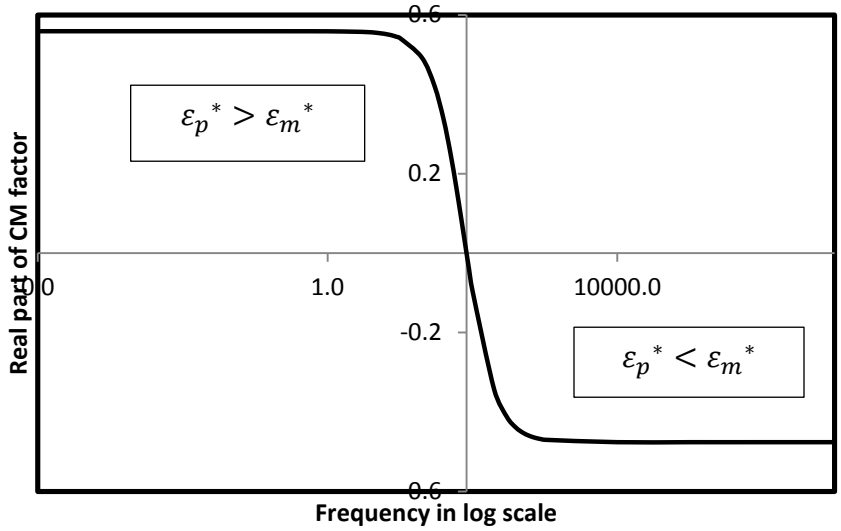

Figure 2.10: When the particle is more polarizable than the medium the Re(f_{cm}) is positive and when the medium is more polarizable than the particle it is negative

Figure 2.10 shows the plot of Re(f_{cm}) against frequency (using equation 2.2) for polystyrene beads suspended in deionized water. In the graph it is seen that at high frequencies the particles are less polarizable than the medium and experience nDEP, and at low frequencies the particles are more polarizable than the medium and undergo pDEP.

For polystyrene beads suspended in deionized water over flat plate electrodes ideally at frequencies well below 20 MHz (1 kHz–1 MHz) all the beads should move to regions of maximum field gradient at the tips of the electrodes, consistent with the polarizability of the particle exceeding the medium. Similarly at frequencies >20 MHz (20 MHz–250 MHz) all the beads are collected at low field gradient regions in the electrode setup [22].

2.2. Fabrication of electrodes

Fabrication of the electrodes is a very important step in the manipulation of particles using DEP. This process combines photolithography and etching to fabricate electrodes with a smooth surface and of desired thickness. In photolithography UV light is used to transfer a geometric pattern on a predesigned mask to a metal substrate coated with a photoresist (light sensitive material). It is followed by a series of chemical treatment that etches the uncovered metal film on the substrate.

For example, a layer of titanium (20nm thick film) and a layer of gold (100nm thick film) are deposited using electron beam evaporation to form the electrode layer on the glass slides (substrate). S1818, a positive photoresist is used to mask the gold where it is not desired to be etched away. Once the S1818 has been developed and baked on sufficiently, the gold is etched away by dipping the electrode in a potassium iodide solution for about 30 seconds. The titanium is then etched away using a dilute hydrofluoric acid dip until the glass appears transparent. The photoresist is removed from the remaining metal, revealing the patterned electrode. This electrode can be used for DEP experiments.

2.3. Advantages of using DEP for particle manipulation

The main advantages of dielectrophoresis include:

- Use of an electric field for manipulation requires no moving parts
- Faster and less expensive approach
- Noninvasive method
- Less heating of the system (comparatively lesser joule heating observed)
- Operates at lower voltage
- Minute dimensions allows high electric field intensity at lower voltages [23]
- Does not require fluorescent staining or chemical tagging [24]
- Polarization forces in DEP acting on particles are insensitive to its charge [25]
- Easy adaptability to electronics and thus can be incorporated easily into micro-systems.

2.4. Comparison with conventional techniques

DEP has few advantages over electrophoresis. Movement by electrophoresis is determined by a net intrinsic electrical charge carried by that particle. It usually occurs in a homogeneous DC field. Whereas the movement of particles due to DEP is determined by the magnitude and polarity of charges induced in the particle by an applied field. It occurs in a DC field as well as in an AC field of a wide range of frequency. The electric field has to be non-homogeneous in this case [26].

Capillary electrophoresis (CE) was considered as the preferred technique for charge based separation of particles as it can be employed for the separation and

characterization of a variety of biological and biomimetic structures [27] including liposomes [28], bacteria, subcellular components and mammalian cells [29]. But CE lacks enhanced selectivity for biological particles. On the other hand DEP has better selectivity to target particles as it is based on the particle's dielectric properties.

Cell density, molecular weights, immunologic assays and receptor-ligand interactions are the common factors that are exploited for particle sorting. However, they are inadequate and have lot of drawbacks. They produce insufficient pure cell populations. Additionally, they are slow, harmful to cells and are limited to certain type target cells. Hence there is an essential need for improving sorting methodologies. According to a review by Pethig *et al.* DEP can be used to isolate and trap single particles better than optical tweezers and ultrasonic manipulation because of the simplicity of the instruments and the ability of DEP to induce both positive and negative forces [30].

2.5. Applications

A number of DEP based devices have been developed to address challenges in biomedical engineering, focusing on life sciences and analytical chemistry. DEP is now considered a viable tool for lab-on-a-chip systems for separating a heterogeneous population of particles into homogeneous subpopulations, manipulating and concentrating biologically relevant molecules, and distinguishing between damaged and healthy cells. Cells, cellular components, DNA etc. can be collected, separated, concentrated, and transported using electrode structures having dimensions of the order

1 to 100 μm. [31]. It should be noted that DEP forces can manipulate even DNA particles, which are about 10^4 orders of magnitude smaller than cells. Recent progress in the development of new electrode structures has led to new techniques for the dielectrophoretic characterization and sorting of cells, microorganisms and other bioparticles using non-uniform AC electric fields.

2.5.1. Particle Sorting

Muller *et al.* designed a 3D microelectrode for caging yeast cells. They found that DEP allows selective manipulation of synthetic as well as biological particles, as it relies on the fact that particular types of particles have unique frequency-dependent dielectric properties [32]. Gossett *et al.* studied the application of DEP to diagnostics and therapy for diseases. It was found that cell reactions to drugs can be studied with DEP as the drugs mainly have an effect on the bioparticle's surface conductivity, membrane capacitance and cytoplasm conductivity [33]. There has also been a study on the dielectric properties of drug sensitive and resistant leukaemic cells for DEP application [34]

There are several advancements in the field of particle trapping and manipulation on a chip [35]. A novel type of particle sorting system consists of extruded quadruple electrodes [36, 37], which can simultaneously load, interrogate, and sort an ensemble of single cells. Pethig *et al.* were able to demonstrate the collection of yeast cells using both nDEP into pDEP on interdigitated castellated electrodes [38].

Virus identification is an important step for disease diagnostics. The separation of two different viruses, Tobacco Mosaic Virus (TSV) and Herpes Simplex Virus (HSV) has been demonstrated using DEP [39]. The HSV is trapped under nDEP forces at the field minimum in the center of the electrode array, while TMV experiences pDEP and collects at the electrode edges (where the electric field is high) and thus can be separated out. This can be extended to other viruses too.

Selectively targeting cancer cells has been a major challenge. Morgan *et al.* worked on the separation of submicron particles by DEP using suitable electrode arrays. DEP exhibits high specificity in separating normal cells from cancer cells [40]. Gascoyne *et al.* [41] showed DEP separation of treated and untreated leukemic mouse cells.

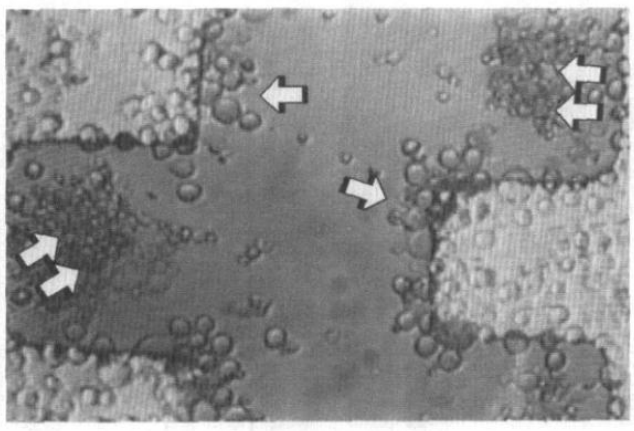

Figure 2.11: Separation of normal murine erythrocytes and erythroleukemia cells using DEP. Double arrows point to where the normal murine erythrocytes are and single arrow shows where the erythroleukemia cells [41]

Treated leukemic cells display negative collection at about 22kHz while untreated leukemic cells showed pDEP. Dielectrophoretic separation of mammalian cells studied

by computerized image analysis permits individual subpopulations to be discriminated within cell mixtures. From the Figure 2.11 it can be seen that the normal murine erythrocytes (smaller cells) aggregate in the gap region between the electrodes and erythroleukemic cells aggregate at the edge of the electrodes. Because normal erythrocytes are smaller than erythroleukaemic cells, a simple size discrimination algorithm allows the image of all cells to be split into separate images containing only erythrocytes or only leukemic cells. These separate images are then analyzed using the same spatial overlap integrals as before.

2.5.2. Live and Dead Cell Separation

DEP filters are used to separate out viable cells before feeding to the bioreactor as non-viable cells produce adverse metabolic products. For example, the use of autologous bone marrow transplants in the remediation of advanced cancers requires the removal of cancer cells from the patient's marrow [42] and the study of signaling between blood cells requires purified cell subpopulations [43]. DEP filters can be employed for such applications.

Ling *et al.* made asymmetric and periodic microelectrode array for continuous particle separation [44]. Jen *et al.* showed the selective trapping of live and dead cells using insulator based electrode array. It was done by utilizing the difference in polarizability of cells and suspending media [45]. Using DEP to distinguish between live and dead cells has advantages over using chromogens and fluorophores. The separation has been addressed theoretically and quantified as a function of membrane conductivity

[46], thickness, cell cytoplasm conductivity [47], permittivity, and cell radius [48]. DEP filters have been made that work by controlling the potential applied and frequency for cell-specific bioparticle manipulation [49].

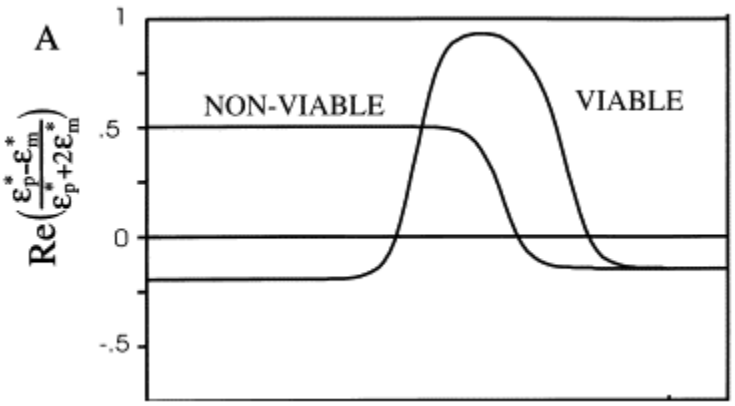

Figure 2.12: Huang *et al.* in 1999 showed separation of live and dead cells based on the CM factor. The optimum of frequency was determined. Model and data taken from published paper [50]

Figure 2.12 shows the difference in crossover frequency curves for live and dead cells based on work by Huang *et al.* combining DEP and electrorotation [50]. Markx *et al.* reviewed the biotechnology application of DEP to separate viable and non-viable cells [51] according to which dead cells have significantly lower dielectrophoretic mobility than live cells. When a cell dies, the cell membrane becomes permeable, and its conductivity increases by a factor of 10^4. Although batch-wise separation of cells is commonly done, DEP also allows continuous operation to separate live and dead cells. Markx *et al.* constructed the electrode array for the continuous separation of live and dead cells was done by [52].

2.5.3. Cell patterning

Cell patterning arranges cells into desired patterns, mimicking the real tissue by applied external guiding or manipulation. This technique is demonstrated by Ho *et al.* and is also called biomimetic patterning [53]. Most of the existing techniques have several drawbacks including cell pre-treatment requirement, difficulty in working with heterogeneous batch of cells, low spatial resolution, complex equipment, cytotoxicity etc. Due to the advantages that DEP has it is becoming one of the powerful tools to pattern biomaterials, bioactive scaffolds and even porous scaffolds [54].

Verduzco-Luque et al. studied the use of cell patterning using DEP to form biofilms using interdigitated array electrodes [55]. These electrodes can be used for various applications like analyzing how the cell-cell interaction affects gene expression [56] and metabolism in biofilms [57].

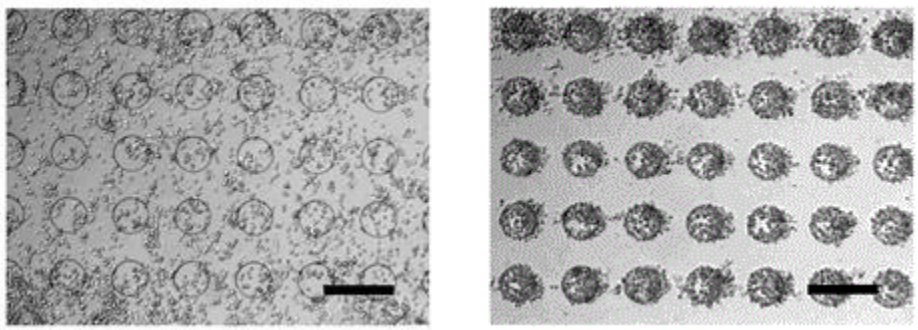

Figure 2.13: Left picture shows cell before DEP and right picture shows the monolayer formation after the DEP force acts on them. They are collected in the microwells [58]

In Figure 2.13 the cells are randomly placed on the electrode in the first picture. After the electric field is applied, the cells start aligning themselves as monolayers over the wells based on nDEP [58]. Tsutsui et al. [59] fabricated an array of PEG hydrogel

microwells on top of the electrode using pDEP. Captured cells formed a homogenous monolayer, thus producing a large array of engineered tissue samples.

The application of cell patterning using DEP to tissue engineering for making multilayer aggregates and scaffolds is a relatively new technique and has great scope. In nDEP as the particles are moved to the lower electric field there might be less energy acting on the cell possibly leading to cell aggregation. pDEP is capable of manipulating thousands of cells in parallel with the single-cell resolution. Markx et al. [60] used DEP to trap and pattern Jurkat T cells, Mouse AC3 stromal cells and SAOS-2 osteoblast cells into an organized multilayered hematon-like (blood producing) structure (see figure 2.14).

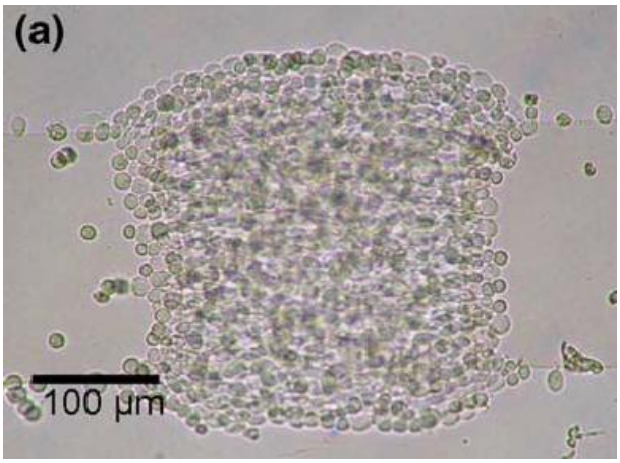

Figure 2.14: Brightfield image of an aggregate of Jurkat cells using DEP at 1 MHz. Introduction of stem cell helped in formation of a multi-layered hematon like structure [60]

In the case of tissue engineering, immobilization of cells is very important to determine the stability of the cell. Gray et al. [61] used a fibronectin coated membrane to help specific binding of cells that were aligned using DEP. Albrecht et al. [62] demonstrated the formation of various PEG hydrogel microstructures containing living

cells using DEP and illustrated their compatibility with a fluorescence-based assay (Figure 2.15). They used crosslinking for binding the cells.

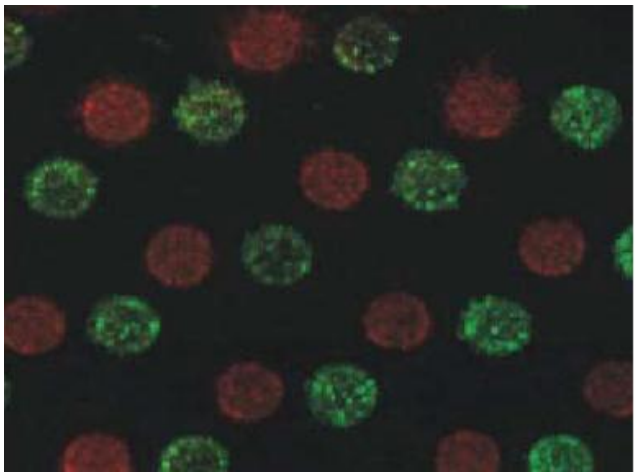

Figure 2.15: Cells encapsulated within an array of micropatterned hydrogel islands [62]

Ho et al. [53] demonstrated the patterning of multiple cells to mimic organs and their functions using pDEP (see Figure 2.16). They worked on the patterning of heterogeneous cells (hepatic cells and endothelial cells) into pearl chains to mimic the lobular morphology of real liver tissue. Concentric-stellate-tip array electrode was constructed in which the concentric-ring array electrodes provide a global radial electric field for the initial formation of cell patterning and the concentric stellate-tips act as the local destination directors (providing the local maxima of electric-field gradients to precisely snare the cells to form the desired cell pattern). This helps in the formation of the radial pearl-chain cell patterns of Human liver cell line (HepG2) and Human umbilical vein endothelial cells (HUVECs).

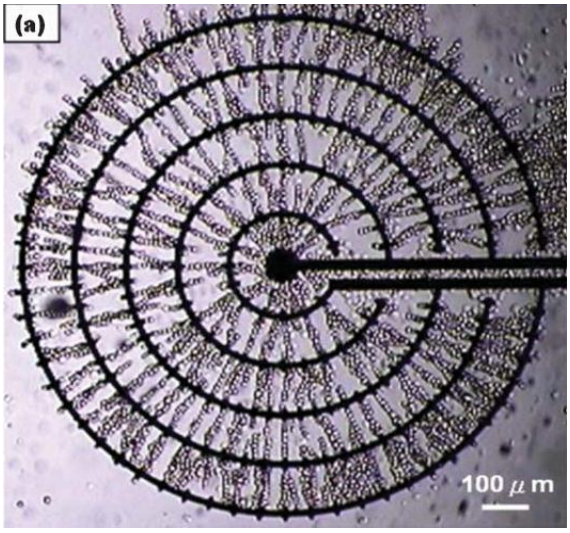

Figure 2.16: Cells flowing over the cell patterning region are manipulated by pDEP and hydrodynamic forces [53]

The cells are guided to the stellate-tips, string into pearl-chain patterns and are snared from individual local strings to a net, and finally form the radial pearl-chain patterns [53].

2.5.4. DNA concentrator

Normal DNA concentration includes several steps of purification and isolation. The series of steps can be avoided using a DNA concentrator shown in Figure 2.17. AC electroosmosis and AC-DEP using gold electrodes are the underlying concept to a DNA concentrator [63]. DNA molecules in solution carry a negative charge and migrate toward the positive pole when placed in an electric field.

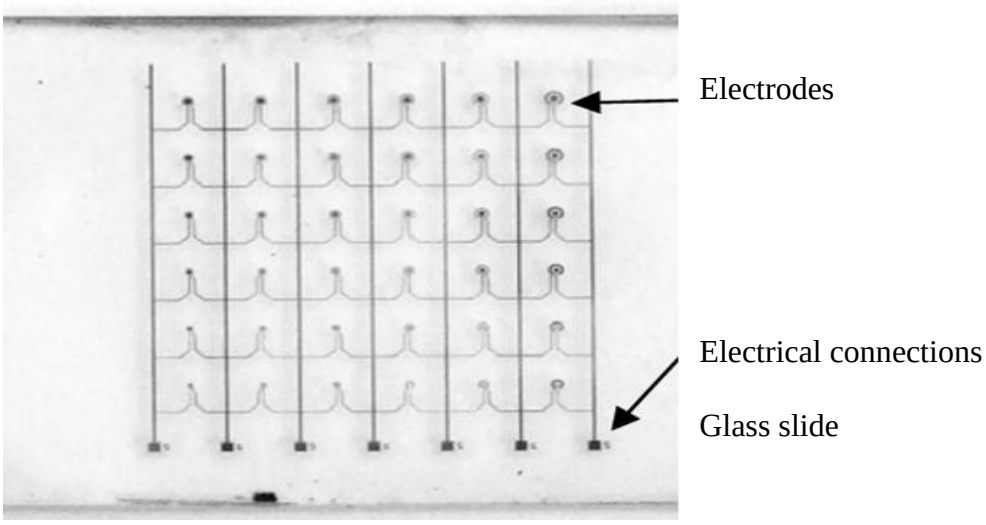

Figure 2.17: DNA concentrator used for purification, stretching and uncoiling of DNA. It allows the instant collection of DNA on the electrode surface [64]

In addition to the net charge, the electric field induces a dipole in the molecules which renders the molecules sensitive to field gradients [65]. For this process the DNA is fluorescently labeled and injected into the microfluidic chamber. When an AC potential is applied, the DNA is manipulated by n-DEP and hydrodynamic force. The randomly distributed DNA is repelled to focus in between the electrode and caused to bounce over the sensing elements.

However, at high frequency the DEP force dominates and the DNA will be attracted to the entire surface of the electrode. At intermediate frequencies, the drag force draws the DNA to the center of the electrode and prevents it from moving after that. Thus, the DNA concentrator has to be operated at this optimum frequency to stretch and uncoil DNA for its separation (e.g., for action of restriction enzymes) [66]. The DNA in the polyacrylamide gel is placed in between the gold electrodes and when electric field is applied stretching of DNA begins. Dipole traps are used to hold DNA

molecules to wash out debris and other contaminants and to direct small amounts of sample to specific locations within a device (e.g., an area for hybridization).

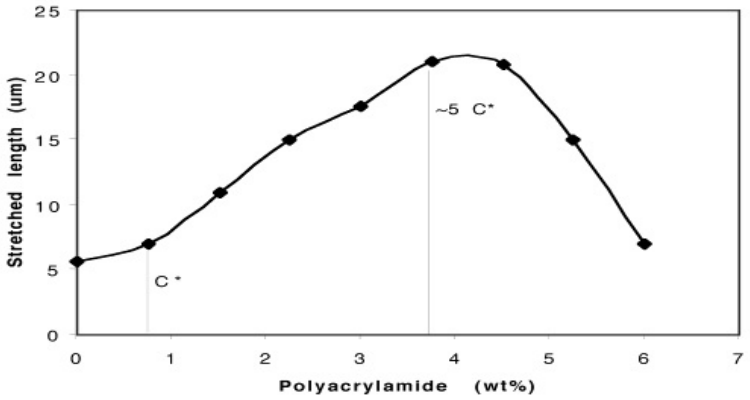

Figure 2.18: DNA stretching as a function of linear polyacrylamide concentration [67]

The stretching of DNA molecules is exhibited as a function of polyacrylamide concentration (see Figure 2.18) [67]. Initially there is an increase in length of DNA (DNA stretches or uncoils) as the concentration of polyacrylamide increases. When the polyacrylamide concentration reaches to about 3.8% the DNA begins to coil again.

2.5.5. Nano-colloid assay and pathogen detection

Miniaturization plays an important role in molecular detection and identification. The DEP nano-colloid assay proves to be a promising technique. Target molecule hybridization onto the probe functionalized nano-colloids changes their surface conductance and consequently their dielectrophoretic crossover frequencies. It has been shown that nano colloid assays can be employed for diagnostics, therapeutics, ecological monitoring and drug discovery [68].

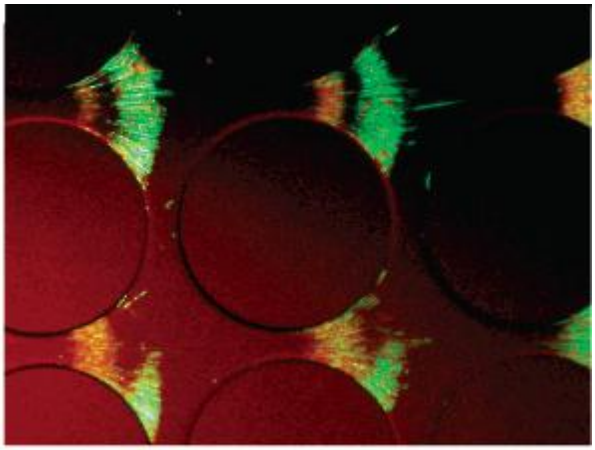

Figure 2.19: Differential trapping of live (green) and dead (red) cells shown by fluorescent tagging. Live cells exhibit more nDEP and are trapped in the wider region while dead cells exhibit lesser nDEP and are trapped in the narrower region [69]

In the case of water analysis, presence of even a single pathogenic bacterium per liter of water is a cause of concern. Such instances require high fluid throughput and the ability to concentrate particles. Because of the comparatively large concentration of dead and inert particles in water samples, selective concentration is desirable (see figure 2.19) [69]. The purification of contaminated water supplies is done by eliminating parasites such as Giardia and Cryptosporidium.

DEP can also be used to purify industrial suspensions. Industrial suspensions contain different organic and nonorganic compounds than resin, which can coagulate and concentrate in circulating water and thus worsen the quality of paper and the function of the paper making devices [70]. The dielectric properties of components of industrial suspensions can also be found using DEP methods.

2.5.6. Other applications

The dielectric properties of cells can be determined using DEP by fitting them to the respective spectra [6]. DEP can be used for the electrofusion of cells which is made use of in the production monoclonal antibodies production and the cloning of mammalian cells [71].

Although DEP is widely applied in many different areas recently, most efforts are now being directed towards biomedical applications [72]. It opens up potentially important applications of DEP as a tool to address needs in stem cell research and therapy (e.g., use of DEP to identify and sort cells for cell based therapies). There has been work characterizing the electric field effect on cell clustering [73], pearl chain formation, the effect zwitterion buffers on cell levitation [74] and the use of digited or castellated electrode structures for viable and nonviable cell separation by DEP [75].

2.6. Related techniques

2.6.1. Electro-rotation and twDEP

Electro-rotation and travelling wave dielectrophoresis (twDEP) are derivatives of DEP. Electro-rotation is the circular movement of an electrically polarized particle due to a phase lag between an applied rotating electric field and the respective relaxation processes. Travelling-wave DEP is achieved using DEP electrode array with quadrature sinusoids covering one phasor rotation. (e.g., twDEP induced micropumping)

2.6.2 Field Flow Fractionation

Field-flow fractionation (FFF) was invented by Calvin Giddings and is a widely used separation technique based on laminar fluid flow. In FFF, an electric field perpendicular to the flow of suspension is applied. The particles get separated based on their mobilities (depends on the size, mass and charge of the particle) [76].

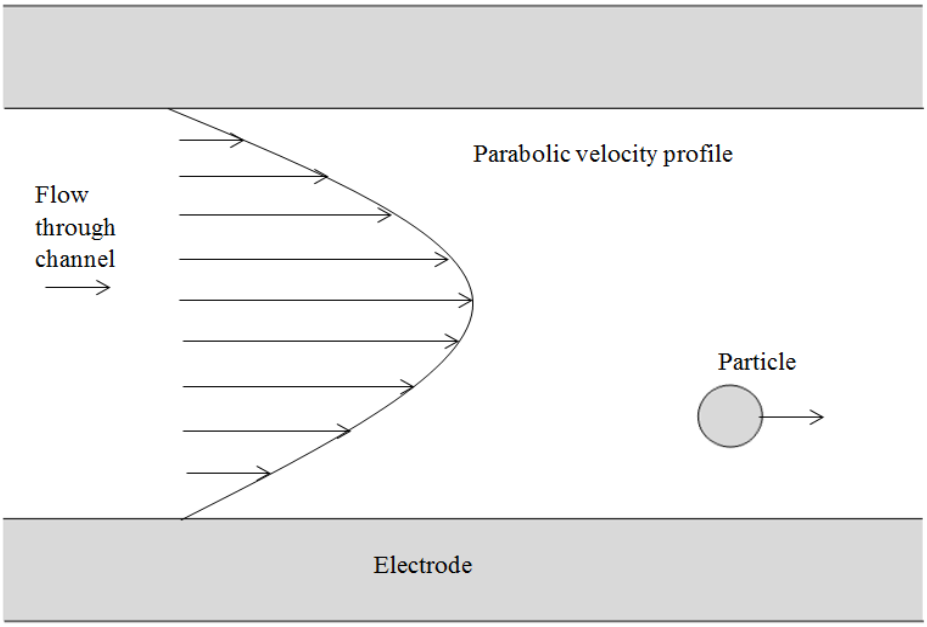

Figure 2.20: Illustration of the combination of DEP and FFF. Particles are levitated by DEP and positioned on different planes in the velocity profile

FFF is generally combined with DEP for effective separation of particles and is one of the most important flow-assisted separation methods [77]. A combination of DEP and FFF is demonstrated in Figure 2.20. In DEP-FFF a non-uniform electric field is applied perpendicular to the fluid flowing through a long and narrow channel. DEP force is used to levitate particles in to different planes in the parabolic velocity profile of liquid flowing through the chamber. As the particles are levitated to different planes on the

velocity profile, they attain different velocities and elution times [78]. Although, it is used for a wide range of sizes at a very good resolution in case of colloidal mixtures effort has to be taken to make sure the results are not skewed by the concentration of particles [79]. It can be employed on different particles including polystyrene beads, viruses and proteins etc.

2.7. COMSOL Multiphysics

COMSOL Multiphysics (previously called FEMLAB) is Finite Element Analysis (FEA) solver and simulation software which contains packages for various applications. COMSOL Multiphysics is compatible with MATLAB and its toolboxes help compile different physics to simulate a real world system. It can be applied for numerous physical and engineering applications where a large variety of programming, preprocessing and postprocessing have to be done. The packages are cross-platform and in addition to conventional physics-based user interfaces, COMSOL Multiphysics also allows for entering coupled systems of Partial Differential Equations (PDEs). The PDEs can be entered directly or using the weak forms. In this project COMSOL was used to understand the underlying concepts of AC-DEP.

CHAPTER III

COMMON PROBLEMS

3.1. Particle size

Particle size is an important factor affecting DEP because the force acting on the particle is proportional to particle's volumetric size ($4\pi r^3/3$) (see equation 2.1). Thus, the DEP force is proportional to r^3, where r is the radius of the particle. However, it has to be noted that the radius also affects the conductivity of the particle, which is determined by its radius, bulk conductivity and surface conductivity. It was found that the effect of radius on conductivity has been ignored in some research works. It has been assumed in these works that the radius will affect the DEP solely by being proportional to the cube of the particle radius [80]. The consequences of ignoring the radius effect have been discussed in Chapter V.

3.2. Shell model of particles

In DEP and related AC electrokinetical phenomena like electrorotation and twDEP dielectric properties are usually assumed to be homogeneous. However, this assumption is not valid in the case of biological particles with which shell models are often used to define the non-uniform dielectric properties of the particles.

In some micro-organisms (e.g. gram positive bacteria) and other cells, the cell wall contains high concentrations of charged species and counter-ions which can form a conductive screen and effectively dominate the dielectric properties. Even if there is less charge, electrorotation measurements have shown that the cell wall plays a significant

role in affecting the electrokinetic properties of the cell in low-conductivity media [81]**.** Large sized vacuoles found in yeasts and other cells in cell require the use of a vesicle inclusion model [82]. Thus considering the cell to be homogeneous can produce skewed results when trying to validate the experimental results with the theoretical results.

3.3. Influence of electric double layer

Problems can arise when calculating the cross-over frequency if the conductivity of the particle is much lower than that of the medium. In this case according to the equation for crossover frequency given below, a value for the crossover frequency should not exist, but this is not the case in reality [83].

$$f_{cross} = \frac{1}{2\pi}\sqrt{\frac{(\sigma_p - \sigma_m)(\sigma_p + 2\sigma_m)}{(\varepsilon_p - \varepsilon_m)(\varepsilon_p + 2\varepsilon_m)}}$$

For example for particles like latex and silica, the conductivity is even lesser than deionized water itself but they still exhibit crossover DEP. This is found to be due to the presence of a stern layer and a small diffuse layer leading to a double layer around the object [84]. Double layer appears on the surface of an object like a solid particle, gas bubble, liquid droplet or a porous body, when it is exposed to a fluid. At lower frequencies the polarizability of the particles increases due to the presence of the ionic double layer resulting in an increase in the DEP force on the particle. It is important to consider this double layer when working with DEP force as they affect the conductivity of the particle.

3.4. Other Forces

For a particle placed in a non-uniform electric field there will be other forces apart from the DEP force acting on them. The net force determining the movement of the particle can be calculated only when all the forces are calculated and their directions determined. The possible forces that have to be considered include gravitational force, buoyancy force, drag force and in some cases electrothermal forces [12]. The importance of including these forces is demonstrated in Chapter V.

3.5 Other problems

Particles exhibit pDEP when they are more polarizable than the suspension medium. Thus, DEP requires a low conductivity medium to effectively manipulate the particles. However, cells require culture media having high conductivity due to their different components. Cells cannot survive when introduced into the low conductivity solution. In some cases (e.g., tissue engineering) which require further growth of cells after patterning, suspending cells in low conductivity solution has its drawbacks [53]. The electrodes can be manipulated accordingly to accommodate high conductivity media. The interaction between particles also affects the particle movement. This has not been considered in most experiments. The numerical calculation of particle interactions is complicated especially when particles have high conductivity or are much closer to each other [85]. The same charges repel each other and different charges attract each other.

One other issue is the interaction of particles with the electrode. Some experiments use a cover layer to protect the particles from direct exposure to the electrodes. The thickness of this cover region is crucial as it determines the magnitude of the DEP force. Electric potential is one important factor that affects the DEP force. It is necessary to optimize the potential applied to the electrodes. Higher potentials might lead to bubbling (e.g. oxygen molecules) of the solution and disrupt the particle aligning.

CHAPTER IV

COMPUTATIONAL MODELING FOR DEP FORCE

Analysis and illustrations using COMSOL modeling is performed to illustrate the consequences of the common problems identified in Chapter III. Different 2D and 3D models are developed to study the factors affecting the DEP force through parametric studies.

The modeling part includes defining the parameters and variables, defining the geometry, applying and configuring the necessary physics, finding the results and plotting the graphs. Analysis of all the parameters is done using mesh plots, point graphs, surface plots and arrow diagrams. Further analysis is done using MS Excel and SigmaPlots to study the relationships between each of the factors and how these relationships affect the DEP force.

4.1. Parameters and Variables

Both global and geometry specific variables were used in this model. Different parameter and variables used in this model are listed in tables 4.1 and 4.2.

Parameters		
Name	**Expression**	**Description**
lm	we + wg	Length of model
we	100[um]	Width of electrode
ratio	1	Ratio of we to wg
wg	ratio*we	Width of gap
pot	15.9[V]	Electric Potential
f	100[kHz]	Frequency
tm	we+wg	Thickness of water region
tc	1[um]	Thickness of cover region

Table 4.1: Parameters for the model. They can be swept to different values and varied easily.

Variables 1		
Name	**Expression**	**Description**
ε_m	78.5	Dielectric constant of medium
ε_p	2.6	Dielectric constant of particle
σ_m	1E-4[S/m]	Conductivity of medium
r	5[um]	Radius of particle
σ_p	4.8E-4[S/m]	Conductivity of PS beads

Table 4.2: Variables for the model whose geometric entity level is the entire model.

4.2. Geometry

The model to determine the DEP force includes positive and negative electrodes with insulation in between them. After the validity of the model, parameters and equations used are checked, other electrode models are made and similar simulation is carried out. Cover layer and water region are made according to the specified dimensions.

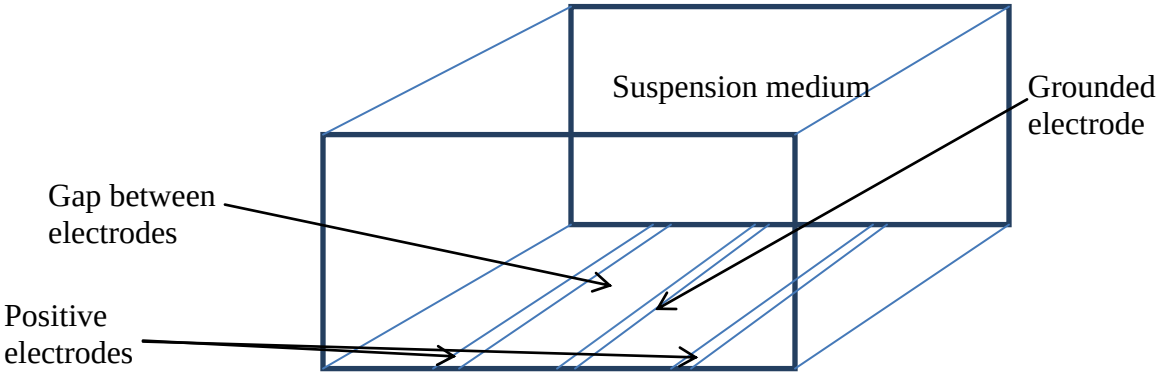

Figure 4.1: Proposed 3D model of the electrode setup used in determing the factors

Figure 4.1 shows the electrode setup in a 3D model. Similar electrode setup is made using COMSOL (Figure 4.2). In Figure 4.2 the gap between the electrodes is given as a ratio. The electrode width is fixed and with the change in ratio the gap between the electrodes could be varied. Gap between the electrodes is ratio times the electrode width. The other parameters used in making the model are defined under parameters and variables in Table 4.1 and Table 4.2. The shape and dimension of the electrodes are an important factor that determine the positioning and separation of particles using DEP.

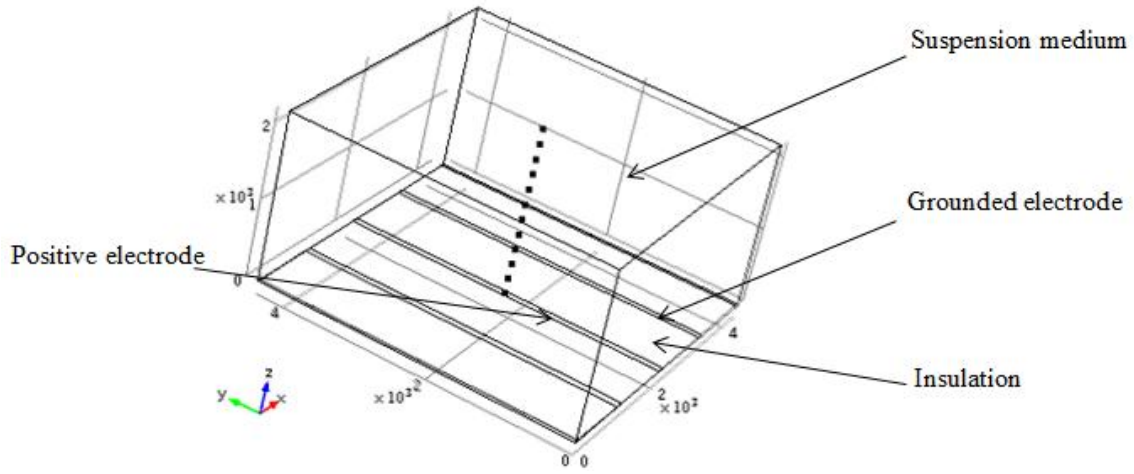

Figure 4.2: Model of the electrode setup used in determing the factors. 3D model with length, breadth and width of electrode included.

COMSOL allows the user to add and couple different physics to under the mechanism behind any process. For our study the electrostatics physics was used to study DEP.

4.3. Materials

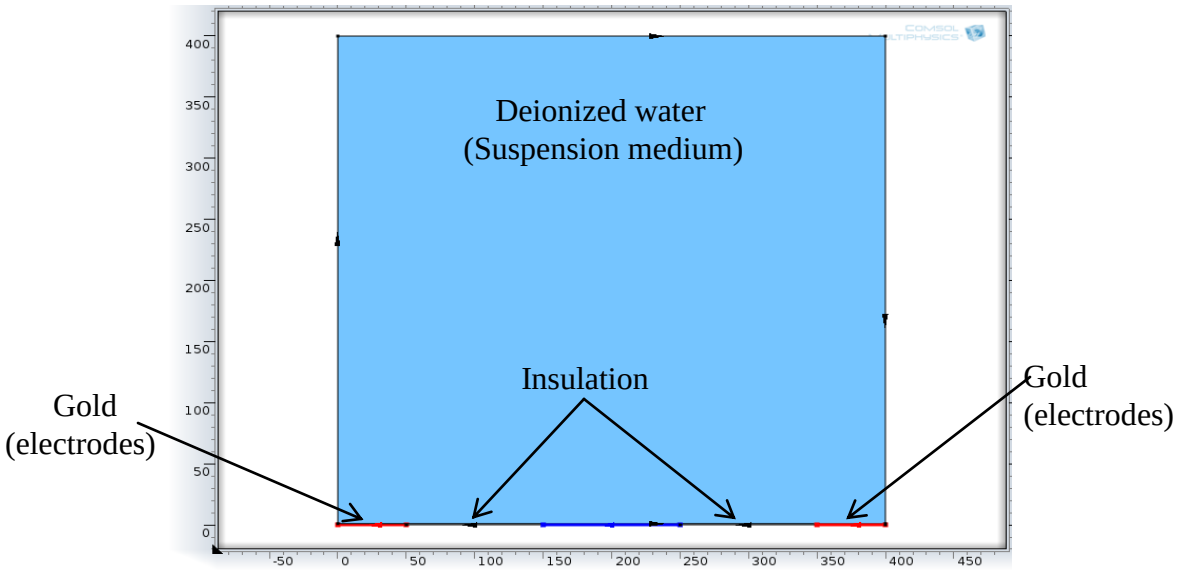

Figure 4.3: Different materials used in making the electrode setup

The materials used for the different components of the electrodes are crucial as they determine the DEP force. The electrodes are made of gold/platinum and cover layer is placed on top to protect the electrodes [86]. The cover layer is generally an oxide coating made to shield direct exposure of a cell to the energized electrode end reducing exposure to undesirable AC field exposure effects [87, 88]. Deionized water is the medium used to suspend the particles in this model.

4.4. Electrostatics

A positive potential is given to the positive electrodes and the other electrodes are grounded. The input potential is given as a parameter so that different values can be substituted if required.

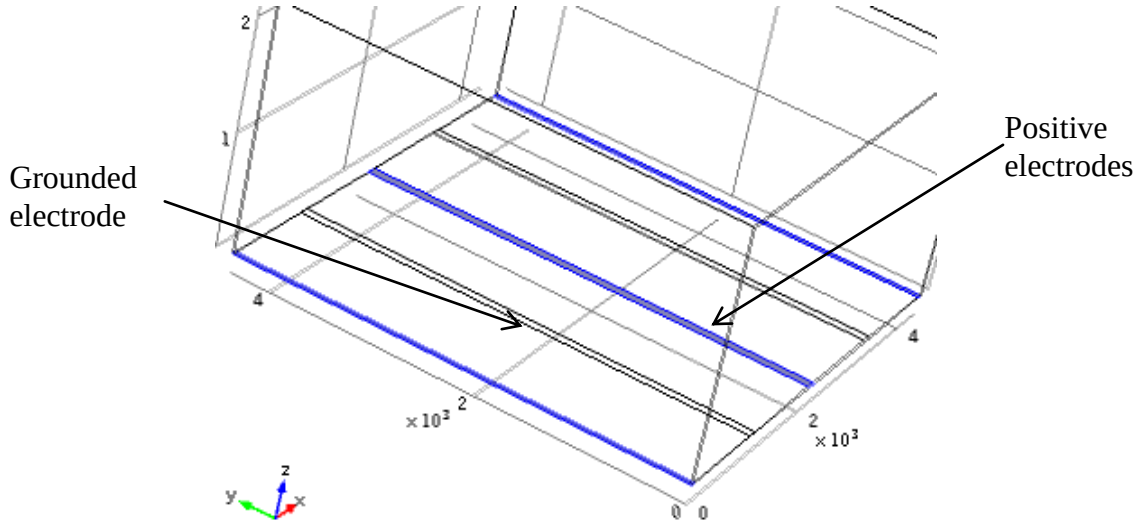

Figure 4.4: Electrodes with positive potential alternating with ground electrodes

The electric field is the negative gradient of the electric potential. Thus, the electrostatics physics is bound by the following equations.

$$D = \varepsilon_o E + p$$

where, D is the electric displacement, E is the external electric field and p is the polarisation. When this is expressed we can use Gauss law. Because of polarisation Gauss law is given as the following:

$$\nabla . D = \rho_v$$

where ρ_v is the free volume charge density. Also, we know that the electric field is the negative gradient of the electric potential.

$$E = -\nabla V$$

For some analysis (e.g., twDEP models) time dependent inputs are given. In these cases the voltage is defined as a sine wave with the adjacent electrodes having a phase lag. This helps analyze the change of forces with time.

4.5. Mesh

The mesh in COMSOL model contains a network of elements of different sizes to discretize the physical domain. Over the elements, often in tetrahedron or triangle shapes, a set of polynomial functions are used to approximate the structural displacement field. The domain for the electrode is assigned a finer mesh than the remaining region due to the expected higher electrical field gradients nearby.

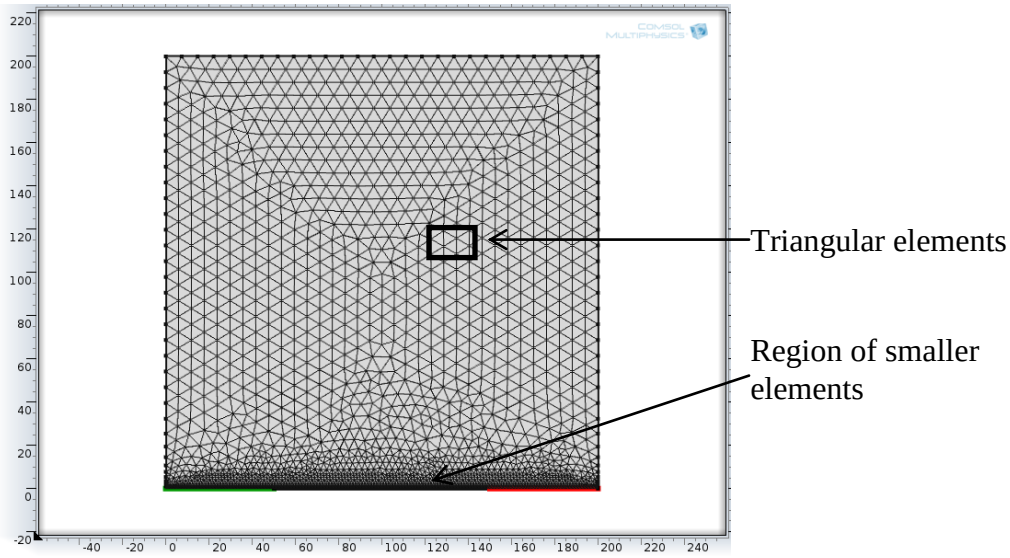

Figure 4.5: Geometry (2D model) meshed finely

4.6. Study

Parametric sweeps are done to analyze the different factors affecting the forces acting on the particles. Four different parametric sweeps are done. The first one is for electric potential varying from 1V to 40V. The second is for the ratio (between the width of gap and width of electrode) to change the gap between the electrodes. The ratio value is swept from 0.1 to 10 with a step of 0.1.

The third parameter is the frequency which is swept for a wide range of values. The equation for force is then plotted and the magnitude of force was verified, in turn verifying the creditability of the model. Finally the radius is swept for different values and also analysis on the effect of radius on conductivity is studied. Parametric sweep showed the trend of change of force with these parameters.

In some cases it is necessary to use two sweeps in the same study. Both frequency and radius affect the CM factor which in turn affects the DEP force directly. The sign of

the CM factor determines if the particle is going to move towards the electrode or away from the electrode. The results from COMSOL are obtained from 3D, 2D and 1D plot groups in case of 3D models and 2D and 1D plot group in the case of 2D models. Particle tracing is done to determine where the particles will end up when a particular factor in the model is changed. Results of these models helped illustrate the consequences of the problems in the literature.

CHAPTER V

REASONS FOR THE PROBLEMS AND THEIR CONSEQUENCES

5.1 CM factor derivation

In Section 2.1.2 the importance of CM factor for determining the direction of the DEP force was discussed. Wang *et* al. studied the polarizability of cells in sugar containing media and the effect of the polarization on the CM factor. The CM factor not only modifies the strength and imposes a direction on the DEP force it also translates the difference in polarization between the particle and the medium [86]. The equation for calculating the Re(f_{cm}) varies with the geometry of the particle. Hence it has to be derived for each shape of the particle. The analytical derivation of the Re(f_{cm}) for a spherical particle is done for this research. Substituting equation 2.3 in equation 2.2 we get the following equation.

$$f_{cm}(\omega) = \frac{(\varepsilon_p - i(\sigma_p/\omega) - \varepsilon_m + i(\sigma_m/\omega))}{(\varepsilon_p - i(\sigma_p/\omega) + 2*\varepsilon_m - 2i(\sigma_m/\omega))}$$

$$= \frac{\omega(\varepsilon_p - \varepsilon_m) - i(\sigma_p - \sigma_m)}{\omega(\varepsilon_p + 2*\varepsilon_m) - i(\sigma_p + 2\sigma_m)}$$

Multiplying by its conjugate we get,

$$f_{cm} = \frac{\omega^2(\varepsilon_p - \varepsilon_m)(\varepsilon_p + 2\varepsilon_m) + (\sigma_p - \sigma_m)(\sigma_p + 2\sigma_m) - \omega i((\sigma_p - \sigma_m)(\varepsilon_p + 2\varepsilon_m) - (\sigma_p + 2\sigma_m)(\varepsilon_p - \varepsilon_m))}{\omega^2(\varepsilon_p + 2\varepsilon_m)^2 + (\sigma_p + 2\sigma_m)^2}$$

Thus, the real part is

$$\mathrm{Re}(f_{cm}) = \frac{(2*pi*f)^2(\varepsilon_p - \varepsilon_m)(\varepsilon_p + \varepsilon_m) + (\sigma_p - \sigma_m)(\sigma_p + 2\sigma_m)}{(2*pi*f)^2(\varepsilon_p + 2\varepsilon_m)^2 + (\sigma_p + 2\sigma_m)^2} \quad (5.1)$$

and the imaginary part is

$$\mathrm{Im}(f_{cm}) = \frac{-(2*pi*f)((\sigma_p-\sigma_m)(\varepsilon_p+2*\varepsilon_m)-(\sigma_p+2\sigma_m)(\varepsilon_p-\varepsilon_m))}{(2*pi*f)^2\,(\varepsilon_p+2*\varepsilon_m)^2+(\sigma_p+2\sigma_m)^2} \quad (5.2)$$

The real part is used to calculate the DEP force. It determines the direction of particle movement and the crossover frequency.

5.2. Effect of radius on conductivity

Radius affects the DEP force directly as well as indirectly through the particle conductivity. O'Konski *et al.* derived the relationship between the radius and the conductivity of the particle which is explained below [22]. Further evidence is drawn from the work of Arnold *et al.*, [8]**.**

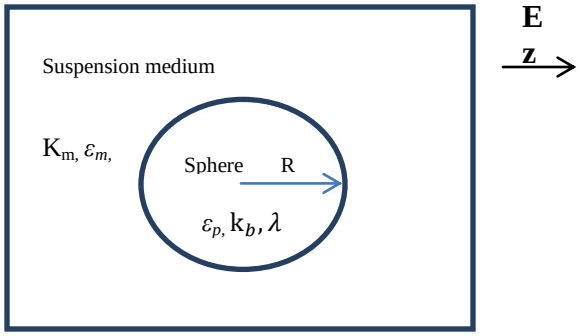

Figure 5.1: Sphere of radius R suspended in a homogenous medium under the influence of an external electric field E

There are few assumptions that have to be made and the expression is derived thereafter.

Assumptions:

1. Joule heating and electrochemical effects are assumed negligible. This is because the electric field is low and frequency is high.
2. Both surrounding medium and system are considered to have uniform bulk conductivities and dielectric constants. Hence no space charge within the system.

At a large distance (r) from the sphere, the electric potential is given by the following equation

$$V = -\int_0^r E.dl \qquad r>>R$$

$$V = -E\, r \cos\theta \qquad (5.1)$$

Where V is the total potential arising from applied electric field. Since there is no space charge within either of the region, the Laplace equation can be used.

$$\nabla^2 V_p = \nabla^2 V_m = 0$$

Where V_p is the potential in the sphere and V_m is the potential outside the sphere (suspension medium). At the surface of the sphere boundary conditions are given by,

1. $V_p = V_m$ at $r = R$ (input potential = output potential at the surface)
2. By Gauss law at any instant,

$$\varepsilon_p \frac{\partial V_p}{\partial r} = \varepsilon_m \frac{\partial V_m}{\partial r} = 4\pi\sigma \quad \text{at } r = R \qquad (5.2)$$

where, ε_p is the real part of complex dielectric constant of the sphere and σ is the density of free charge at the surface.

The periodic electric field is given by

$$E = E_o e^{i\omega t} \qquad (5.3)$$

where, E_o is the space mean value of the peak field intensity in the suspension and ω is the angular frequency.

To solve the equation for the periodic field shown above the differential equation for surface charge density has to be derived. The surface charge density undergoes a time variation two processes.

a) Transport of ions to and from an element of surface due to bulk conductivities of the two media. It is given by σ_a. For an isotropic medium the differential equation is given by

$$\frac{\mathrm{d}\sigma_\mathrm{a}}{\mathrm{dt}} = \mathrm{k_m}\ \frac{\partial \mathrm{V_m}}{\partial \mathrm{r}} - \mathrm{k}_b \frac{\partial \mathrm{V_p}}{\partial \mathrm{r}} \tag{5.4}$$

Where, k is the bulk conductivity of the particle and k_m is the conductivity of the medium.

b) The transport of ions along the surface as a result of the surface conductivity. It is given by σ_b. Continuity equation for process b for an axially symmetric spherical surface is

$$\frac{\mathrm{d}\sigma_\mathrm{b}}{\mathrm{dt}} = \frac{\lambda}{R^2 \sin\theta}\ \frac{\partial}{\partial \theta}\left(\sin\theta \frac{\partial \mathrm{V_p}}{\partial \theta}\right) \tag{5.5}$$

Where, λ is the surface conductivity of the sphere.

Considering $\lambda, k_b\ and\ k_m$ as constants we can sum up (5.5) and (5.6) we have

$$\frac{\mathrm{d}\sigma}{\mathrm{dt}} = \frac{\mathrm{d}\sigma_\mathrm{a}}{\mathrm{dt}} + \frac{\mathrm{d}\sigma_b}{\mathrm{dt}}$$

Thus,

$$\frac{\mathrm{d}\sigma}{\mathrm{dt}} = \frac{\lambda}{R^2 \sin\theta}\ \frac{\partial}{\partial \theta}\left(\sin\theta \frac{\partial \mathrm{V_p}}{\partial \theta}\right) + \mathrm{k_m}\ \frac{\partial \mathrm{V_m}}{\partial \mathrm{r}} - \mathrm{k}_b\ \frac{\partial \mathrm{V_p}}{\partial \mathrm{r}} \tag{5.6}$$

Equation (5.6) has to be solved to get the equation for σ.

Substituting equation (5.1) and (5.2) we get

$$\frac{d\sigma}{dt} = \frac{\lambda}{R^2 \sin\theta} \frac{\partial}{\partial\theta}\left(\sin\theta \frac{\partial(-ER\cos\theta)}{\partial\theta}\right) + k_m \frac{4\pi\sigma}{\varepsilon_m} - k_b \frac{4\pi\sigma}{\varepsilon_p}$$

Solving the partial derivative gives the following

$$\frac{d\sigma}{dt} = \frac{\lambda}{R^2 \sin\theta} \frac{\partial}{\partial\theta}(ER \sin^2\theta) + 4\pi\sigma \left(\frac{k_m}{\varepsilon_m} - \frac{k_b}{\varepsilon_p}\right)$$

$$\frac{d\sigma}{dt} = \frac{\lambda}{R^2 \sin\theta} (2ER \sin\theta \cos\theta) + 4\pi\sigma \left(\frac{k_m}{\varepsilon_m} - \frac{k_b}{\varepsilon_p}\right)$$

$$\frac{d\sigma}{dt} = \frac{2\lambda}{R} (E\cos\theta) + 4\pi\sigma \left(\frac{k_m}{\varepsilon_m} - \frac{k_b}{\varepsilon_p}\right)$$

$$d\sigma - \left[\frac{\lambda}{R^2 \sin\theta} (2ER \sin\theta \cos\theta) + 4\pi\sigma \left(\frac{k_m}{\varepsilon_m} - \frac{k_b}{\varepsilon_p}\right)\right] dt = 0$$

Solving using software gives the value of σ to be the following

$$\sigma = 3iE\cos\theta \frac{(\varepsilon_p k_m - \varepsilon_m (k_b + \frac{2\lambda}{r}))}{\omega\left(\varepsilon_p^* + 2 * \varepsilon m^* - 8 * \pi * i * \frac{\lambda}{\omega r}\right)} \quad (5.6)$$

where, r is the radius of the particle, ε_p is the dielectric constant of the particle and ε_m is the dielectric constant of the medium. In equation 5.6 we can see the conductivity and permittivity term that resembles the term $\varepsilon_p k_m - \varepsilon_m k_p$. Thus we infer that

$$k_p = k_b + \frac{2\lambda}{R} \quad (5.7)$$

where, k_p is the effective particle conductivity, k_b is the bulk conductivity, λ is the surface conductivity and R is the radius of the particle [89]. The effective particle conductivity is equal to the increase of the bulk conductivity by the term $\frac{2\lambda}{R}$.

The conductivity of a cell's interior can be as high as 10^3μS/mm, since cells contain many ions and charged particulates. In contrast, the conductivity of cell membranes tends to be 10^{-4}μS/mm. Thus σ_b and λ, both play an important role. However,

in the case of the very good insulator (e.g., polystyrene beads) it is safe to assume that σ_b can be neglected as the field does not penetrate as deep into the synthetic particles.

The effect of radius on the dielectric properties of the particle has been largely ignored. For example in Kralji *et al.* a series of polystyrene bead sized 4.13 ± 0.35, 5.09 ± 0.44, 5.63± 0.69 and 6.02 ±0.37 μm were used [90]. In the theoretical explanation of the experiment they have considered that the radius affects DEP force only in the form of equation 2.1. It is mentioned in the paper that all the particles (considering all of them are made of the same material-polystyrene) will have uniform dielectric properties. But this is not true, as the radius (size of the particle) affects the conductivity and hence the CM factor. Thus the assumption made in Page 5021 of the publication that all polystyrene beads exhibit nDEP under specified conditions is not valid [90]. Different sized particles could still exhibit different DEP behavior and could lead to erroneous results of their experiments. This is evident from Figure 5.2.

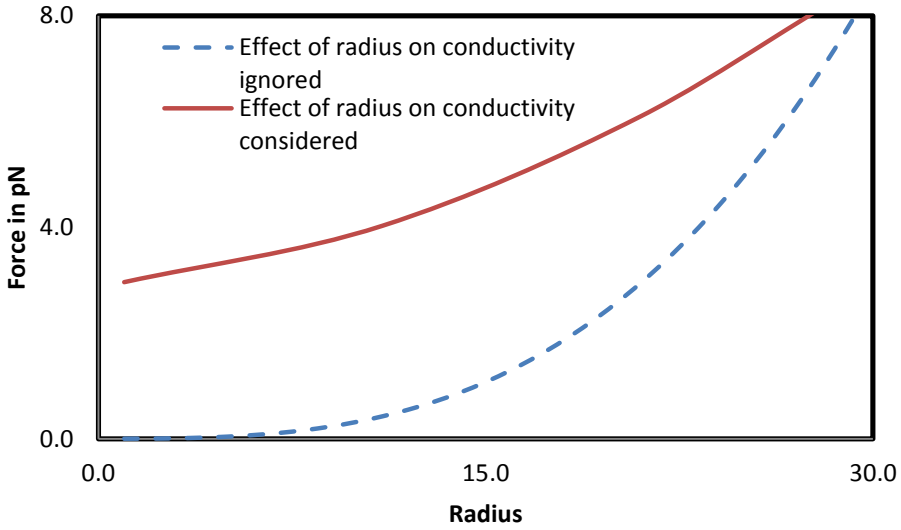

Figure 5.2: Difference in DEP force between when effect of radius on conductivity is considered and when it is neglected. (Data collected from COMSOL model)

In Figure 5.2 the DEP force is plotted against the radius of the particle. Two different cases are analyzed. The first one is when the effect of radius on conductivity is considered and the second one is when this effect is ignored. We can see that when it is assumed that the DEP force is proportional only to the r^3 term a cubic curve is obtained. However when the radius effect on the conductivity is also considered the DEP force curve is not cubic. Clearly ignoring the effects of radius on conductivity has significant effect on the final DEP force. It is important to consider the radius-conductivity concept when working with beads of different size because particles of different sizes will experience different DEP forces. This mechanism is utilized in the DEP filters (H shaped channels) to perform the separation of particles by size, which has a potential in separating cells of different sizes for biomedical applications [92].

Similar assumption is found in Cetin *et al.*, [91] where the authors attempted continuous particle separation based on size using AC-DEP. They considered different sized beads and assumed that the radius affected only the volume and not the conductivity. They demonstrated successful separations of 10 and 5 μm diameter latex particle mixture and mixture of yeast cells and WBCs using a device operated at low electrical potential. However, the DEP force acting on the particle is different from their theoretical calculation. They had to use scaling factors to make up the difference. One of the reasons for incorrect theoretical value might be due to ignoring the radius effect of the dielectric properties.

5.3 Effect of shell model

The shell model is used to consider the contribution of the dielectric properties of various layer structures surrounding a cell. The non-homogeneous nature of cells and other bioparticles (shown in Figure 5.3) cannot be neglected.

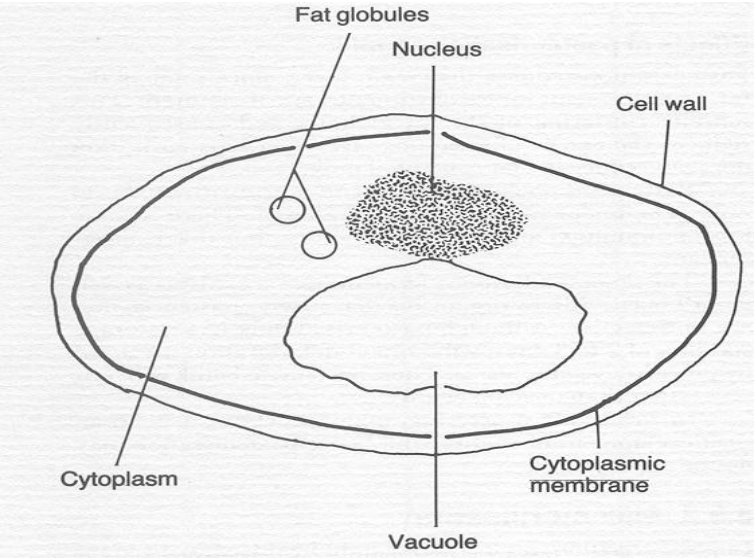

Figure 5.3: Structure of yeast cell having different organelles with different dielectric properties [93]

Figure 5.3 shows the structure of the yeast cell. Its components include vacuole, vacuole membrane, cytoplasm, plasma membrane and cell wall [93]. It is important to consider the large vacuole that plays an important role in determining the conductivity and permittivity of a yeast cell [110]. Most of the works dealing with yeasts cells have ignored the large vacuole and nucleus present while determining the dielectric properties. Kadaksham *et al.* studied the clustering of yeast cells under DEP. They examined the DEP force and mutual DEP force due to neighboring particles [73]. However, they did not consider the fact that the cell is highly non-homogeneous due to the different

components. A vesicle inclusion model has to be adopted for a yeast cell. Karan *et al.* did quasi-elastic light scattering studies on yeast cells undergoing DEP [81]. The dielectric properties of the cells were studied and the non-homogeneity of the cell was ignored.

In a review by Gossett *et al.* label-free cell separation and sorting of cells is discussed and the shell model of cells is not considered [33]. Only the theoretical part of the concept is discussed. By substituting ε_p^* for the shell model in the CM factor equation to get the new CM factor using symbolic complex numbers in Matlab and entering those numbers in COMSOL, we can take advantage of computational simulation approach to examine the shell model.

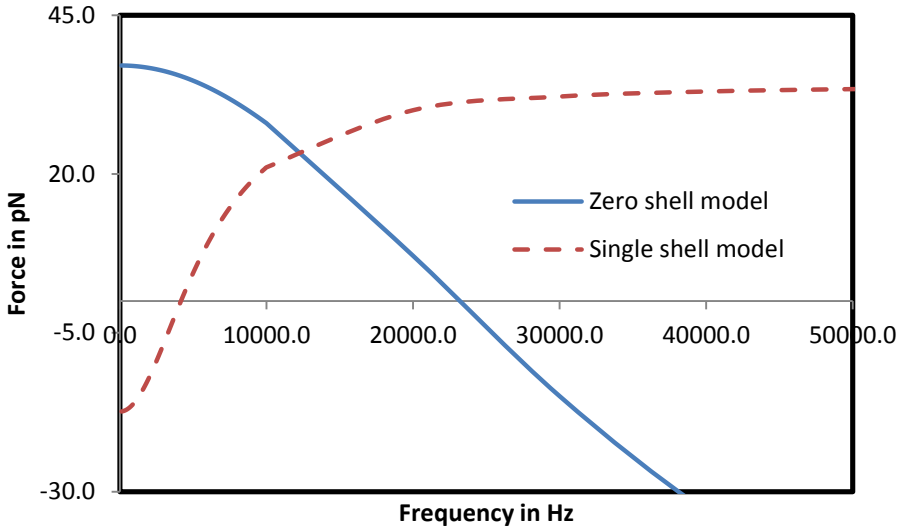

Figure 5.4: Change of force with frequency in the shell model considering non-homogeneous dielectric properties and change of force with frequency when the shell model is not used.

In Figure 5.4 shell model was applied to E.*coli* cells and the DEP force is plotted against frequency. It shows the change of force when the shell model of cells has been ignored. It gives a cross-over frequency of about 23 kHz. If the shell model of the cells

has been considered then there is a shift in the cross-over frequency to 4.2 kHz. It can also be noted from the graph that the direction in which the particles travel might be different. When the shell model is ignored at low frequencies the particles exhibit pDEP and then cross-over occurs. It is the other way around in the case where shell model is considered. The result is justified using experimental results from a publication by Pethig *et al*. according to which the cells exhibit nDEP at lower frequency and pDEP at higher frequency.

5.4 Effect of electric double layer on cross-over frequency

As discussed earlier the crossover between positive and negative DEP response is dependent on the properties of the particle and the suspension medium. The crossover frequency is calculated from equation (5.8) and the COMSOL model in this chapter [94].

$$f_{cross} = \frac{1}{2\pi}\sqrt{\frac{(\sigma_p-\sigma_m)(\sigma_p+2\sigma_m)}{(\varepsilon_p-\varepsilon_m)(\varepsilon_p+2\varepsilon_m)}} \tag{5.8}$$

For polystyrene beads suspended in deionized water the parameters are substituted and the cross over frequency is calculated to be 83 kHz.

$$f_{cross} = \frac{1}{2\pi}\sqrt{\frac{-2.584E-7}{-9.499E-19}}$$

$$f_{cross} = \frac{1}{2\pi} * 521561 = 83kHz$$

It can be plotted graphically as shown in Figure 5.4 using COMSOL.

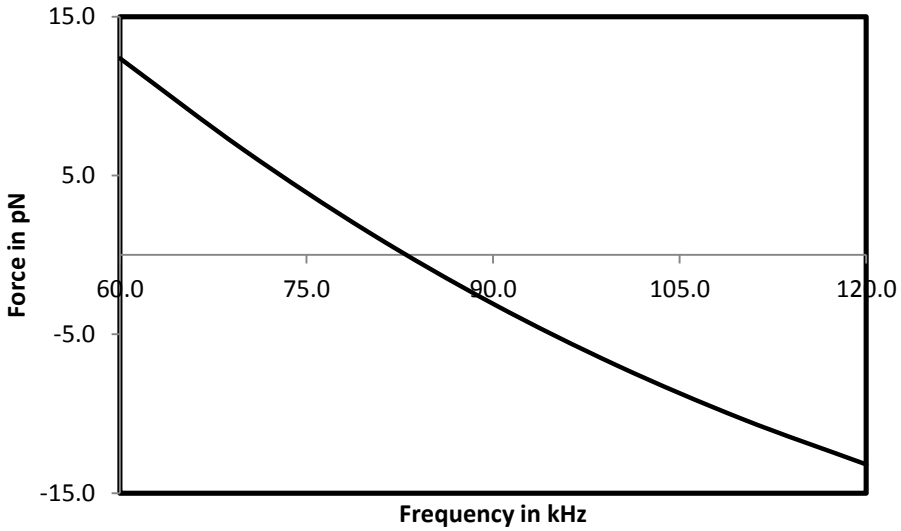

Figure 5.5: DEP force changing from positive to negative with increase in frequency. Data is obtained from COMSOL model.

In Figure 5.5, the frequency is plotted against the DEP force for polystyrene beads suspended in deionized water. Both the COMSOL model and CM factor calculation show that at a frequency of 83 kHz the DEP changes from positive to negative. However this cannot be held true in all cases. When the conductivity of particles are much lower than the suspension medium, equation (5.8) can be reduced as follows.

$$f_{cross} = \frac{1}{2\pi}\sqrt{\frac{(-\sigma_m)(\sigma_p+2\sigma_m)}{(\varepsilon_p-\varepsilon_m)(\varepsilon_p+2\varepsilon_m)}} \tag{5.9}$$

In equation (5.9) the crossover frequency is the square root of a negative number and hence cannot exist. On the contrary a crossover always takes place from pDEP to nDEP in experimental results in systems where the particle is more polarizable than the medium. This is contributed to the presence of an electric double layer, which is not considered in most of the work.

Stern suggested the combination of the Helmholtz and Gouy-Chapman models, giving an internal Stern layer (i.e. Helmholtz layer), and an outer diffuse layer (i.e. Gouy-Chapman layer) [84]. It is composed of two parallel layers of charge surrounding the object (see Figure 5.6). The Stern layer is the first layer with the surface charge and is made of ions that are absorbed directly onto the object due to chemical interactions. Stern layer is assumed to be a nanometer-thick of conducting ionic layer around the particle where the ions are strongly bound to the surface to allow tangential electric flux. The conducting Stern layer increases the nanocolloid conductivity to produce pDEP of latex and silica nanoparticles in low-conductivity buffer solutions [95].

The second layer (diffuse layer) is composed of ions attracted to the surface by the Coulomb force. The second layer electrically screens the first layer and is made of free ions which move in the fluid due to electric absorption and thermal effects and are not firmly anchored to the object. The combined Gouy-Chapman-Stern model is most commonly used for describing the electric double layer effect.

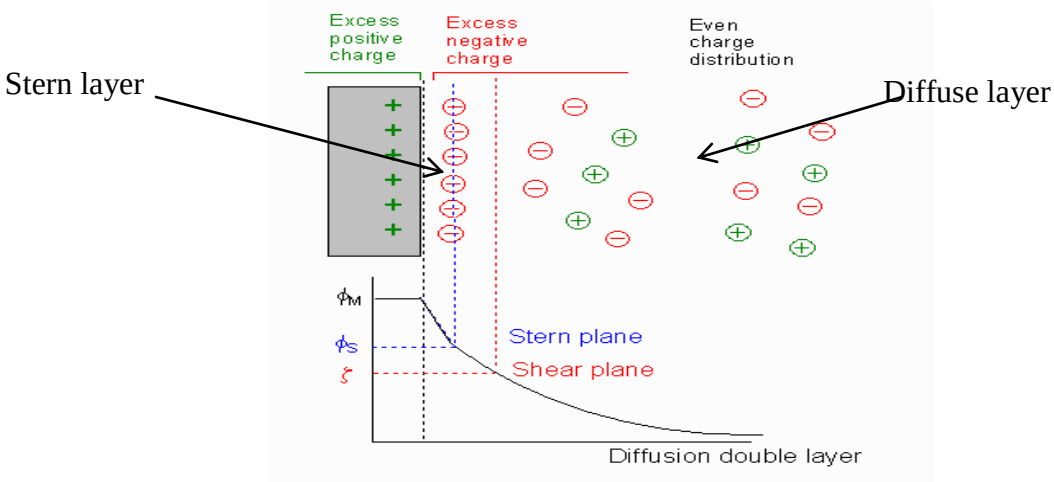

Figure 5.6: Double layer model with the internal Stern layer and the outer diffusion layer which affects the complex conductivity used in determining the Clausius Mossotti factor [96].

The double layer is used to describe the electro-osmotic component [97]. The AC electric fields produce a force in the induced charges in the electric diffuse layer of the electrodes. This gives rise to the electro-osmosis phenomena and hence necessities the discussion of Brownian movement. DEP forces produce a tangential electric field at the electrode–electrolyte double layer [98].

The conductivity calculation in the presence of a double layer involves a complex dependence on polar and azimuthal angles. However a simplified calculation can be carried out by system of spherical coordinates for our research. Analytical formula is derived for calculation of the empirical constant with the capacitance of the stern and diffuse layer to facilitate the calculation.

$$\sigma_p = \sigma_b + \frac{2(k_s + k_d)}{r}$$

where k_s and k_d are the conductivity of the diffuse layer and stern layer respectively.

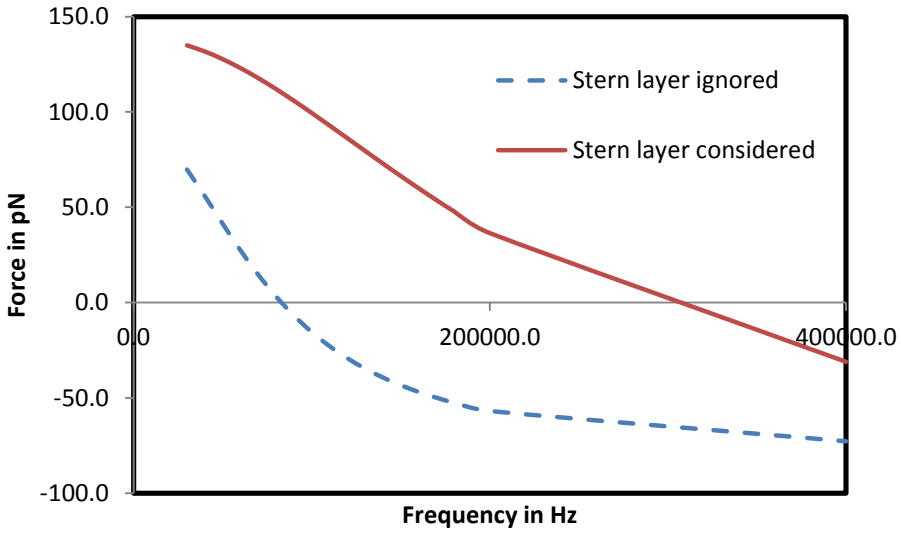

Figure 5.7: Shift in crossover frequency and magnitude of DEP force when the conductivity of the stern layer is included in the model

Figure 5.7 compares the DEP force when the stern layer conductivity is included and when it is ignored for latex beads suspended in deionized water. It is seen that there is a considerable shift in the frequency and there is a change in the magnitude of the force as well. Thus defined by Basuray *et al.* Stern layer increases the nanocolloid conductivity to produce pDEP [95]. However, mostly due to the lack of experimental evidences to examine the distinct contribution of Stern and diffuse layer conductions the understanding of the polarization due to double-layer remain unclear. This is because, most of the DEP experiments focusing on colloids on monodisperse systems have not been able to explain the mutual DEP response of an individual particle affected by the presence of polarized neighbor particles in polydisperse systems and in different aggregation states [99].

5.5 Net force acting on the particle

In section 3.4 the other forces that might act on the particle were discussed. The gravitational and buoyancy are the vertical forces that determines the levitation of a particle. Gravitational force is the force by which particles experience an attractive force which is directly proportional to its mass and inversely proportional to the square of the distance between them. Buoyancy force acts in the opposite direction to gravitational force (Figure 5.8). It is an upward force exerted by a fluid which opposes the gravity (weight) of an immersed object [12].

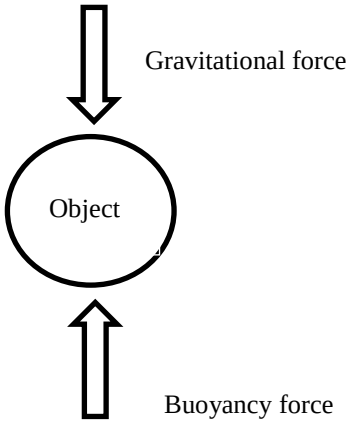

Figure 5.8: Directions of gravitational and buoyancy force

The net gravitational and buoyancy forces are given by the following formula:

$$F_{grav+bouy} = \frac{4}{3}\pi r^3 \left(\rho_w - \rho_p\right) g$$

$$= \text{-2.57E-13 N}$$

where, r (radius of the particle) is 5µm, ρ_w (density of suspending medium) is 1000 kg/m^3, ρ_p (density of particle) is 1050 kg/m^3 and g (acceleration due to gravity is 9.81 m/s^2

Drag force is the force that acts on a particle due to the fluid flow velocity. It is given by the following formula:

$$F_{drag} = 6\mu\eta r v$$

where, r is radius of the particle, v is the velocity of the particle and η is the viscosity of the suspension medium. In our experiment we have not considered the fluid flow as the particles and medium are already present over the electrodes. In that case the drag force can be neglected. Markyx *et al.* [89] studied the levitation of particles by DEP. For this only the gravitational settling was considered to be the balancing force for nDEP force.

Buoyancy force and the possible drag force have not been considered. This might lead to the development of incorrect prediction equation when combining DEP with FFF.

Cui *et al.* tried to understand the force equation for a time varying electric field [80]. The net force was calculated by balancing the particle with DEP force and drag force. The terminal velocity was calculated. However the effect of gravitational and buoyancy force were ignored.

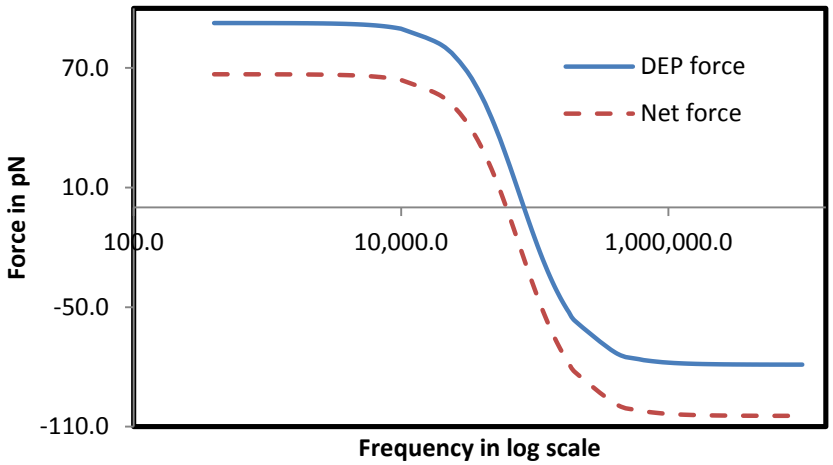

Figure 5.9: DEP force compared to the net force which includes gravitational and buoyancy force

The difference in movement of the particle when other forces are considered is plotted in Figure 5.9 for polystyrene beads suspended in deionized water. There is a shift in the cross-over frequency observed when the gravitational and buoyancy force are included. The crossover takes place at 83 kHz when DEP force alone is considered. However, it takes place at 65 kHz when the other forces are included. Thus, it will be important to consider these forces when working with DEP.

CHAPTER VI

FACTORS AFFECTING DEP

In this chapter, the influence of various factors on DEP force is examined using COMSOL modeling. The problems identified and explained in the previous chapter are combined with these factors to analyze their effects on the DEP force. These factors fall under four categories: physical conditions, electrode properties, particle properties and suspension medium properties.

6.1 Physical Conditions

The physical conditions that affect the DEP force include electric potential, frequency and CM factor. The effects of these conditions are examined by using the COMSOL model with flat plate electrodes.

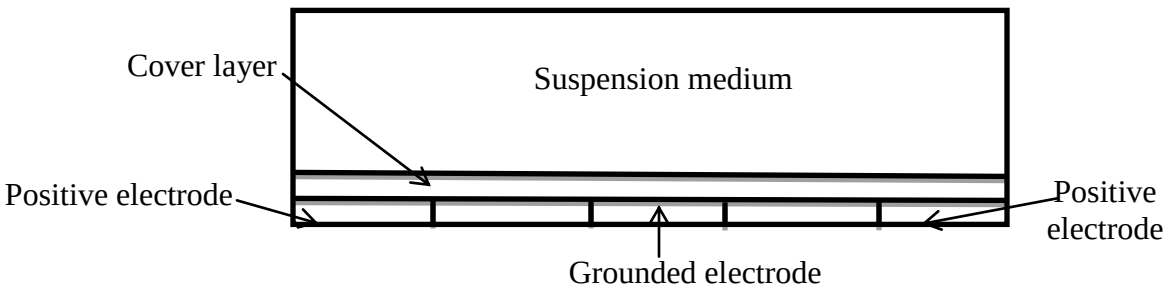

Figure 6.1: Single cell of flat plate electrodes setup with alternating positive electrodes and grounded electrodes with insulation in between.

Figure 6.1 depicts a unit cell of the model with interdigitated electrodes having alternating positive electrodes and grounded electrodes with insulation in between them to produce non-uniform electric field. The electrodes have a cover layer on top of them to

protect the electrodes from the medium and the particles from strong electric fields. Figure 6.2 shows the developed COMSOL.

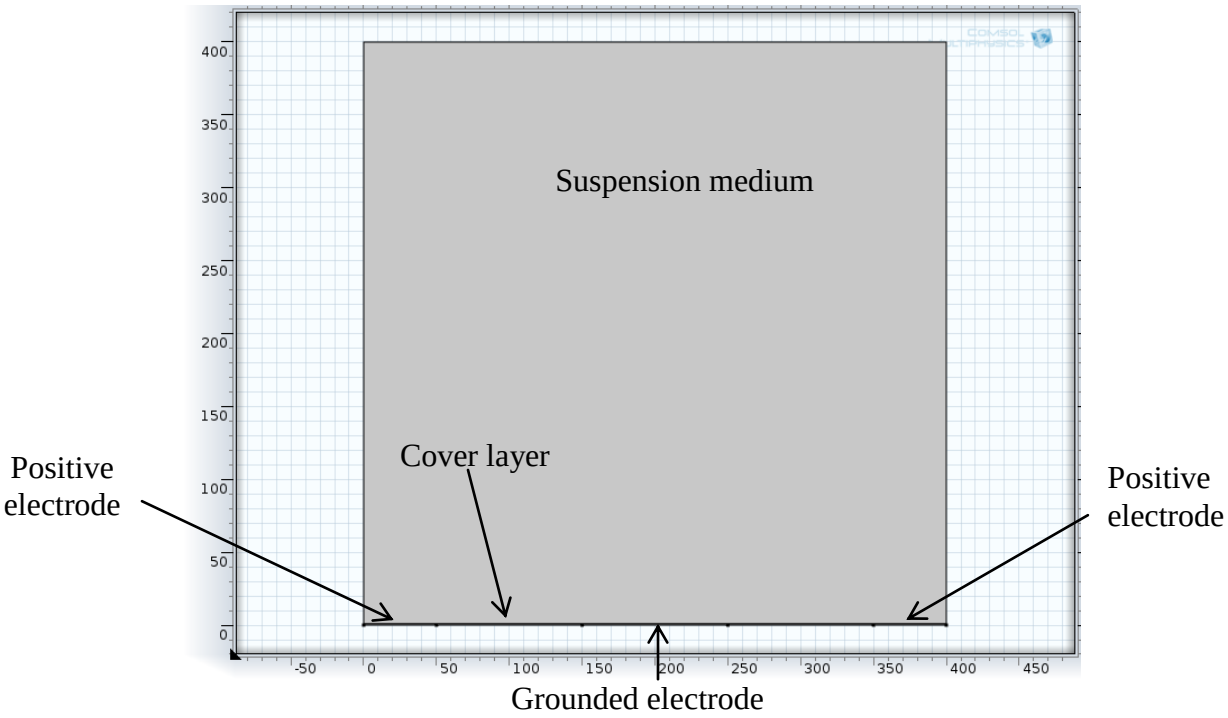

Figure 6.2: COMSOL model for flat plate electrodes (corresponding to Figure 6.1)

6.1.1. Electric potential

The electric field intensity depends on the applied electric potential. From equation 2.1 we know that the DEP force increases exponentially as the electric potential increases.

$$F_{DEP} = 2\pi r^3 \varepsilon_m Re(f_{CM}) \nabla E^2$$

$$E = -\nabla V$$

Figure 6.3 illustrates this effect using a system of E.*coli* cells in low conductivity medium. The change in the curve when the shell model and effect of radius on

conductivity are included is also analyzed using the COMSOL model described in Figure 6.2.

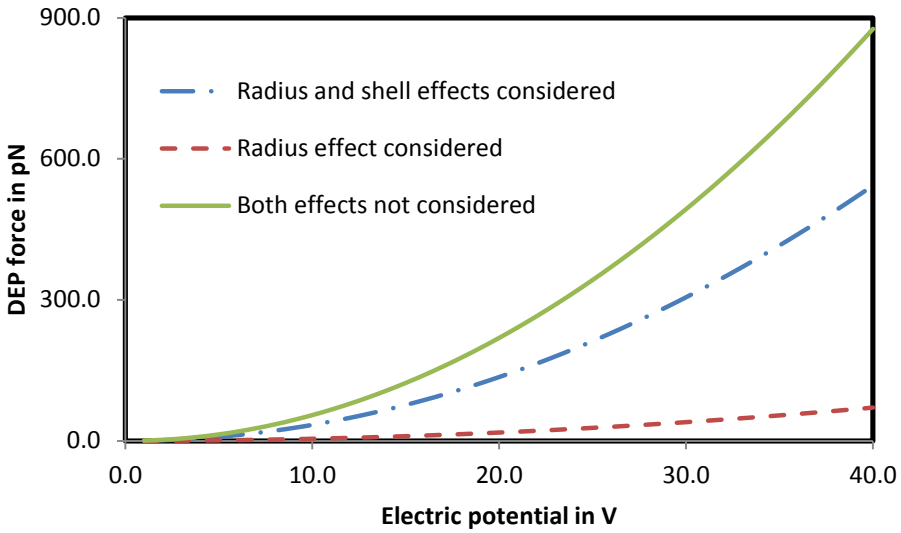

Figure 6.3: Variation of DEP force with electric potential in three different cases

Figure 6.3 shows the effect of electric potential on the DEP force under three conditions. They are 1) when only the effect of radius on conductivity is considered 2) when the effect of both radius and shell model are considered 3) when both the effects are ignored. Although in all the three cases the DEP force increases with the electric potential there is difference in the magnitude of the force. It is seen that when the radius effect on the conductivity is ignored the force has higher magnitude. This is because the radius is inversely proportional to the conductivity of the particle (see equation 5.7).

$$k_p = k_b + \frac{2\lambda}{r}$$

The conductivity of the particle in turn affects the CM factor. Considering the shell model also has its effect on the DEP force. The E.*coli* cells have a homogeneous core surrounded by a cell membrane with different dielectric properties. Thus there is once

again a change in the conductivity of the particle caused by the shell model and the CM factor is affected.

Large electric field strengths cause localized heating of electrode structures which gives rise to discontinuities in conductivity, permittivity and viscosity of the medium. Thus it is advantageous that DEP can produce the required force at lower electric potentials. Although magnitude of force is compared with the previously published papers to check the correctness, validation by statistical data analysis is an important step in understanding the correctness of our theory. Figure 6.4 shows the curve fitting between the data obtained from COMSOL and the theoretical equation.

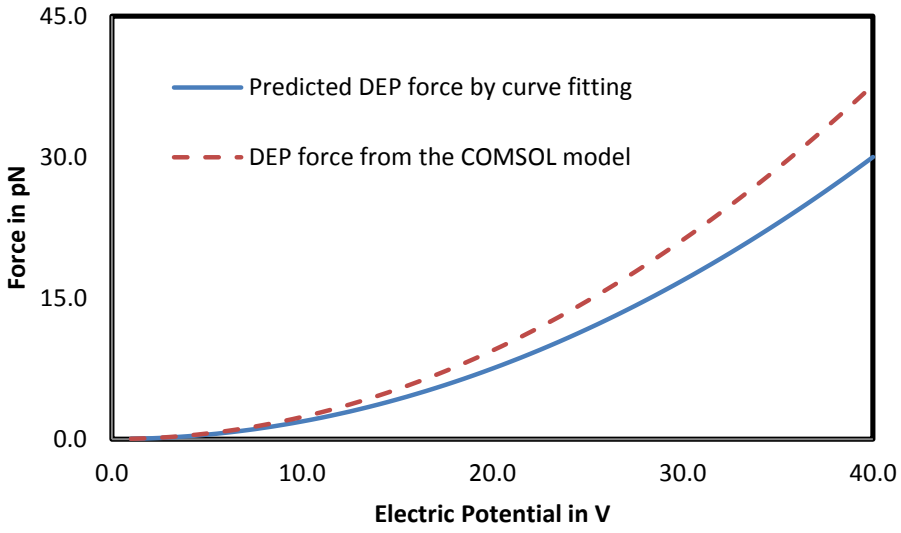

Figure 6.4: Curve fitting for electric potential

A close fit is obtained only when the effect of radius on conductivity and shell model for the particles are included. The discrepancy in the fitting (see Figure 6.4) is due to the 1D nature of the theoretical formula. The theoretical formula does not account for the DEP force in the y and z directions.

Figure 6.5 shows the arrow diagram for electric field of the flat plate electrode model described in Figure 6.2. The direction of flow of charge is from the positive to the grounded electrode .

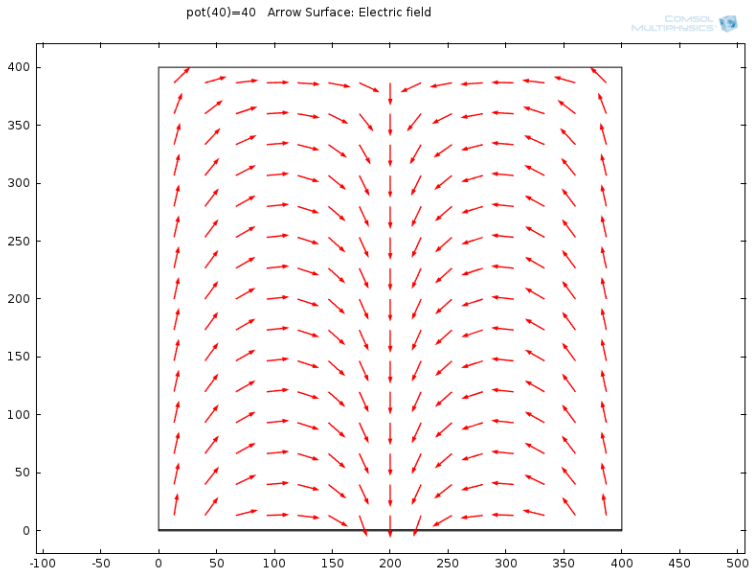

Figure 6.5: Flow of electric charge resulting in the non-uniform electric field

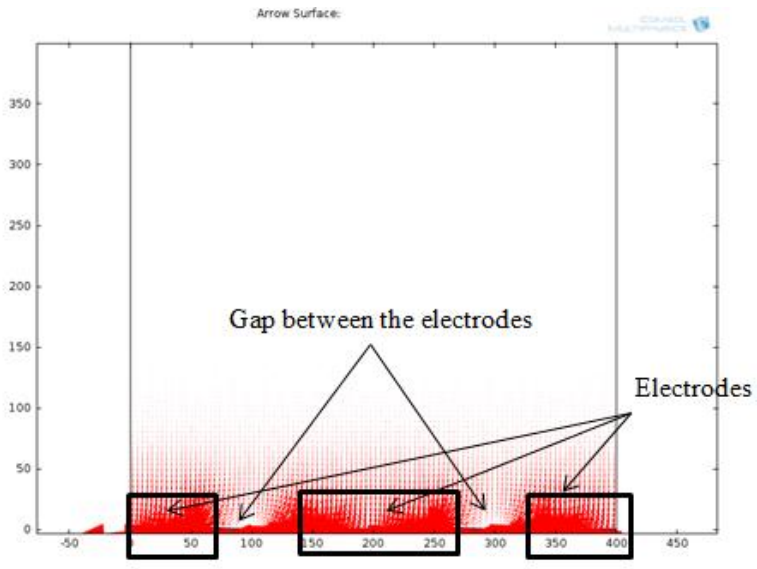

Figure 6.6: Arrow diagram for the DEP force

From Figure 6.6 it can be see that the DEP force accumulates on the top of the electrodes and is lesser at the gap between the electrodes. This leads to the collection of particles over the gap between the electrodes. The particles are pushed to region of lower fields by the DEP force.

6.1.2. CM factor and frequency

The CM factor is unique for every particle. It is a major factor that controls the direction in which the particles move. Polystyrene beads do not have bulk conductivity as they are insulators. However, they have a surface conductivity. The surface conductance arises from the movement of the ions in the double layer and is directly proportional to the surface charge density. The radius of the polystyrene beads used here is 5μm. Thus the particle conductivity is computed as shown in Section 3.3. The permittivity can be found from relative permittivity. Relative permittivity of the particle is 2.55 and permittivity of vacuum is $\varepsilon_0 \approx 8.85\times 10^{-12}$ F/m. Thus, the permittivity of the particle is $\varepsilon_p = 2.25 * 10^{-11}$ F/m.

Name	Value	Unit
Dielectric constant of DI water	78.5	1
Conductivity of DI water	2.00E-04	S/m
Dielectric constant of PS beads	2.6	1
Conductivity of PS beads	4.80E-04	S/m

Table 6.1: Dielectric properties of a polystyrene beads and deionized water [102]

The conductivity and permittivity values in Table 6.1 are used in the model to compute the DEP force. Conclusions are drawn by analyzing the CM factor. The change in CM factor with frequency is illustrated using Figure 6.7 considering the particle to be polystyrene and the suspension medium to be deionised water. From Figure 6.7 it can be seen that Re(f_{cm}) varies drastically in frequency ranges 1-1000 kHz for polystyrene beads.

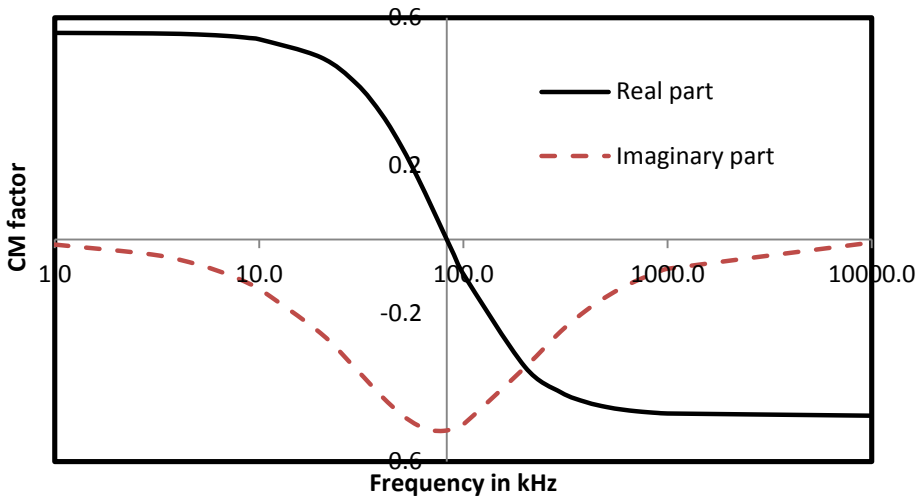

Figure 6.7: Change in real part and imaginary part of CM factor with change in frequency

The Re(f_{cm}) is used to calculate the DEP force and the Im(f_{cm}) is used for electrorotation and twDEP. In the publication by Markx *et al.* [52] equation 5.1 was further simplified by considering the cases of low and high frequencies. At a low frequency the first term of equation reduces to zero. Considering f tends to zero in equation 5.1 gives rise to the following [100]

$$\mathrm{Re}(f_{cm}) = \frac{(\sigma_p - \sigma_m)(\sigma_p + 2\sigma_m)}{(\sigma_p + 2\sigma_m)^2}$$

$$\mathrm{Re}(f_{cm}) = \frac{(\sigma_p - \sigma_m)}{(\sigma_p + 2\sigma_m)}$$

Similarly, when the frequency is high only the first term is used simplifying the equation to (5.4).

$$\mathrm{Re}(f_{cm}) = \frac{\varepsilon_p - \varepsilon_m}{\varepsilon_p + 2\varepsilon_m}$$

Thus, the CM factor depends on the frequency. COMSOL illustration of change in the direction of the DEP force when the CM factor switches from positive to negative is illustrated below.

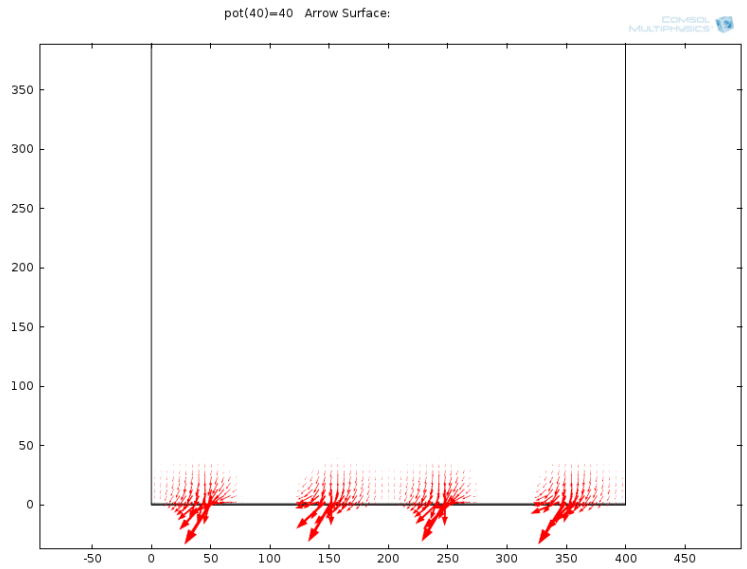

Figure 6.8: Direction of DEP force using an arrow diagram when the CM factor is positive

The same experimental conditions are used for the two conditions (see Figure 6.8 and 6.9) and the change in direction of the DEP force is observed. When the CM factor is positive the DEP force is directed towards the electrodes and when it is negative the DEP force is directed away from the electrode.

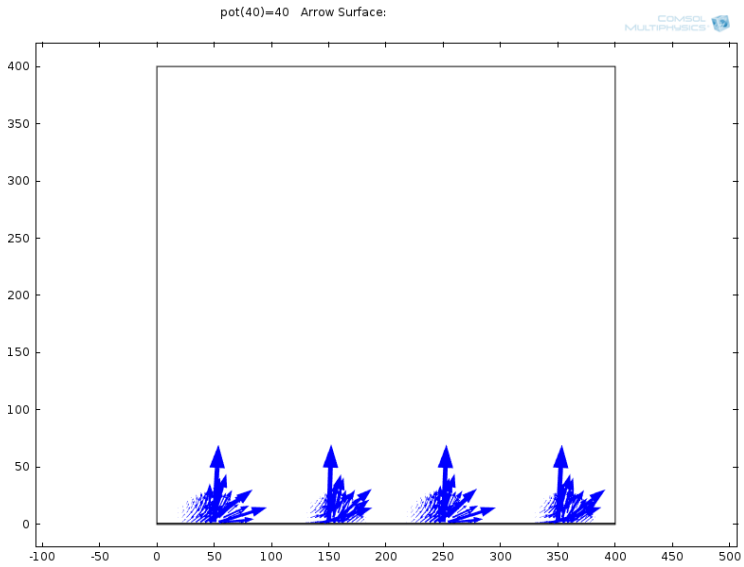

Figure 6.9: Direction of DEP force using an arrow diagram when the CM factor is negative

Thus the direction of DEP force depends on the CM factor. The CM factor in turn depends on the frequency as seen in equation 5.1.

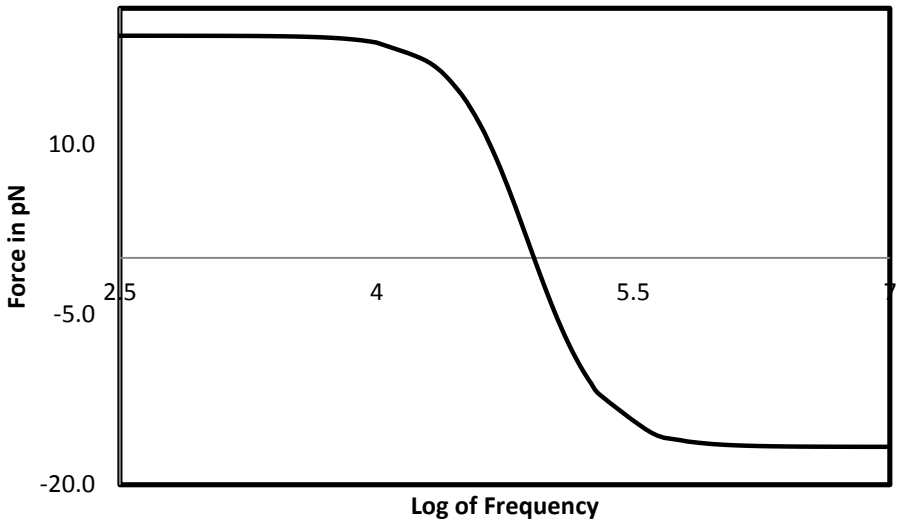

Figure 6.10: Change of DEP force with frequency

A sigmoidal curve is obtained when the frequency was plotted against the force corresponding to Re(f_{cm}). In Figure 6.10 the data of E.*coli* cells suspended in deionized

water is used to plot the DEP force against frequency. The curve gives a range for frequency at which pDEP, nDEP and crossover are exhibited.

Further validation is done by curve fitting. The curve from the computational model is fitted with the mathematical model. This is done to see if our results match with the theoretical values. Data from the model is imported and both these values were plotted simultaneously.

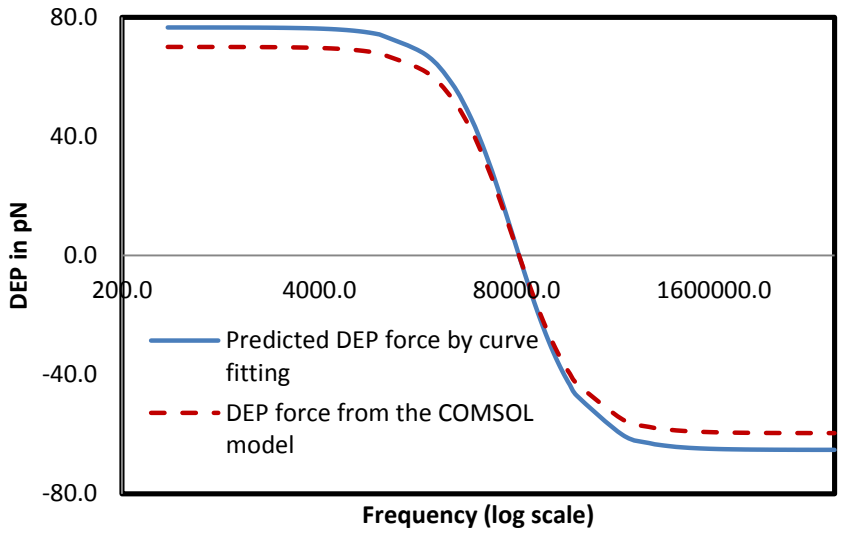

Figure 6.11: Curve fitting for change of DEP force with frequency

In Figure 6.11 the frequency is plotted against the DEP force for the same system. The mathematical data and COMSOL model data are compared. The small discrepancy seen in Figure 6.11 is because the COMSOL model has three dimensions (x, y and z directions). However theoretically we do not have it. A close enough curve is obtained by including the shell model and radius-conductivity effects.

Mesh plots are made to illustrate the effect of radius and frequency on the

CM factor. 3D mesh plots are made to analyze how the CM factor and DEP force are affected by the radius and frequency. Figure 6.12 shows the plot for radius, frequency and CM factor.

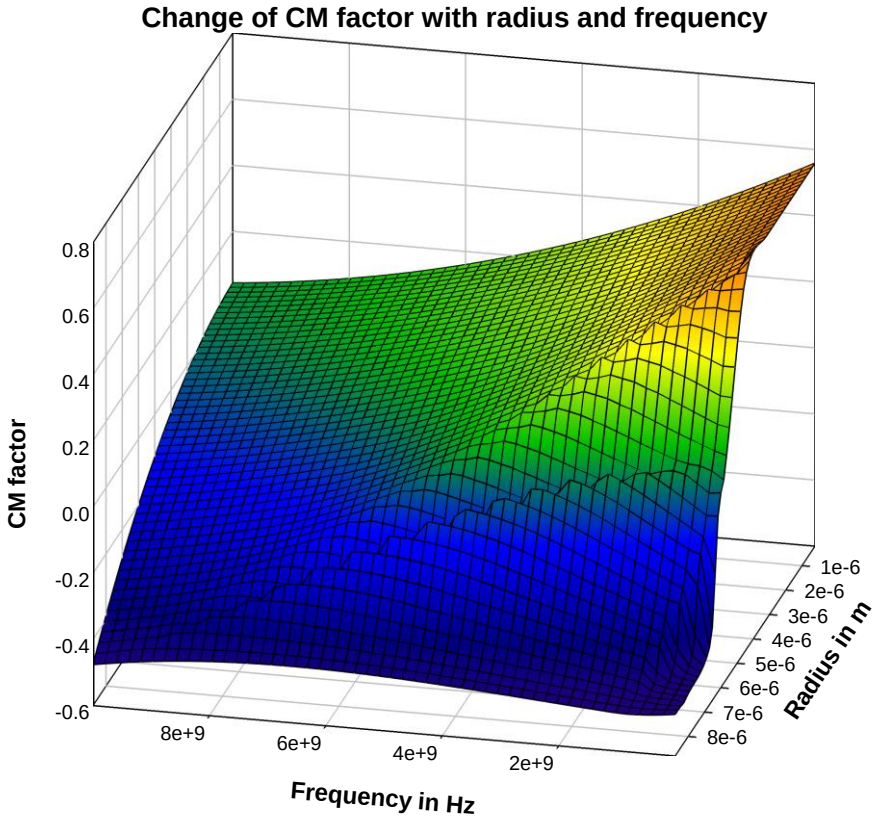

Figure 6.12: 3D mesh plot showing the change of CM factor with radius and frequency

3D mesh plots are also made to analyze the change of DEP force with radius and frequency. The same pattern in not observed because DEP force is also dependent on the r^3 term apart from the CM factor. The plot for DEP force is shown in Figure 6.13.

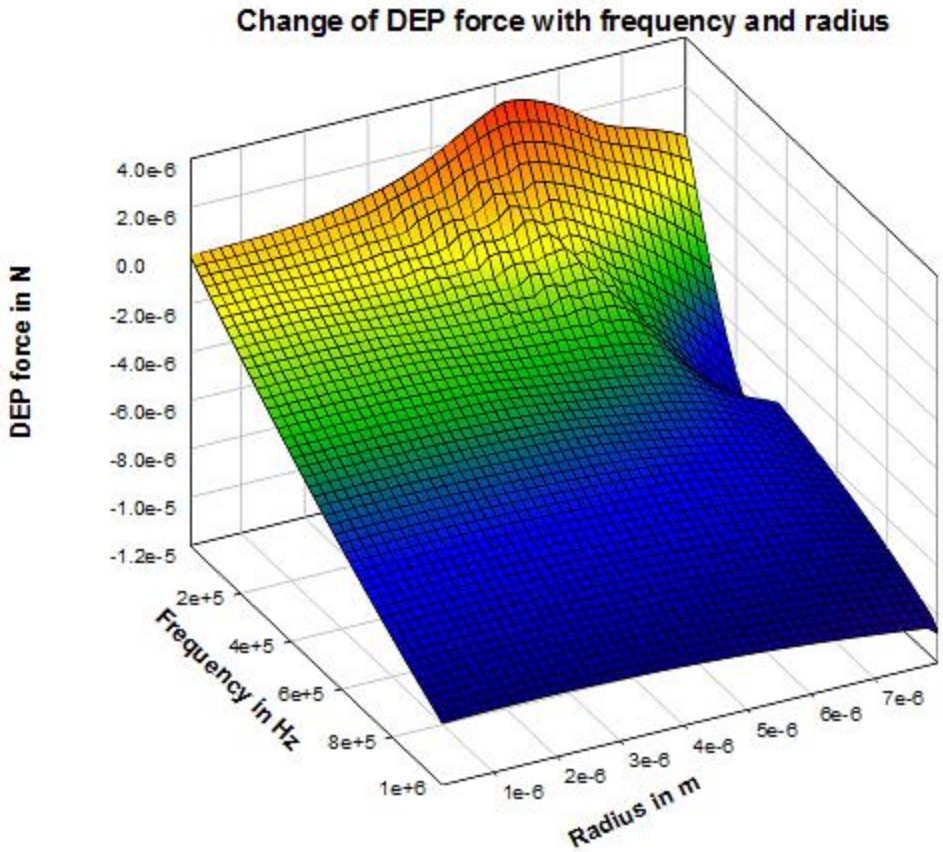

Figure 6.13: 3D mesh plot showing the change of DEP force with frequency and radius.

From Figure 6.13 it can be seen that with the change in frequency there is a change of direction of DEP force. It should also be noted that radius also has an effect on the direction of force. For radius greater than 5μm the DEP force decreases again and might lead to a cross-over. This confirms the radius effect on the CM factor (affects the conductivity which affects the CM factor.

6.2. Electrode Setup

6.2.1. Electrode shapes

The interdigitated castellated electrode is a commonly used type of electrode to trap particles between the electrodes. Interdigitated electrodes to trap yeast cells in the electrode bay region and on top of the electrodes are demonstrated in Figure 6.14 [38].

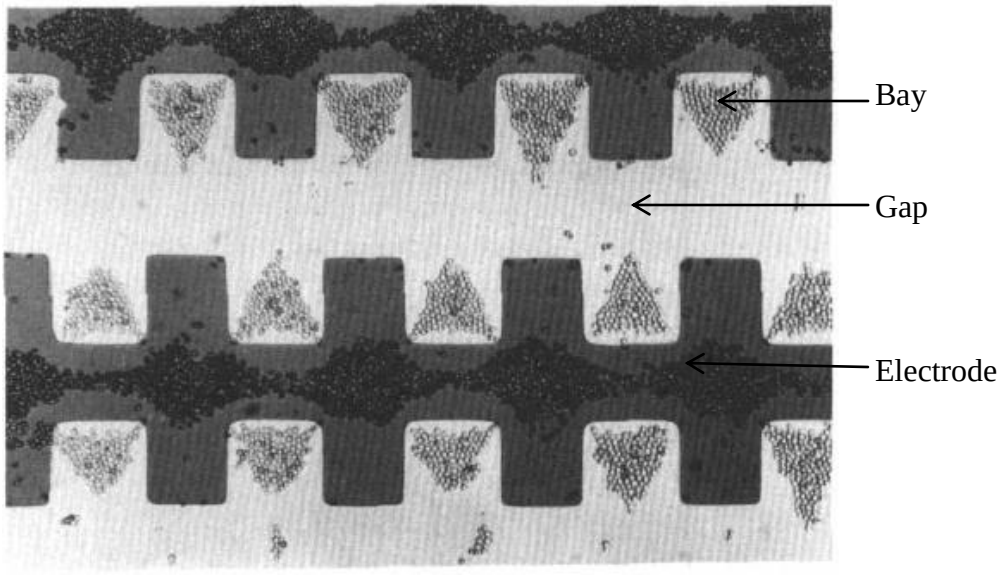

Figure 6.14: Yeast cells are collected in the bay region and on top of the electrodes [38]

From 6.14 it can be seen that the particles are collected in triangular segments between the electrode and in diamond segments on top of the electrodes. To understand the underlying mechanism, this electrode setup is modeled using COMSOL. The electric potential distribution can be seen in Figure 6.15. It has alternating positive and grounded electrodes with insulation in between which gives rise to the DEP force. Yeast cells are used demonstrate the DEP movement.

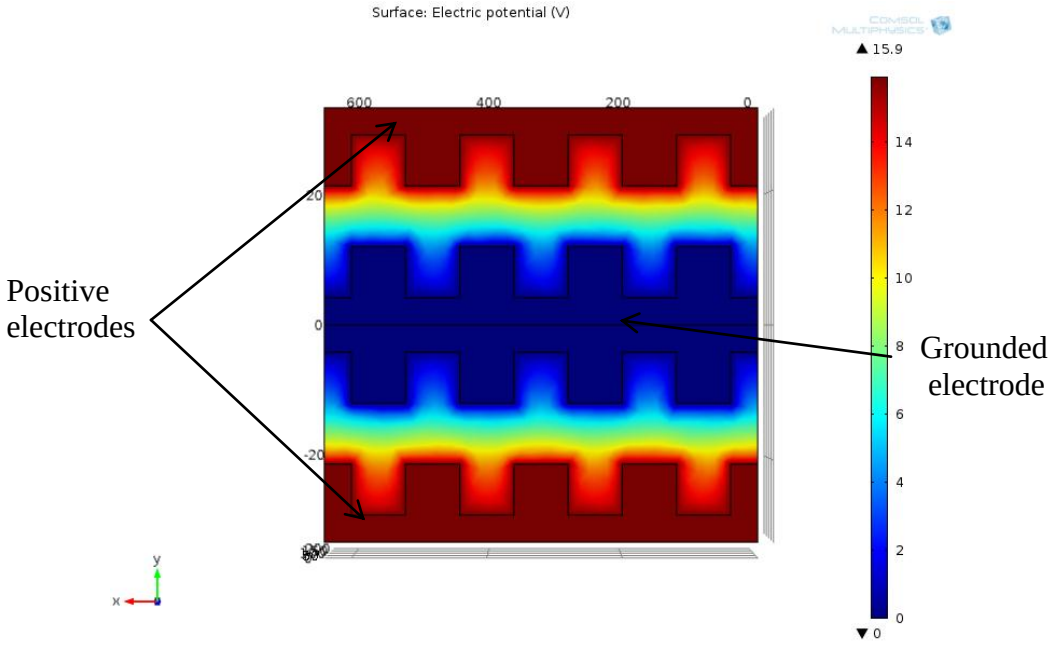

Figure 6.15: Flow of charges from the positive electrode to the negative electrode

Yeast cells used for the study do not have isotropic dielectric properties. Hence a shell model is used to determine the CM factor. The system is operated at an electric potential of 15.9V and a frequency of 10-150 kHz. In the case of nDEP the cells are pushed to lower field regions away from the regions of concentration of DEP force. In Figure 6.16 and 6.17 the arrows denote the magnitude and direction of the DEP force. In the proportional arrow diagram larger arrows signify higher magnitude. Thus the particles (as they are pushed to the lower field regions) will be collected in the regions where there is lesser DEP force acting.

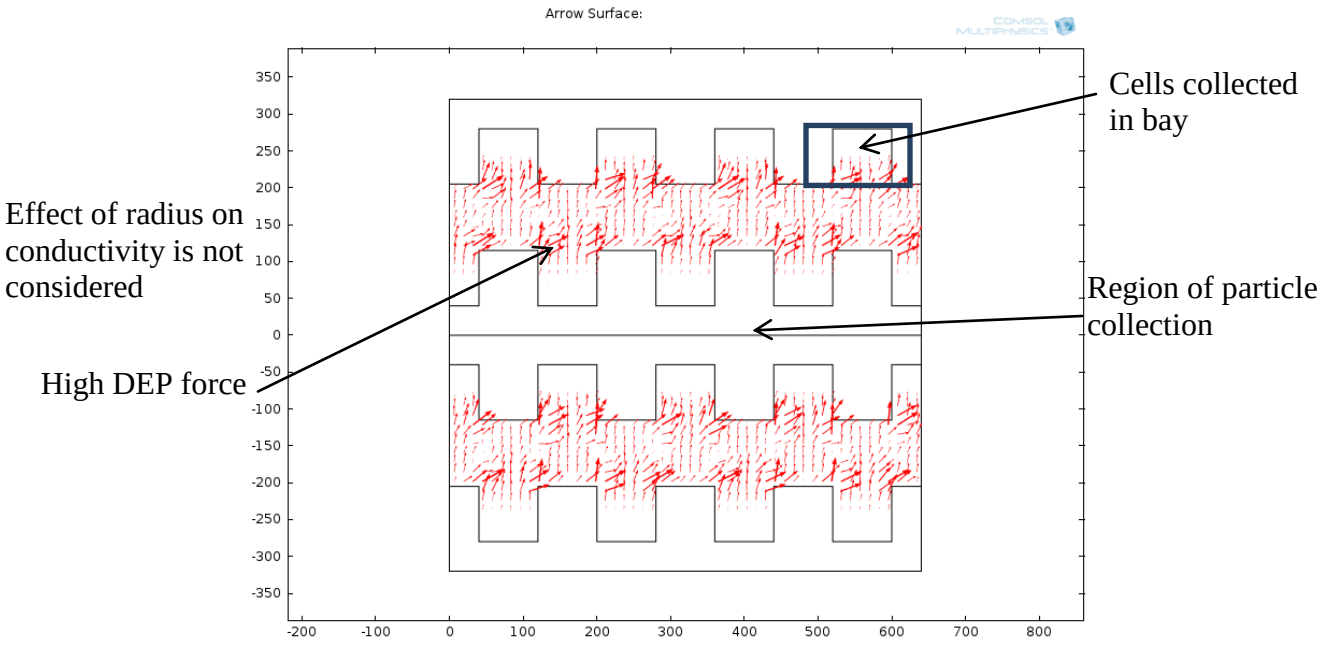

Figure 6.16: Arrow plots for the DEP force when the radius-conductivity effect is not considered

Figure 6.16 has the arrows concentrated in the gap between the electrodes. The position to where the arrows point shows the region of higher DEP. The effect of radius on conductivity is ignored in this case. Thus from Figure 6.16 we can see the particles will be collected in the bay between the electrodes and on top of the electrodes. However this does not explain the triangular and diamond collection patterns and the magnitude of DEP.

It is interesting to observe that the collection pattern found in Figure 6.16 was seen when the radius-conductivity effects were included (see Figure 6.17). Cells in the inter-electrode space are pushed away from the electrode edges towards the bays in a triangular pattern. Similarly, cells on the electrodes are directed towards central regions

of the electrode surfaces in a diamond pattern due to high nDEP force on the electrode edges.

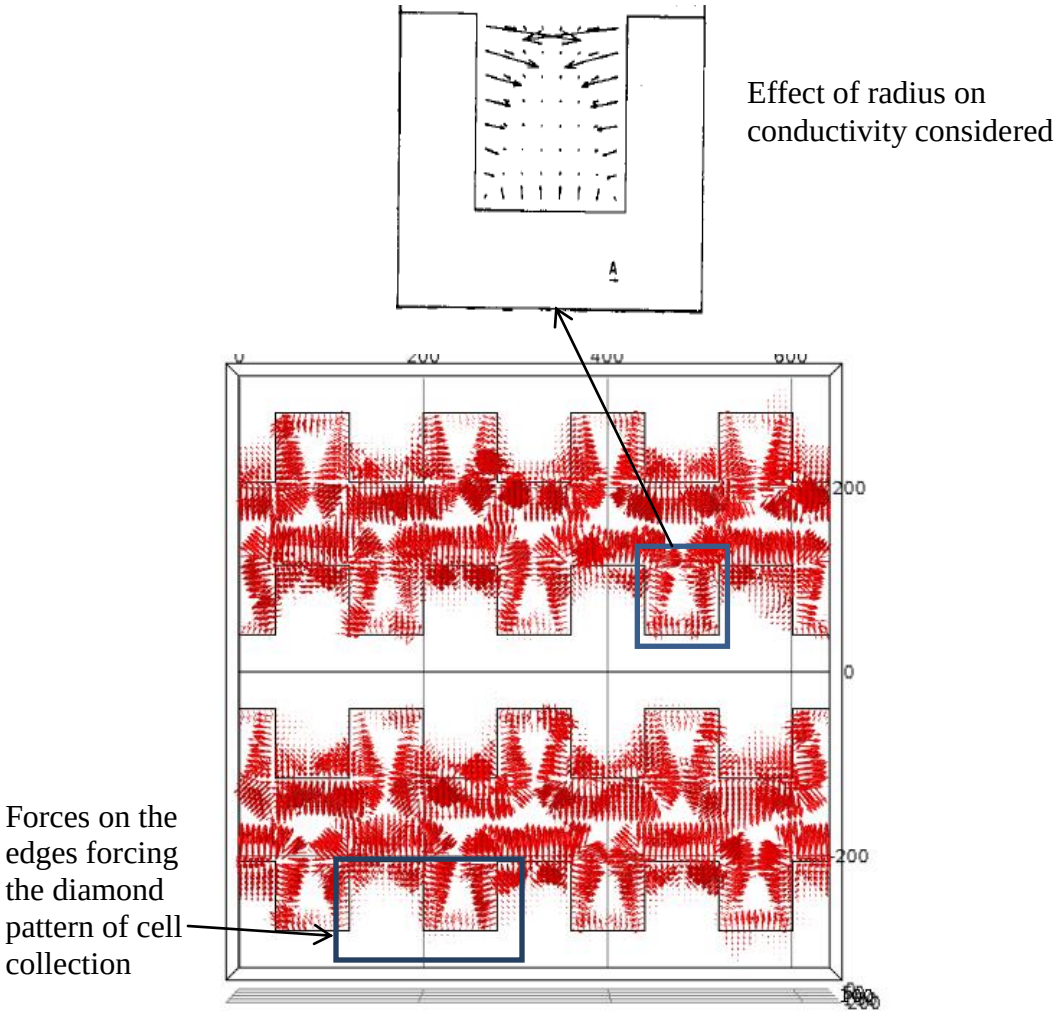

Figure 6.17: Particle collection after radius-conductivity effect is included, resembles figure 6.15 more closely

Although there are some spaces in the gap region between the electrodes the particles will not get collected there. This is because the DEP force is higher and directed away from the region and hence the particles will not be stable. In the bay region however, the forces are directed towards the region and hence leads to the collection of

particles. The above result is observed when the effect of radius on conductivity is considered.

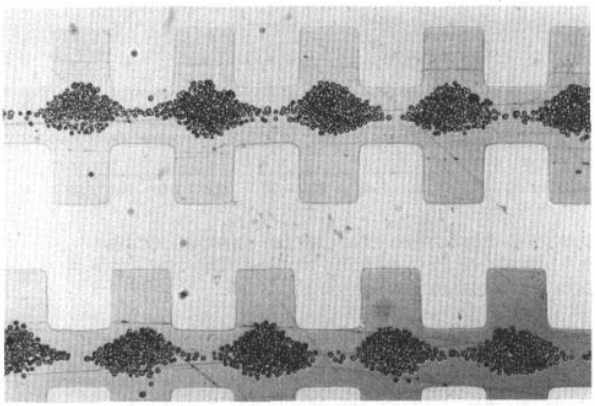

Figure 6.18: Diamond patterning observed on the top of the electrodes whereas the triangular bay patterning not observed at 500Hz [38]

From Figure 6.18 it can be seen that at very low frequencies under the same experimental conditions although the diamond pattern was formed there is no triangular collection in the bay area. This is demonstrated in the COMSOL model (see Figure 6.19).

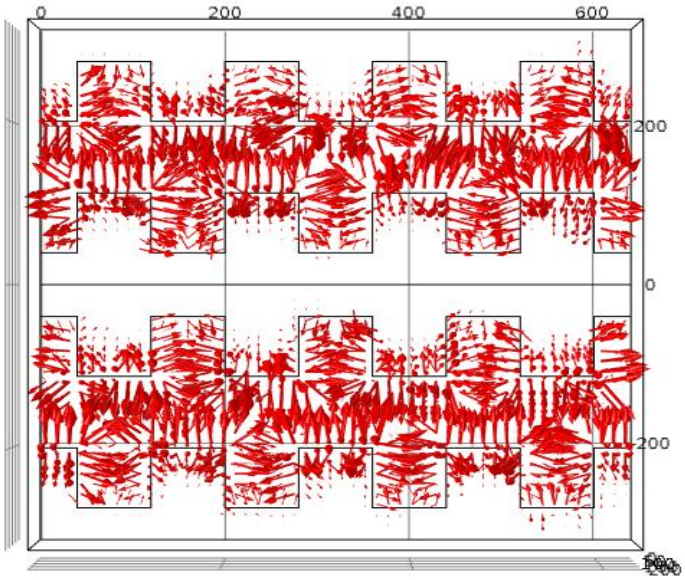

Figure 6.19: COMSOL results illustrating the phenomenon observed in Figure 6.18

Although at 500 Hz the particle is still going to exhibit nDEP there is no collection of particles in the bay area. This is because $(E \cdot \nabla)E$ has a minimum value at the center of the electrodes. Thus during nDEP at low frequency the cells will have a lower potential energy when aggregated in a diamond-shaped pattern on the electrode surfaces than when aggregated in a triangular pattern in the electrode bays.

Due to higher DEP forces at the electrode edge it becomes necessary to calculate the force acting at the electrode tips. A stronger and highly non-uniform electric field is created near the edge of the electrode.

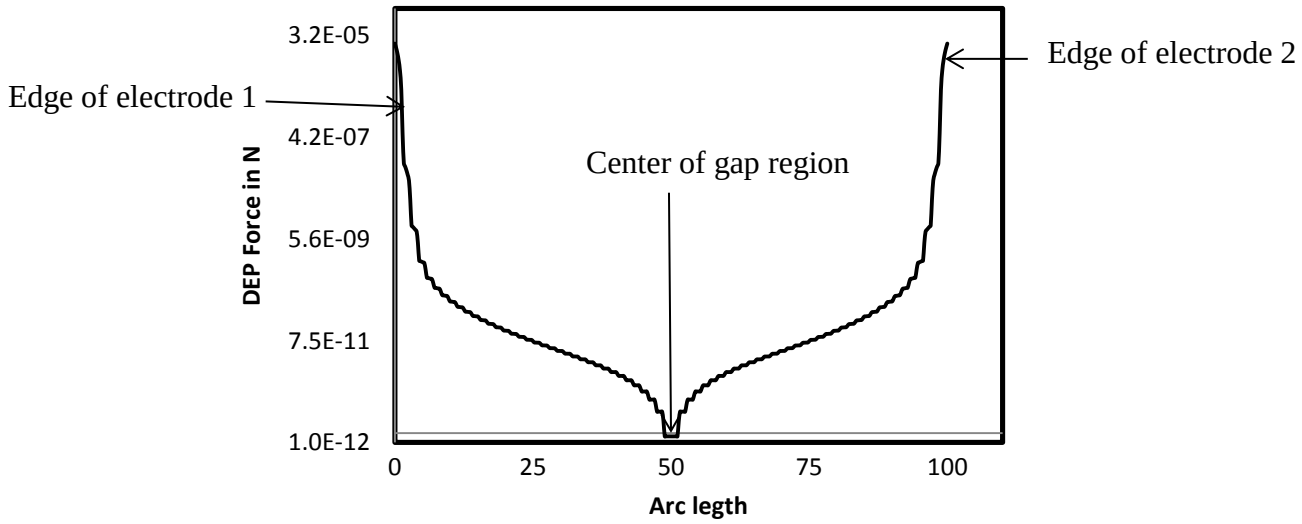

Figure 6.20: Line graph showing how the forces change as we move between the electrodes

Figure 6.20 shows the change in magnitude of the force as we move from one edge of the electrode to other. Arc length of 50 signifies the center of the gap region. The magnitude of the DEP force is the highest at an arc length of 50, showing that the maximum force is at the edge of the electrode.

Elliptical shaped electrodes have been used in several applications. The force that directs the particles to particular positions can be determined by adjusting the length of the major and minor axis [101]. The electrode setup generally has a micro-channel for the removal of the particles. The micro-channel is surrounded by the inner electrodes so that the collection of particles takes place at the inner electrodes.

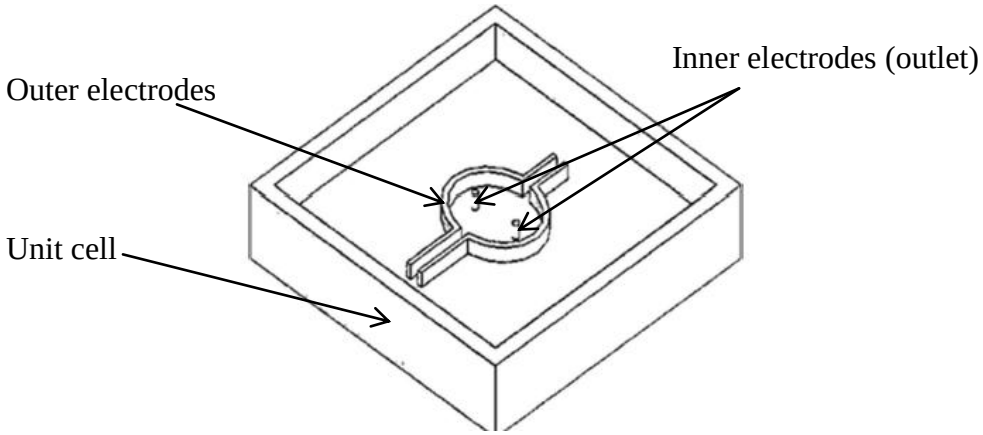

Figure 6.21: 3D electrode model with the inner and outer elliptical electrodes [101]

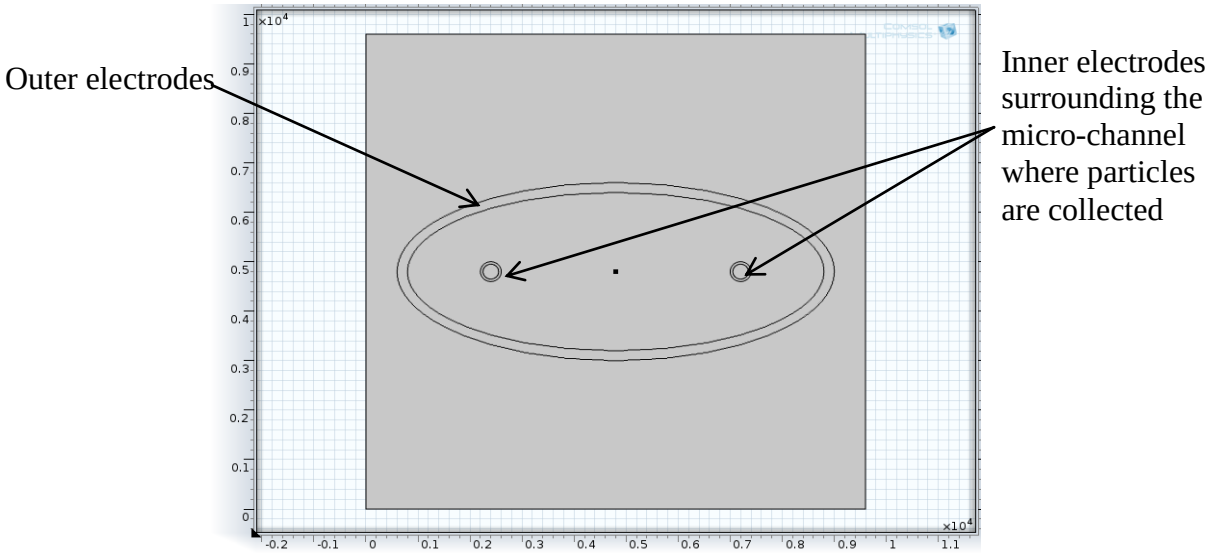

Figure 6.22: COMSOL model when the ratio between semi-minor and semi-major axis is 0.4

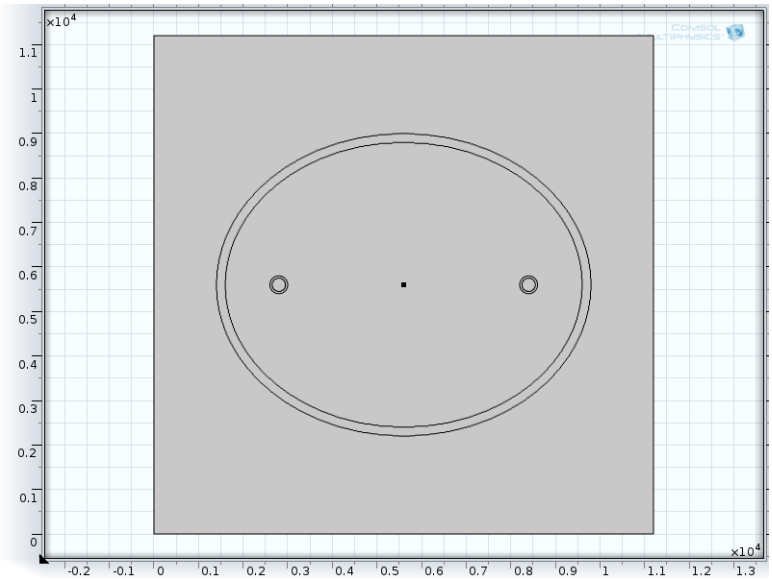

Figure 6.23: COMSOL model when the ratio between semi-minor and semi-major axis is 0.8

Generally the length of the semi-major axis is kept constant and the length of the semi-minor axis is varied. This can be easily done in modeling by considering a ratio between the length of the semi-minor axis and the length of the semi-major axis. This ratio is swept to optimize the electrode shape. Desired results were achieved when the ratio between the major and minor axis were greater than 0.7.

The particle considered here is polystyrene beads varying in radius and the suspension medium is deionized water. The properties of PI beads and DI water are found in Table 6.1. Figure 6.24 shows the electric potential distribution of the electrode setup. The inner electrodes are grounded and the outer electrodes are given a positive potential.

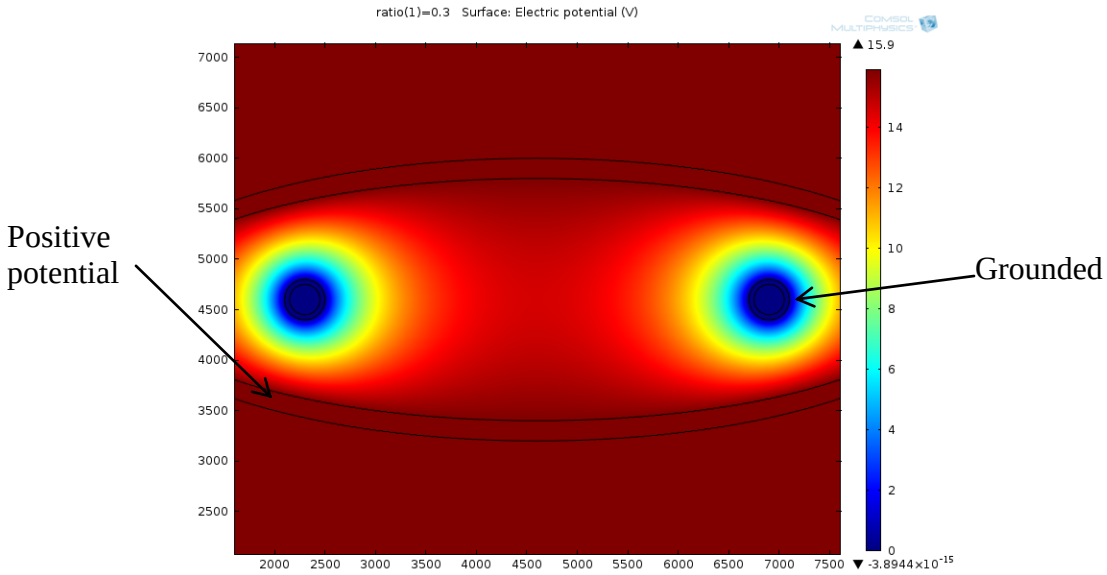

Figure 6.24: Electric potential on the elliptical electrode

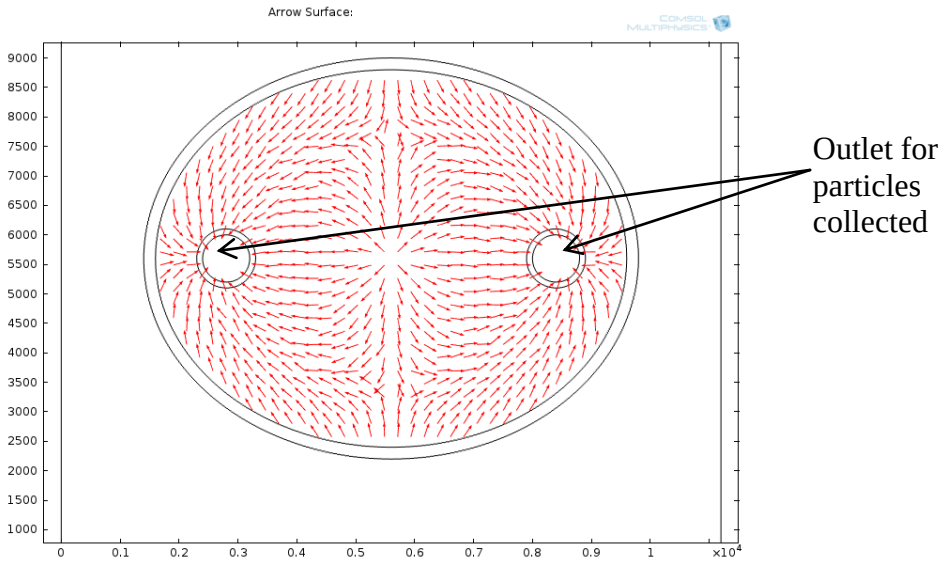

Figure 6.25: Arrow diagram showing the DEP force directed to the micro-channel (inner electrodes) where the particles get collected when the ratio is 0.7 or greater

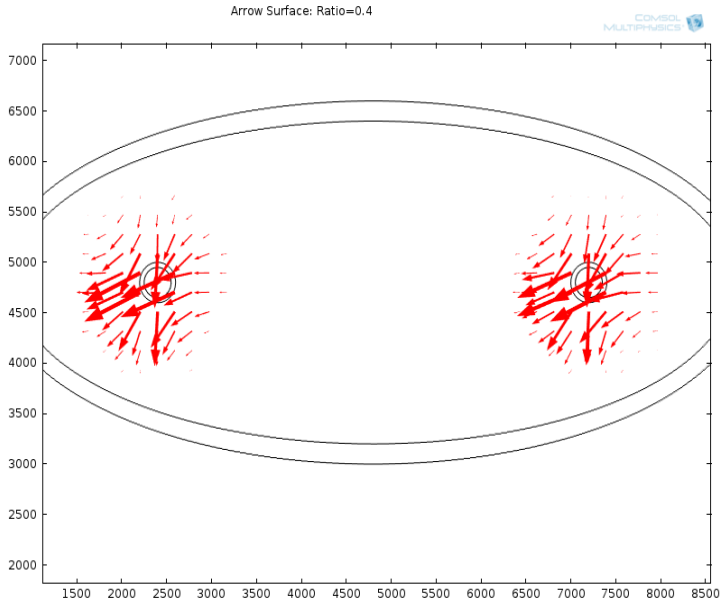

Figure 6.26: Arrow diagram showing the DEP force directing the particles away from the micro-channel when the ratio is less than 0.7

The arrows point to where the DEP force is higher. From Figure 6.25 and 6.26 it can be seen that the particles are directed towards the micro-channel and collected through them when the ratio between the major and minor axis is 0.7 or greater. In Figure 6.25 the DEP force is higher around the inner electrodes and hence the particles are pushed towards the inner electrodes which act as outlet. The particles do not align as desired when the ratio is less than 0.7.

6.2.2. Electrode dimension

The ratio between the electrode width and the gap between the electrodes is varied and the change in force is observed. Thus the electrode width is kept constant and the gap between the electrode changes with change in the ratio.

$$w_g = \text{ratio} \times w_e$$

where w_g is the width of the gap between electrodes and w_e is the width of the electrodes. The force decreases with increase in ratio. This can be explained using equation 2.1. In equation 2.1

$$F_{DEP} \propto \nabla |E|^2$$

The electric field intensity is inversely proportional to the distance between the electrodes. Thus, the DEP force decreases when the electrodes are moved apart.

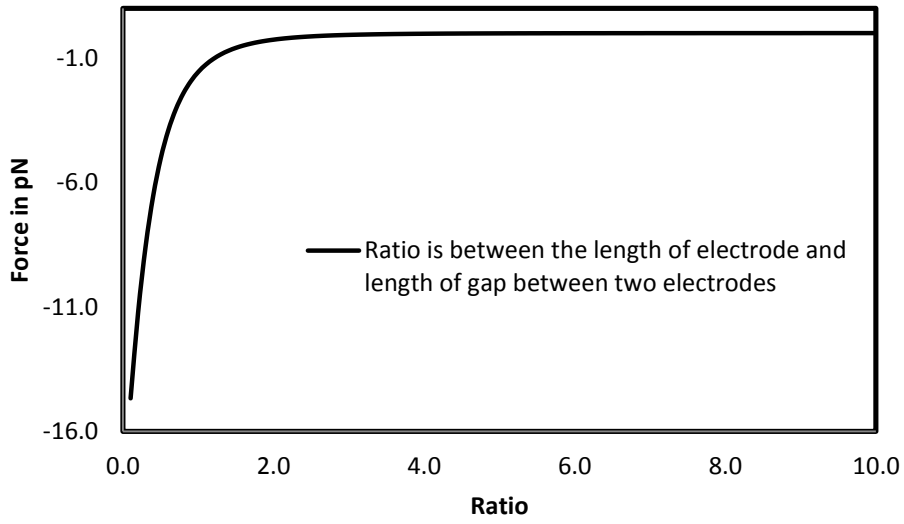

Figure 6.27: Decrease of force with increase in the distance between the electrodes

6.2.3. Insulation

The presence of insulators between the electrodes distorts the distribution of the local electric field and creates zones of higher and lower field intensity. Thus a non-uniform electric field is created [103]. Insulation also increases the effective wire diameter and limits some factors which would lead to acceleration [104]. Figure 6.28 and

6.29 show how the DEP force changes with the size of the insulation between the electrodes.

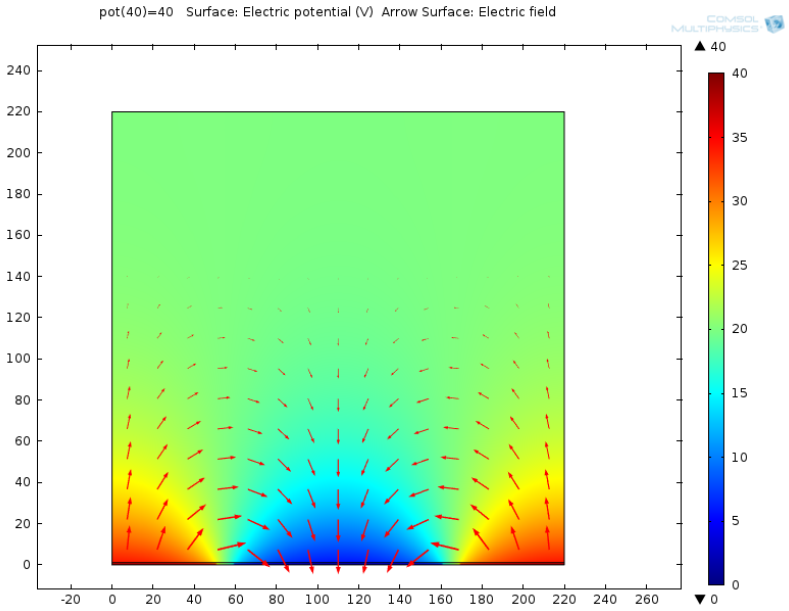

Figure 6.28: Arrow diagram for electric potential when ratio between electrode length and insulation length is 0.1

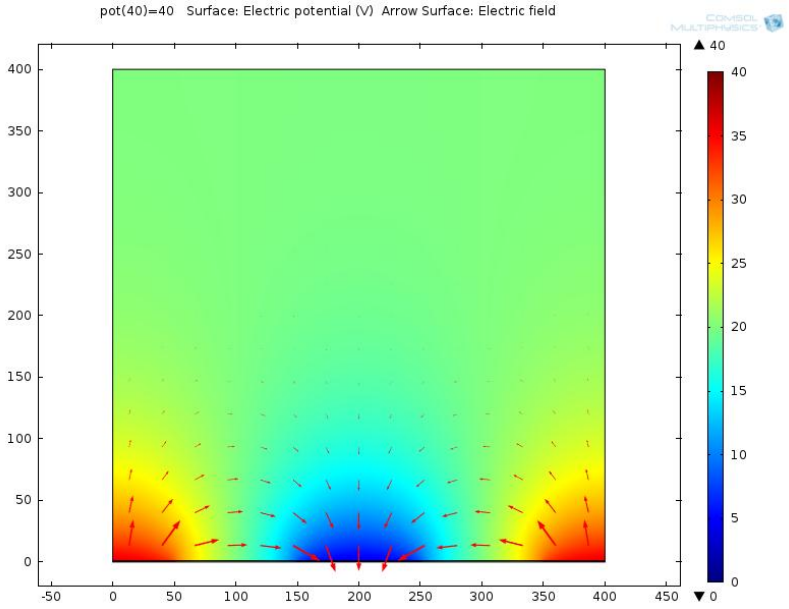

Figure 6.29: Arrow diagram for electric potential when ratio between electrode length and insulation length is 1

The arrow diagram shows the direction of the field and the length of the arrow is proportional to the magnitude of the force. It can be seen from the figures that with the optimal insulation length there is a proportional, non-uniform and wide spread field.

6.3. Particle Properties

6.3.1. Synthetic particles

Most synthetic beads used for DEP experiments have uniform properties. Bulk conductivity is assumed to be zero for synthetic beads as they are insulators. The surface conductivity of the beads is a function of its radius. Latex, polystyrene and silica beads are used as models to mimic cells [8]. The table below consolidates the general properties of latex and silica beads of radius 10μm [105]. The properties of polystyrene beads are listed in table 6.1.

Particle/Parameters	Latex beads	Silica beads	Units
Conductivity	1.50E-12	1E-12	S/m
Permittivity	2.21E-11	4.87E-11	F/m

Table 6.2: Dielectric properties and sizes of synthetic beads generally used in DEP experiments

The conductivity of silica beads and latex beads are lower than the cells [106]. Silica beads are used as probe in bead-based immunoassay and in flow cytometry applications [107].

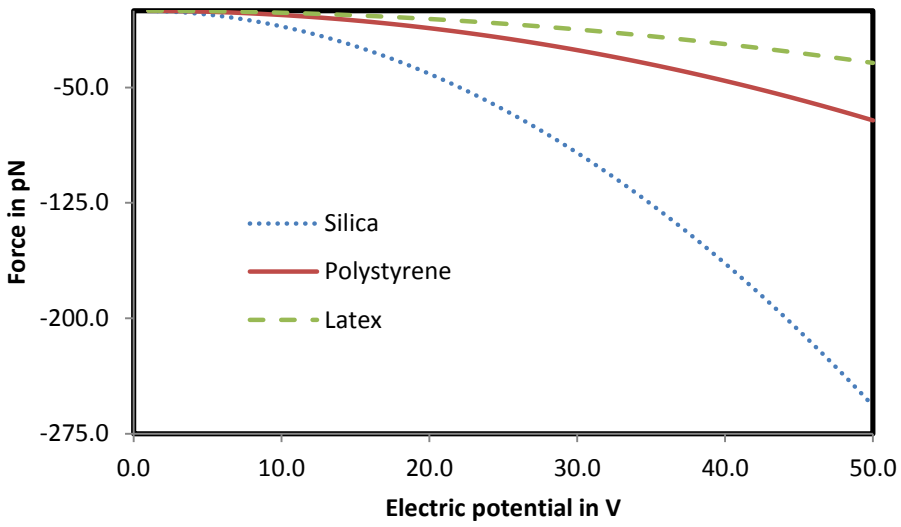

Figure 6.30: Force distribution with respect to electric potential for different synthetic particles

The aligning of particles by DEP is demonstrated experimentally in Figure 6.31 and 6.32. Polystyrene beads of 10 µm radius are introduced into the electrode system. The particles start aligning in the form of chains in the gap region between the electrodes when an electric potential is applied to the electrodes.

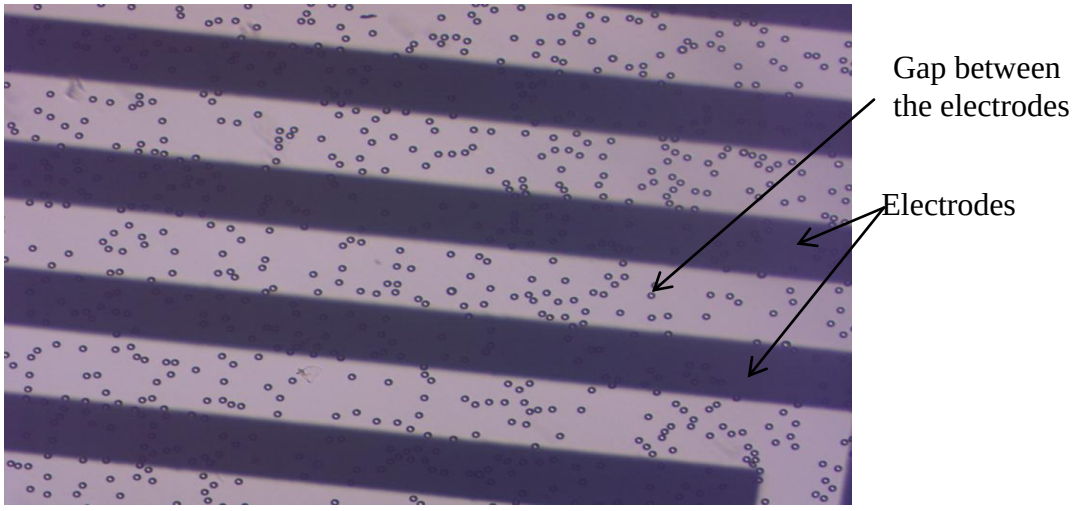

Figure 6.31: Microscopic image of polystyrene beads when electric potential is not applied

The 10 µm beads are randomly distributed over the electrodes and the gap region in Figure 6.31.

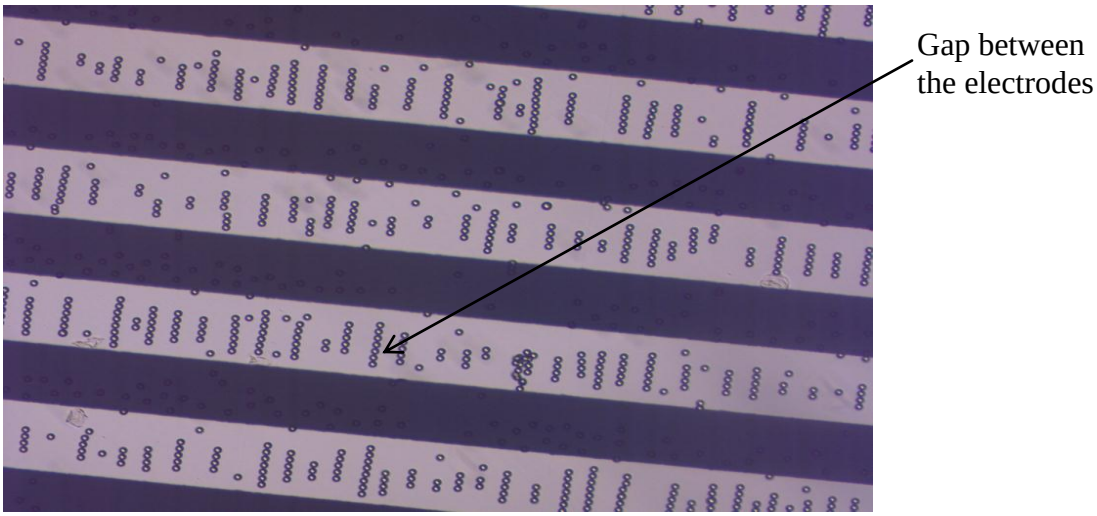

Figure 6.32: Microscopic images of the aligning of polystyrene beads electric potential is applied

The beads form long chains on the top of the gap region between the positive and negative electrodes.

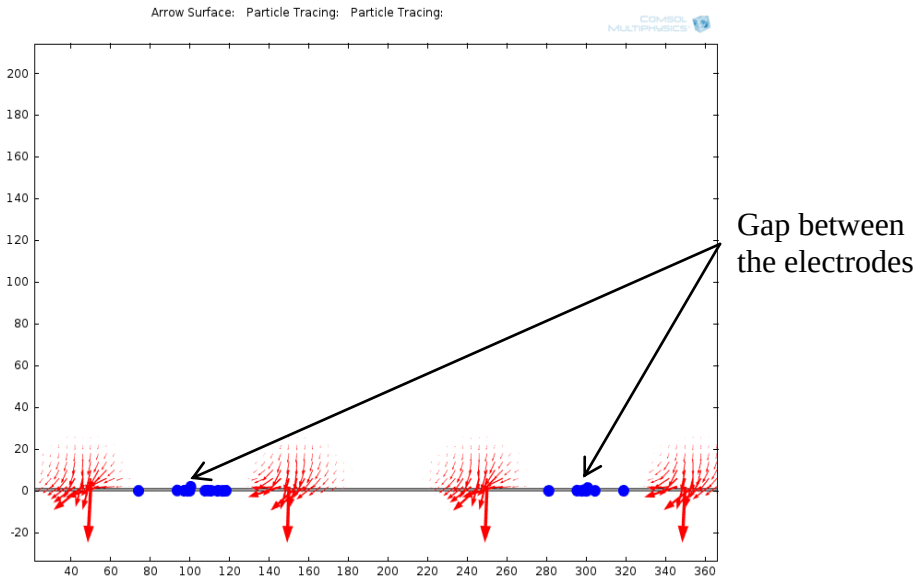

Figure 6.33: Arrow diagram (red) for the DEP force and particle tracing showing the particles (in blue) aligning between the electrodes

This can be explained using the COMSOL model shown in Figure 6.2. Figure 6.33 shows the particles aligned between the electrodes in the gap region. The red arrows show where the DEP force acts. This force pushes the particles (in blue in figure 6.33) to the gap region. This leads to the particles forming chains in the gap region as observed in Figure 6.32. Hence the particle alignment observed experimentally can be explained using COMSOL when the effect of radius on conductivity and shell model are considered.

6.3.2 Biological particle

Manipulation of biological particles using the DEP force is different from manipulation of synthetic particles because of the non-homogeneous nature of the biological particles. Figure 6.34 shows frequency-force curve for polystyrene beads and E.*coli* cells where the cells and the beads have different crossover frequency. Hence the cells cannot be manipulated under the same conditions as synthetic beads.

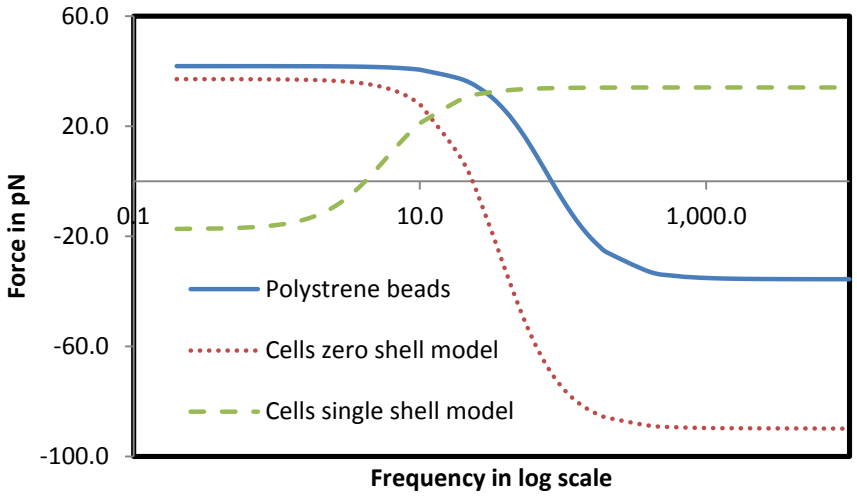

Figure 6.34: Comparing the crossover frequency curve for polystyrene beads and E.*coli* cells

As shown in Figure 6.34 the crossover for the polystyrene beads take place at about 83 kHz and for cells it is much lower. It is also important to note from the figure that there is a shift in the cross-over frequency when the shell model for cells is ignored. When a single shell model is assumed for E.*coli* cells then the crossover takes place at 4.2 kHz instead of 22 kHz. Also the single shell model exhibits nDEP at lower frequency and pDEP at higher frequency. The single shell model demonstrates the DEP movement of E.*coli* cells better than the zero shell model. This is justified from the experimental work carried out by Kuczenski *et al.* where they studied the separation of E.*coli* cells and their viability under DEP [108]. They observed nDEP at the given frequency range. Hence it is important to consider the shell model when working with cells.

Data for the properties of a cancer cell and healthy cell are listed in table 6.3 [10]. DEP has been widely used to separate healthy cells from damaged cells. The cells cannot be expressed as a homogeneous particle. Shell model is used to determine the dielectric properties of biological particles [109].

Cell	Healthy Cell	Myeloma cell	Unit
Membrane Conductivity	1.00E-07	8.00E-09	S/m
Membrane Permittivity	8.85E-11	7.08E-11	F/m
Cytoplasm Conductivity	0.2	0.5	S/m
Cytoplasm Permittivity	6.64E-10	4.43E-10	F/m

Table 6.3: Comparison of dielectric properties of healthy cell and cancer cell [106].

In the case of blood cells it is observed that normal cells get aligned at the electrode edges while the cancer cells did not. For dead and live cell separation, the properties of the dead cells remain the same at all frequencies while the live cells have

different properties at different frequencies [45]. The relative dielectric permittivity and conductivity of dead cells are 47.5 and 0.845 S/m, respectively for all frequencies. As for viable cells, the relative dielectric permittivity and conductivity are calculated as 1.073E4 and 1.1E10 S/m at 500 Hz. Thus, the dead cells were seen to exhibit a pDEP response while the viable cells underwent nDEP.

A comparative study is done to combine the different problems identified and to show the effects. In Figure 6.35, the effect of radius on conductivity is studied in a shell model.

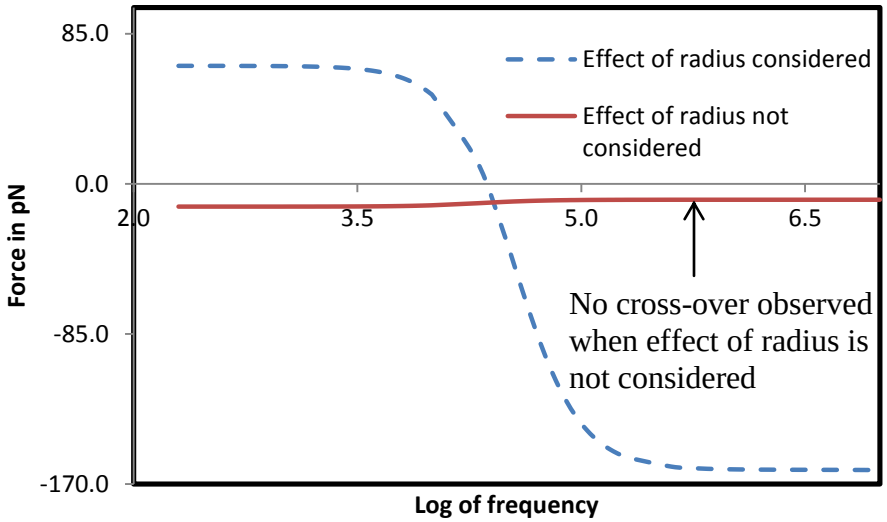

Figure 6.35: Shell model comparing the frequency curve when the effect of radius on conductivity is considered and when it is ignored

In the shell model two different cases are examined, considering the effect of radius on conductivity and ignoring it. The crossover for shell model takes place at 22 kHz. However, from Figure 6.35 it is seen that cross-over did not take place at 22 kHz when the effect of radius is ignored.

6.4. Suspension Medium

Depending on whether the permittivity of particle is higher or lower than the suspension medium there will be a change in direction of DEP force. Hence it is important to consider the suspension medium while analyzing the factors that affect the DEP force. Cells are grown on specific medium that has conductivity much different from deionized water used to suspend the particles.

Before cell patterning experiments, the cells are passaged by trypsinization and suspended in low conducting buffer solution. This is made of deionized water combined with HEPES, calcium chloride, D-glucose and sucrose, and its pH is adjusted to 7.35 by aqueous NaOH. The conductivity of this suspension is 0.02S/m [59]. The cells have lesser viability when suspended in the low conductivity medium.

However, low conductivity medium are generally preferred to achieve the desired movement of cells. But research has been conducted to show that even high conductivity medium like the medium containing sucrose and BSA [110] or Saline media [111] can be used when suitable electrode setup is made for DEP. Hemisodium EDTA is used to adjust the conductivity of the medium to increase the cell viability [112] .

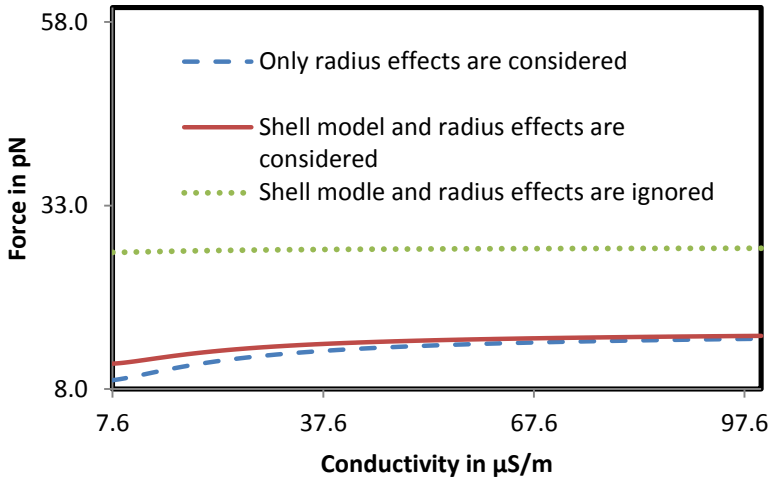

Figure 6.36: Change in DEP force with the conductivity of the suspension medium

Figure 6.36 shows the change of DEP force with the conductivity of the medium under two cases, 1) When only the radius effects are considered 2) When the shell model and radius effects were considered 3) When both the effects are ignored. The model is swept for a range of conductivity. The shift in the magnitude of the DEP force is observed when the shell model and radius effects are ignored.

CHAPTER VII

CONCLUSION AND FUTURE WORK

DEP serves as a rapid and non-invasive technique that can be exploited for various biomedical applications like particle sorting, cell patterning, pathogen detection etc. This research provides a thorough review of the field of DEP and identifies common problems present in the literature. A complete review of the literature for DEP is done. The problems in the literature are highlighted and their impact on the DEP force is illustrated using COMSOL multiphysics. This allows us to understand the difference in particle movements based on the problems. Finally COMSOL is used to illustrate the effect of several factors affecting DEP considering one or more contradiction in the model.

From the work it is evident that it is important to correct the problems identified. For example ignoring the shell model for non-homogeneous particle leads to the shift in the crossover frequency. The magnitude of the force is found to be incorrect when the radius-conductivity effects and the other forces acting on the particles are ignored. Also, the importance of the double layer and its effect on the conductivity of the particle is illustrated in this research.

Further studies need to be done to analyze the force individually in x and y direction in 2D models and x, y and z direction in 3D models. The force acting in each direction will help predict the direction in which the particle is supposed to move and if a particle levitates or not. This will give an understanding of how exactly the force moves a

particle placed in a non-uniform field and gives more information on why levitation of particles and pearl chain formation occurs. It can be done using COMSOL multiphysics.

Electrical characterization of a pearl chain model yields an ohmic behavior. More research on the effect of electric double layer on the DEP experiments should be done. A suitable equation has to be derived for different geometries of the particle, to calculate the change in conductivity due to the presence of an electric double layer.

It is also important to consider the interaction between particles when they are in close proximity. Two or more particles with the same sign of charges repel each other. The mechanism of interaction between particles is still unclear and future research has to be done on it. In an electrolyte the available free charges screen the particle's charge and the field produced by the particles charge rapidly decays with distance. Thus these interactions can be ignored when the distance between the particles is large. However, when the particles are very close, both electrostatic interactions and van der Waals play an important role in forming long chains.

Application of DEP to tissue engineering is a relatively new field that has great scope in building biomimetic structures of the human organs. Combining heterogeneous mixture of cells and aligning them in the required pattern is challenging. Thus, DEP proves to be an interesting field of study which can be further exploited for molecular biology and stem cell research. For this a thorough understanding of the mechanism is necessary. This work serves to provide deeper insight into the basic concepts of DEP and serves as a reference for future work.

REFERENCES

1. Pohl, H., *The Motion and Precipitation of Suspensoids in Divergent Electric Fields.* J. Appl. Phys. 1951. **22:** p. 869-871.

2. Muller, T., Fiedler, S., Schnelle, T., Ludwig, K., Jung, H., Fuhr, G., *High frequency electric fields for trapping of viruses.* 1996. Biotechnol. Tech. **10**: p. 221– 226.

3. Washizu, M., Kurosawa, O. *Electrostatic manipulation of DNA in microfabricated structures.* IEEE Trans. Ind. Appl. 1990 **26**: p. 1165–1172.

4. Cummings, E.B. and Singh, A.K., *Dielectrophoresis in Microchips Containing Arrays of Insulating Posts: Theoretical and Experimental Results.* Anal. Chem. 2003. **75**: p. 4724-4731.

5. Hernandez, H.M., Cardiel, B., Gonalez, P., Encinas, L., *Insulator-based dielectrophoresis of microorganisms: theoretical and experimental results.* Electrophoresis. 2011. **32(18)**: p. 2502-2511.

6. Irimajiri, A., Hanai, T., and Inouye, A., *Dielectric theory of multi-stratified shell-model with its application to a lymphoma cell*. Journal of Theoretical Biology, 1979. **78(2)**: p. 251-269.

7. Jones, T.B. *Electromechanics of particles.* Cambridge University Press. 1995.

8. Kirby, B.J. *Micro- and Nanoscale Fluid Mechanics: Transport in Microfluidic Devices.*. Cambridge University Press. 2010. ISBN 978-0-521-11903-0.

9. Arnold, W.M., Schwan, H.P. and Zimmermann, U. *Surface Conductance and Other Properties of Latex Particles Measured by Electrorotation*. J. Phys. Chem. 1987**. 91**: p. 5093-5098.

10. Broche, L.M., Labeed, F.H. and Hughes, M.P., *Extraction of dielectric properties of multiple populations from dielectrophoretic collection spectrum data*. Physics in Medicine and Biology, 2005. **50(10)**: p. 2267-2274.

11. Prodan, E., Prodan, C. and Miller, J.H.Jr., *The Dielectric Response of Spherical Live Cells in Suspension: An Analytic Solution.* Biophysical Journal, 2008. **95:** p.4174–4182.

12. Irimajiri, A., Suzaki, T., Asami, K. and Hanai, T. *Dielectric Modeling of Biological Cells: Models and Algorithm.* Bull. Inst. Chem. Res., Kyoto Univ., 199. **69.** No. 4.

13. Ramos, A., Morgan, H., Green, N.G. and Castellanos, A., *Ac electrokinetics: a review of forces in microelectrode structures***,** J. Phys. D: Appl. Phys. 1998. **31:** p**.** 2338–2353.

14. Morgan, H., Green, N.G., *Dielectrophoretic investigations of sub-micrometre latex spheres*, J. Phys. D: Appl. Phys. 1997. 30: p. 2626–2633.

15. Pauly, H. and Schwan, H. *Impedance of a suspension of ball-shaped particles with a shell: a model for the dielectric behaviour of cell suspensions and protein solutions* Chemi. Biochemie. 1959. **14(2)**: p. 125-131.

16. Fuhr, G., Hagedorn, R. and Müller, T. *Simulation of the rotational behavior of single cells by macroscopic spheres.* Stud. Biophys. 1985. **107**: p. 109–116.

17. Oblak, J., Križaj, K., Amon, S., Lebar, A. M. and Miklavčič, D. *Feasibility study for cell electroporation detection and separation by means of dielectrophoresis.* Bioelectrochemistry, 2007. **71(2):** p. 164–171.

18. Arnold, W. M. and Zimmermann, U., *Electro-rotation development of a technique for dielectric measurements on individual cells and particles.* J. Electrostat. 1998. **21**:p. 151–191.

19. Schnelle, Th., Müller, T., Fiedler, S. and Fuhr, G. *The influence of higher moments on particle behaviour in dielectrophoretic field cages*. J. Electrostat. 1999. **46**: p. 13–28.

20. Biasio, A.D. and Cametti, C., *Effect of shape on the dielectric properties of biological cell suspensions,* Bioelectrochemistry. 2007. **71**: p. 149–156.

21. Hughes, M.P., Pethig, R., Wang, X-B. *Forces on Particles in Travelling Electric Fields: Computer-Aided Simulations*. J. Phys. D: Appl. Phys. 1996. **29**: p. 474-482.

22. O'Konski, C. *Electric properties of Macromolecules. V.theory of ionic polarization in polyelectrolytes.* J. Phys. D: Appl. Phys. 1997 **30:** p. 2470–2477.

23. Pohl, H. Dielectrophoresis; Cambridge University Press: Cambridge, 1978.

24. Crane, J.; Pohl, H. J. *A Study of Living and Dead Yeast Cells Using Dielectrophoresis.* Electrochem. Soc. 1968, **115**(6): p. 584-586.

25. Germishuizen, W.A., Walti, C., Wirtz, R., Johnston, M. B., Pepper, M., Giles, A. and Middelberg, A., *Selective dielectrophoretic manipulation of surface-immobilized DNA molecules.* Nanotechnology. 2003.**14**: p. 896–902.

26. Pysher, M.D. and Hayes, M.A. *Electrophoretic and Dielectrophoretic Field Gradient Technique for Separating Bioparticles.* 2007. Analytical Chemistry. A-F.

27. Duffy, C. F. Gafoor, S. Richards, D. P. Admadzadeh, H. O Kennedy, R. Arriaga, E. A. *Determination of Properties of Individual Liposomes by Capillary Electrophoresis with Postcolumn Laser-Induced Fluorescence Detection*, Anal. Chem. 2001. **73 (8):** p. 1855-1861.

28. Radko, S. P. Stastna, M. Chrambach, A. *Size-Dependent Electrophoretic Migration and Separation of Liposomes by Capillary Zone Electrophoresis in Electrolyte Solutions of Various Ionic Strengths.* Anal. Chem. 2000. **72**: p. 5955- 5960.

29. Mehrishi, J. N. and Bauer, J. *Electrophoresis of cells and the biological relevance of surface charge***.** Electrophoresis. 2002. **23**: p. 1984-1994.

30. Pethig, R. and Markx, G.H., *Applications of dielectrophoresis in biotechnology. Trends Biotechnol.* 1997, **15**: p. 426-432.

31. Green, N.G., and Morgan, H., *Dielectrophoretic separation of nano-particles*. J. Phys. D: J. Appl. Phys. 1997. **30:** p. L41-L84.

32. Muller, T., G. Gradl, S. Howitz, S. Shirley, T. Schnell, and G. Fuhr, *A 3-D microelectrode system for handling and caging single cells and particles*. Biosensors & Bioelectronics 1999. **14**: p. 247- 256.

33. Gossett, D., Weaver, W., Mach, A., Hur, S.C., Lee, W., Amini, H., and Carlo, D. D. *Label-free cell separation and sorting in microfluidic systems.* Anal Bioanal Chem. 2010. **397(8)**: 3249–3267.

34. Duncan, L., Shelmerdine, H., Coley, H.M. and Labeed, F.H. *Assessment of the dielectric properties of drug sensitive and resistant leukaemic cells before and after ion channel blockers using dielectrophoresis*. NSTI-Nanotech 2006. **2.** ISBN 0-9767985-7-3.

35. Fiedler, S., S.G. Shirley, T. Schnelle, and G. Fuhr, *Dielectrophoretic sorting of particles and cells in a microsystem*, Analytical Chemistry 1998. **70**: p. 1909-1915.

36. Voldman, J., M.L. Gray, M. Toner, and M.A. Schmidt, *A microfabrication-based dynamic array cytometer*, Analytical Chemistry 2002 **74**: p. 3984-3990.

37. Voldman, J., M. Toner, M.L. Gray, and M.A. Schmidt, *Design and analysis of extruded quadrupolar dielectrophoretic traps*, Journal of Electrostatics 2003 **57**:p. 69-90.

38. Pethig, R., Y. Huang, X.B. Wang, and J.P.H. Burt, *Positive and negative dielectrophoretic collection of colloidal particles using interdigitated castellated microelectrodes*, Journal of Physics D: Applied Physics 1992 **24:** p**.**881-888.

39. Xiaoyuan Hu, Paul H. Bessette, Jiangrong Qian, Carl D. Meinhart , Patrick S. Daugherty, and Hyongsok T. Soh, *Marker-specific sorting of rare cells using dielectrophoresis*. Proceedings of the National Academy of Sciences of the United States of America, ISSN 0027-8424, 11/2005, Volume 102, Issue 44, pp. 15757 – 1576.

40. H. Morgan, M.P. Hughes, and N.G. Green, *Separation of submicron bioparticles by dielectrophoresis*, Biophysical Journal. 1999. **77**: p. 516-525.

41. Gascoyne, P.R.C., Y. Huang, R. Pethig, J. Vykoukal, and F.F. Becker, *Dielectrophoretic separation of mammalian cells studied by computerized image analysis*, Measurement Science and Technology 1992 **3:** p. 439-445.

42. Fischer, A. *The use of monoclonal antibodies in allogeneic bone marrow transplantation*. 1993. **83 (4)**: p. 531-4.

43. Hathcock, K.S., Hirano, H. and Hodes, R.J. *CD45 expression by murine B cells and T cells: Alteration of CD45 isoforms in subpopulations of activated B cells.* Immunologic Research. 1993. **12(1)**: p. 21-36.

44. Ling, S.H., Lam, Y.C., and Chian, K. S. *Continuous Cell Separation Using Dielectrophoresis through Asymmetric and Periodic Microelectrode Array*. Anal. Chem. 2012. **84**: p. 6463−6470.

45. Jen, C. P. and Chen, T. W. *Selective trapping of live and dead mammalian cells using insulator-based dielectrophoresis within open-top microstructures. Biomed Microdevices.* 2009. **11**: p. 597–607.

46. Gagnon, Z., Mazur, J. and Chang, H.C., *Integrated AC electrokinetic cell separation in a closed-loop device.* Lab Chip. 2010. **10**: p. 718–726.

47. Chen, C. H. and Santiago, J. G. *A planar electroosmotic micropump.* J. Micromech. Microeng. 2002. **11**: p. 672–683.

48. Gonzalez, A., Green, N. G., Castellanos, A. and Morgan, H. *Fluid Flow induced by nonuniform ac electric fields in electrolyes on microelectrodes II. A linear*

double-layer analysis, Phys. Rev. E: Stat. Phys., Plasmas, Fluids, Relat. Interdiscip. Top. 2000. **61**: p. 4019–4028.

49. H. Morgan, N. Green, *AC Electrokinetics: Colloids and Nanoparticles*, Research Studies Press, Hertfordshire, England, 2003.

50. Huang, Y., Hölzel, R., Pethig, R., Wang, X. B., *Differences in the AC electrodynamics of viable and non-viable yeast cells determined through combined dielectrophoresis and electrorotation*. Phys Med Biol, 1992. **37**: p. 1499–1517.

51. Markx, G., Davey, C., *The dielectric properties of biological cells at radiofrequencies: Applications in biotechnology*. Enzyme and Microbial Technology. 1999. **25**: p. 161–171.

52. Markx, G. H. and Pethig, R. *Dielectrophoretic separation of cells: Continuous separation.* Biotechnol. Bioeng. 1995. **45**: p. 337−343.

53. Ho, C.T., Lin, R.Z., Chang, H. Y., Chang, W. Y., Liu. *Rapid heterogeneous liver-cell on-chip patterning via the enhanced field-induced dielectrophoresis trap.* Lab Chip. 2006. **6**: p. 724–734.

54. Lin, R.Z., Ho, C.T., Liu, C. H., Chang, H. Y. *Dielectrophoresis based-cell patterning for tissue engineering.* Biotechnol. J. 2006. **1**: p. 949–957.

55. Verduzco-Luque, C., Alp, B., Stephens, G. M. and Markx, G. H., *Construction of biofilms with defined internal architecture using dielectrophoresis and flocculation*. Biotechnol. Bioeng.. 2003. **83(1)**: p. 39–44.

56. Mason, V. P., Markx, G. H., Thompson, I. P., Andrews, J. S., Manefield, M., *Colonial architecture in mixed species assemblages affects AHL mediated gene expression.* FEMS Microbiol. Lett. 2005. **244(1):** p. 121–127.

57. Andrews, J. S., Mason, V. P., Thompson, I. P., Stephens, G. M., Markx, G. H., *Construction of artificially structured microbial consortia (ASMC) using dielectrophoresis: Examining bacterial interactions via metabolic intermediates within environmental biofilms.* J. Microbiol. Methods 2006. **64(1):** p. 96–106.

58. Gagnon, Z.R. *Cellular dielectrophoresis: Applications to the characterization, manipulation, separation and patterning of cells.* Electrophoresis. 2011. **32:** p. 2466–2487.

59. Tsutsui, H., Yu, E., Marquina, S., Valamehr, B., Wong, I., Wu, H. and Ho, C.M., *Efficient Dielectrophoretic Patterning of Embryonic Stem Cells in Energy*

Landscapes Defined by Hydrogel Geometries, Annals of Biomedical Engineering. 2010. **38**: p. 3777–3788.

60. Markx, G. H., Carney, L., Littlefair, M., Sebastian, A. Buckle, A. M., *Recreating the hematon: microfabrication of artificial haematopoietic stem cell microniches in vitro using dielectrophoresis.* Biomed. Microdevices. 2009. **11(1)**: p. 143–150.

61. Gray, D. S., Tan, J. L., Voldman, J. and Chen, C. S., *Dielectrophoretic registration of living cells to a microelectrode array.* Biosens. Bioelectron. 2004, **19:** p.1765–1774.

62. Albrecht, D. R., Tsang, V. L., Sah, R. L., Bhatia, S. N., *Photo- and electropatterning of hydrogel-encapsulated living cell arrays*. Lab Chip 2005. **5**: p. 111–118.

63. Bown, M.R. and Meinhart, C.D. *AC electroosmotic flow in a DNA concentrator*. *Microfluid Nanofluid*. 2006. **2**: p. 513–523.

64. Cheng, H., Lei, K., Choy, K., Chow, L., *Single-stranded DNA concentration by electrokinetic forces.* J. Micro/Nanolith. MEMS MOEMS. 2009.8(2): p. 021107.

65. Asbury, C. and Engh, G., *Trapping of DNA in Nonuniform Oscillating Electric Fields*. Biophysical Journal. 1998. **74**: p.1024–1030.

66. Washizu, M., Kurosawa, O., Arai, I., Suzuki, S., Shimamoto, N. *Applications of electrostatic stretch-and-positioning of DNA.* IEEE Trans. Ind. Appl. 1995. **31**: p. 447–456.

67. Namasivayam, V., Larson, R.G., Burke, D.T., Burns, M.A. *Electrostretching DNA molecules using polymer-enhanced media within microfabricated devices.* Anal. Chem. 2002. **74**: p. 3378–3385.

68. Ghallab, Y.H. and Badawy,W. *A novel cmos lab-on-a-chip for biomedical applications*, in Proceedings of IEEE International Symposium on Circuits and Systems (ISCAS ’05). 2005. p. 1346– 1349.

69. Lapizco-Encinas, B.H., Simmons, B.A., Cummings, E.B., and Fintschenko, Y., *Dielectrophoretic Concentration and Separation of Live and Dead Bacteria in an Array of Insulators.* Anal. Chem. 2004. **76**: p. 1571-1579.

70. Ino, K., Shiku, H., Ozawa, F., Yasukawa, T., and Matsue, T. *Manipulation of microparticles for construction of array patterns by negative dielectrophoresis*

using multilayered array and grid electrodes. Biotechnol Bioeng. 2009. **104(4):** p.709-18.

71. Nrumann, E., Sowers, A. E. and Jordan, C. A. *Electroporation and Electrofusion in Cell Biologq, 1989.* Plenum Press.

72. Medoro, G., Manaresi, N. Leonardi, A., Altomare, L. Tartagni, M. and Guerrieri. R., *A lab-on-a-chip for cell detection and manipulation.* IEEE Sensors Journal. 2003. **3(3)**: p. 317–325.

73. Kadaksham, J., Singh, P. and Aubry, N., *Dielectrophoresis induced clustering regimes of viable yeast cells. Electrophoresis*. 2005. **26**: p. 3738–3744.

74. W. Arnold, *Positioning and levitation media for the separation of biological cells*, IEEE Trans. Ind. Appl. 2001. **37**: p. 1468–1475.

75. Markx, G., Talary, M. and Pethig, R. *Separation of viable and non-viable yeast using dielectrophoresis.* J. Biotechnol., 1994. **32:** p**.** 29–37.

76. Kirkwood, J. G. *Statistical mechanics of fusion*. J. Chem. Phys. 1941. **9:** p. 878-881.

77. Giddings, J. C. *Factors influencing accuracy of colloidal and macromolecular properties measured by field-flow fractionation.* Analytical Chemistry. 1997. **69**: p. 552–557.

78. Giddings, C., Yang, F. and Myers, M. *Flow Field-Flow Fractionation: A Versatile New Separation Method*. Science. 1976. **193**. p. 1244-1245.

79. Berg, H. C. and Purcell, E. M. *A method for separating according to mass a mixture of macromolecules or small particles suspended in a fluid*, Theory I. Proceedings of the National Academy of Sciences. 1967. **58**: p. 862–869.

80. Cui, H., Voldman,J. He, X. and Lim, K. *Separation of particles by pulsed dielectrophoresis*. Lab Chip. 2009. **9**: p. 2306–2312.

81. Karan, V.I.S, Kaler, O., Fritz, G. and Adamson, R. *Quasi-Elastic Light Scattering Studies on Yeast Cells Undergoing Dielectrophoresis.* 1986. IEEE Transactions On Industry Applications. **22**: p. 57-62.

82. Einolf, C. W. and Carstensen, E. L. *Passive electrical properties of microorganisms, Low-frequency dielectric dispersion of bacteria*. 1973. Biophys. J. **(13):** p. 8-13.

83. White, C.M., Holland, L.A., Famouri, P., *Application of capillary electrophoresis to predict crossover frequency of polystyrene particles in dielectrophoresis*, Electrophoresis, 2010. **31**: p. 2664–2671.

84. Stern, O. *Z.Electrochem*, 30, 508 (1924)

85. Pethig, R., *Dielectrophoresis-Status of the theory,technology and applications.* Biomicrofluidics, 2010. **4:** p. 022811-022820.

86. Wang, X., Yang, Y., and Gascoyne, P.R., *Role of peroxide in AC electrical field exposure effects on friend murine erythroleukemia cells during dielectrophoretic manipulations*. Biochim. Biophys. Acta 1990 **1426**: p. 53-68.

87. Graham D.M., Messerli, M.A., and Pethig, R., *Spatial manipulation of cells and organelles using single electrode dielectrophoresis.* BioTechniques. 2012 **52**: p.39-43.

88. Voldman, J., *Electrical forces for microscale cell manipulation*. Annu. Rev. Biomed. Eng. 2006. **8**: p. 425-454.

89. Markx, G., Pethig, R., and Rousselet. J., *The dielectrophoretic levitation of latex beads, with reference to field-flow fractionation.* J. Phys. D: Appl. Phys. 1997 **30**: p.2470–2477.

90. Kralji, J.G., Lis, M., Schmidt, M. and Jensen, K., *Continuous Dielectrophoretic Size-Based Particle Sorting.* Anal. Chem. 2006. **78**: p. 5019-5025.

91. Cetin, B., Kang, Y., Wu, Z. and Li, D., *Continuous particle separation by size via AC-dielectrophoresis using a lab-on-a-chip device with 3- electrodes.* Electrophoresis. 2009. **30(5)**: p.766–772.

92. Lewpiriyawong, N., Yang, C. and Lam, Y. C. *Dielectrophoretic manipulation of particles in a modified microfluidic H filter with multi-insulating blocks*. Biomicrofluidics. 2008. **2**: p. 034105 1-11.

93. http://www.ilri.org/InfoServ/Webpub/fulldocs/ilca_manual4/Microbiology.html

94. Arnold, W. M., Jäger, A. H. Zimmermann, U. *The influence of yeast strain and of growth medium composition on the electro-rotation of yeast cells and of isolated walls.* 1989. Dechema Biotechnology Conferences. **3**: p. 653-656.

95. Basuray, S. and Chang, H., *Designing a sensitive and quantifiable nanocolloid assay with dielectrophoretic crossover frequencies,* Biomicrofluidics, 2010. **4**: p. 013205 1-11.

96. Web.nmsu.edu

97. Shilov, V. N. *Dielectrophoresis of Nanosized Particle*. 2008. Colloid Journal. **70(4)**: p. 515–528.

98. Castellanos, A., Ramos, A., Green, N.G. and Morgan, H. *Electrohydrodynamics and dielectrophoresis in microsystems: scaling laws*. J. Phys. D: Appl. Phys. 2003. **36**: p. 2584–2597.

99. Hoffman, P. D. and Zhu, Y. *Double-layer effects on low frequency dielectrophoresis-induced colloidal assembly.* 2008. Applied Physics Letters. **92**: p. 224103-224110.

100. Inoue, T., Pethig, R., Al-Ameen, T. A. K., Burt J P H and Price J A R., *Dielectrophoretic behaviour of Micrococcus lysodeikticus and its protoplast*. J. Electrostatics 1988 **21**:p. 215–223.

101. Hasan, R. and Khurma, A., *AC Dielectrophoresis Using Elliptic Electrode Geometry*. Journal of Sensors, 2011 **2011**: p. 8.

102. Khoshmanesh, K., Zhang, C. and Nahavandi, S., *Size based separation of microparticles using a dielectrophoretic activated system.* Journal of Applied Physics, 2010 **108**: p. 034904-034911.

103. Wang Y. and Afsar M.N., *Measurement of complex permittivity of liquid dielectrics*, Microwave and Optical Technology Letters, 2002 **34**: p. 240–243.

104. Pohl, H. A. and Schwar, J. P. *Factors Affecting Separations of Suspensions in Nonuniform Electric Fields.* J. Appl. Phys. 1959. **30**: p. 69-75.

105. Iliescu, C., Xu, G., Loe, F.C., Ong, P.L. and Tay, F.E.H., *A 3-D dielectrophoretic filter chip, Electrophoresis*. 2007. **28**: p. 1107–1114.

106. Gimsa, J., Marszalek, P., Loewe, U. and Tsong, T. Y., *Dielectrophoresis and electrorotation of neurospora slime and murine myeloma cells*. Biophys. J. Biophysical Society. 1991. **60**: p. 749-760.

107. Zou, Z., Lee, S.H. and Ahn, C.H., *A Polymer Microfluidic Chip With Interdigitated Electrodes Arrays for Simultaneous Dielectrophoretic Manipulation and Impedimetric Detection of Microparticles*, IEEE Sensors Journal, 2008. 8(5): p. 527-536.

108. Bunthawin, S., Wanichapichart, P. and Gimsa, J., *An investigation of dielectric properties of biological cells using RC-model*. Songklanakarin J. Sci. Technol. 2007. **29(4)**: p.1164-1181.

109. Han, K. and Frazier, A.B., *Lateral-driven continuous dielectrophoretic microseparators for blood cells suspended in a highly conductive medium*. Lab Chip. 2008. **8**: p. 1079–1086.

110. Chaurey,V., Polanco,C., Chou, C., Swami, N., *Floating-electrode enhanced constriction dielectrophoresis for biomolecular trapping in physiological media of high conductivity*, Biomicrofluidics. 2012. **6**: p. 012806 1-14.

111. Gascoyne, P., Wang, X., Huang, Y., and Becker, F., *Dielectrophoretic Separation of Cancer Cells from Blood*, IEEE Trans Ind Appl. 1997. **33(3):** p. 670–678.

112. Kuczenski,R., Chang, C. and Revzin, A. *Dielectrophoretic microfluidic device for the continuous sorting of Escherichia coli from blood cells.* Biomicrofluidics. 2011. **5**: p. 032005-15.